Medical University of South Carolina

MEDICA

MUSC Theses and Dissertations

1-1-2020

Antibiotic Disruption of Oral Microbiota Dysregulates the Osteoimmune Response and Alveolar Bone Homeostasis in the Healthy Periodontium

Brooks Albert Swanson
Medical University of South Carolina

Follow this and additional works at: https://medica-musc.researchcommons.org/theses

Recommended Citation

Swanson, Brooks Albert, "Antibiotic Disruption of Oral Microbiota Dysregulates the Osteoimmune Response and Alveolar Bone Homeostasis in the Healthy Periodontium" (2020). *MUSC Theses and Dissertations*. 685.
https://medica-musc.researchcommons.org/theses/685

This Thesis is brought to you for free and open access by MEDICA. It has been accepted for inclusion in MUSC Theses and Dissertations by an authorized administrator of MEDICA. For more information, please contact medica@musc.edu.

Antibiotic Disruption of Oral Microbiota Dysregulates the Osteoimmune Response and Alveolar Bone Homeostasis in the Healthy Periodontium by

Brooks Albert Swanson

A dissertation submitted to the faculty of the Medical University of South Carolina in partial fulfilment of the requirements for the degree of Masters in Biomedical Sciences in the College of Graduate Studies

Department of Microbiology and Immunology

2020

Approved by:

Chairman, Advisory Committee	Chad Novince
	Christopher Davies
	Alexander Alekseyenko
	Sakamuri Reddy

DEDICATION

To my parents, Carolyn and Bob.

To my brother, Robert.

To my sister, Allie.

ACKNOWLEDGEMENTS

I would like to thank Dr. Jessica Hathaway-Schrader for assistance with graphical design.

TABLE OF CONTENTS

LIST OF TABLES

Table

LIST OF FIGURES

Figure

ABSTRACT

BROOKS ALBERT SWANSON. Antibiotic Disruption of Oral Microbiota Dysregulates the Osteoimmune Response and Alveolar Bone Homeostasis in the Healthy Periodontium. (Under the direction of CHAD NOVINCE).

Problem: A balanced relationship between the host and oral microbiota supports periodontal health and alveolar bone homeostasis. Antibiotic perturbation of the gut microbiota critically regulates the osteoimmune response at non-oral skeletal sites. However, the impact of antibiotics on the oral microbiota and osteoimmune mechanisms regulating alveolar bone homeostasis are unknown. Considering that periodontitis driven bone loss is caused by dysbiotic shifts in the oral microbiome, antibiotic disruption of the oral microbiota may have deleterious effects on alveolar bone homeostasis.

Approach: Drinking water of sex-matched C57BL/6T specific-pathogen-free (SPF) mice was supplemented with minocycline (MINO) or vehicle (VEH) control treatment from age 6 to 12 weeks. SPF mice were euthanized at age 12 weeks to assess immediate effects and at age 18 weeks to evaluate sustained minocycline effects. 16S rDNA analysis was performed to evaluate bacterial load and phylum level alterations in the oral microbiome. Micro-CT was utilized to assess linear alveolar bone loss in the maxilla and cortical/trabecular bone microarchitecture in the mandible. qRT-PCR analysis was carried out to assess pro-osteoclastic and pro-inflammatory genes in the mandible bone marrow (MBM) and gingiva. TRAP+ osteoclastic cell outcomes in alveolar bone were evaluated by *in situ* and *in vitro* approaches. Flow cytometric analysis of immune cells was performed in MBM and cervical lymph nodes (CLNs). In a separate experiment, drinking water of male C57BL/6T germ-free (GF) mice was supplemented with MINO or VEH treatment from age 6 to 12 weeks.

Results: MINO treatment increased overall bacterial load and induced phylum level alterations in the oral bacteriome of 12-week-old male SPF mice. Disruption of phylum level bacterial communities were sustained in 18-week-old male SPF mice. The effects of MINO treatment on the oral microbiota were sex-dependent as no alterations were seen in female mice. MINO treatment induced linear alveolar bone loss in both male and female SPF mice at the age 12 weeks and these effects persisted at age 18 weeks. Validating that MINO-induced catabolic effects on alveolar bone is dependent on the oral microbiota, no differences were found in linear alveolar bone loss in MINO vs. VEH treated male GF mice. Cortical bone thickness was decreased in the mandible in response to MINO treatment. Osteoclast cell size and bone interface were increased in maxillary alveolar bone sections from MINO vs. VEH treated male SPF mice. Exogenous MINO stimulation in MBM cultures derived from naïve 12-week-old male SPF mice increased osteoclast size and number of nuclei. Intriguingly, these findings suggest that MINO-induced pro-osteoclastic effects could be in part independent of the microbiota. Pro-inflammatory plasmacytoid dendritic cells (DCs) were upregulated within MBM and CLNs of MINO vs. VEH treated male SPF mice. Paralleling the plasmacytoid DCs, MINO treatment profoundly increased T_H1 and T_H17 cell populations in the MBM and CLNs.
Conclusion: The current investigation reveals that MINO disruption of oral microbiota induces a pro-inflammatory immune response, which upregulates osteoclastogenesis, and drives alveolar bone loss. This novel research shows that oral MINO therapy, a commonly prescribed antibiotic treatment, may have detrimental clinical effects on alveolar bone in the healthy periodontium.

CHAPTER 1: INTRODUCTION

1.1 Problem Statement

The commensal oral microbiota is a critical regulator of health and disease in the human body, having effects on food digestion, dental caries, oral cancer, and oral infectious diseases, specifically periodontitis.[1,2] Periodontal disease is a chronic inflammatory disease of the periodontium and is the most common oral condition of the human population.[3] Important to this proposal, the homeostasis between the commensal oral microbiota and host immune response regulates alveolar bone remodeling in the healthy periodontium.[4] Studies utilizing the specific pathogen free (SPF) vs. germfree (GF) mouse model have discerned that the commensal oral microbiota enhances osteoclastogenesis and has catabolic effects on alveolar bone homeostasis during health.[4-7] The commensal oral microbiota increases alveolar bone loss and enhances osteoclast precursor cell potential to differentiate into osteoclastic cells lining alveolar bone.[4] Increased pro-inflammatory cytokines (IL17, IL6, IL-1β), which enhance osteoclastogenesis, correlate with decreased alveolar bone height in SPF vs. GF mice.[5,7] Irie, Novince, and Darvaeu (2014) recently showed that the commensal oral microbiota increased the frequency of $TRAP^+$ osteoclastic cells and $RANKL^+$ cells at the alveolar bone surface, as well as significantly increased numbers of neutrophils, which highlights that the oral microbiota drives pro-inflammatory immune response effects that lead to alveolar bone loss.[4] Recent human periodontitis studies demonstrating a link between the disruption of the oral microbiota and host inflammatory response, have shown an oral microbial imbalance induces alterations in gene expression lineage and leads to increased local T_H17 cells to promote periodontal disease.[8] Periodontal mouse model studies have shown that bone loss was decreased after administration of soluble

decoy receptors for IL-1α, IL-1β, or TNF[9-11] and also in mice deficient in host inflammatory mediators, such as IFNγ, IL-6, or TNF receptor 1.[12,13]

Antibiotics are well known to induce shifts and alterations in the microbial composition within the gut, which have indirect effects on host immunity and physiology.[14-16] We have previously shown that the antibiotic disruption of gut microbiota composition alters host immune response effects, which increased osteoclast activity and impaired bone mass accrual at non-oral skeletal sites.[17] However, the effects of an antibiotic-disrupted commensal oral microbiota and its impact on the osteoimmune response and alveolar bone homeostasis is currently unknown.

1.2 Hypothesis

Antibiotic perturbation of the oral microbiota regulates the osteoimmune response and alveolar bone homeostasis.

1.3 Specific Aims

Aim 1: Evaluate the persistence of minocycline treatment effects on the oral microbiome and alveolar bone homeostasis.

Aim 2: Investigate the impact of antibiotic treatment effects on skeletal homeostasis and osteoimmune response mechanisms within the alveolar bone complex.

1.4 Background and Significance

General background on the periodontium and alveolar bone complex

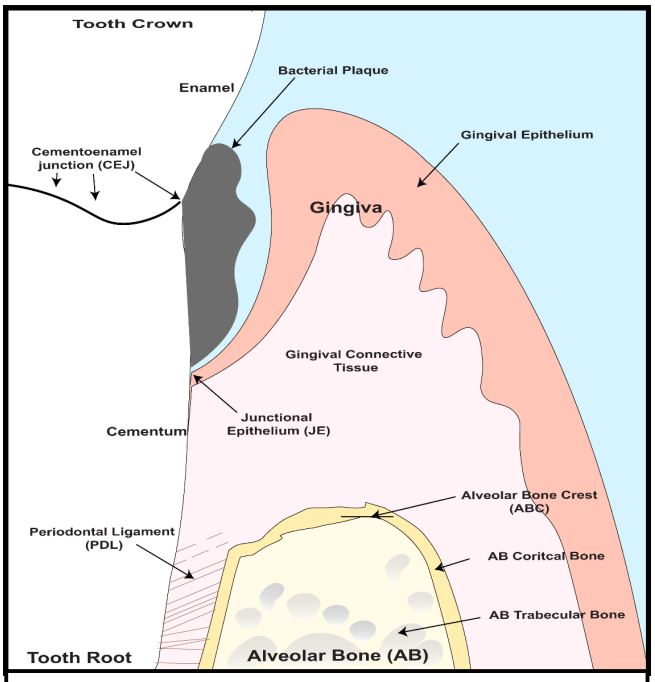

Figure 1: Structure of the Periodontium
Note: Figure was adapted from Hathaway-Schrader and Novince (2020).[1]

The major components of the periodontium are the gingiva, periodontal ligament, cementum, and alveolar bone **(Figure 1)**. The periodontium supports the teeth, dynamically acting as a suspensory apparatus resilient to normal functional and mastication forces.[18] Continuously adapting to masticatory demands, each of the periodontal tissues is unique in location, structure, and biochemical properties.[18]

The gingiva is the external barrier tissue of the periodontium, and functions to offer immediate protection for the underlying alveolar bone **(Figure 1)**. The gingiva surrounds the tooth like a collar and is firmly bound to the alveolar bone and cervical portion of the tooth.[19] The dentogingival junction, which consists of the epithelial and connective tissue attachment to the tooth, serves to protect to subjacent alveolar bone

from dental plaque biofilm resident microbes.[20,21] While epithelial tissues at external body surfaces act as an impermeable barrier to colonization of microbial biofilms, the junctional epithelium **(Figure 1)** attachment at the tooth surface is known to be highly permeable.[20]

The main function of the junctional epithelium is to form a unique seal between the root surface and gingiva to provide protection against the constant exposure of oral microbes and their byproducts.[20] Salivary proteins accumulate on the tooth surface to form the acquired pellicle.[22] Primary colonizers have adhesins that bind to complimentary salivary protein receptors in the acquired pellicle. Primary colonizers then provide receptors for secondary colonizers.[22] As a result of poor oral hygiene, the accumulation of dental plaque occurs, which provides a reservoir for the increase in periodontal pathogenic (perio-pathogenic) bacteria. Perio-pathogenic bacteria have invasive / evasive abilities and synthesize proteases that break down the epithelial physical barrier.[22] If the periodontium is constantly subjected to challenge by perio-pathogenic bacteria, the periodontal immune defense mounts an exacerbated pro-inflammatory response.[22]

The cementum is a specialized mineralized surface layer of the tooth root and attaches the teeth to the alveolar bone by anchoring the periodontal ligament (PDL) **(Figure 1).**[23] The PDL is a specialized connective tissue that attaches the teeth to surrounding alveolar bone.[24] Since teeth are not embedded into the alveolar bone directly, the periodontal ligament uses sensory receptors to ameliorate the impact of compressive forces generated during mastication on the alveolar bone.[25] The PDL also contains pluripotent stem cells that aid in regeneration and maintenance of the tissues within the periodontium.[26]

Continuous challenge by perio-pathogenic bacteria induces chronic inflammation which dysregulates collagen tissue remodeling. Apical migration of the junctional epithelium and periodontal pocket formation occurs due to degradation of collagen in the periodontal ligament and gingival connective tissue.[20] If poor hygiene persists, gram negative perio-pathogenic bacteria will continue to drive a chronic pro-inflammatory immune response state which leads to progressive tissue destruction and alveolar bone loss.[22]

The cementoenamel junction (CEJ) represents the anatomic limit between the enamel crown and cementum root surface, and is located at the cervical region of the tooth **(Figure 1).**[27] One of the most important parameters for assessing periodontal destruction is evaluating the linear distance from the CEJ to alveolar bone crest (ABC). In periodontal disease states, the crest of the alveolar bone migrates apically, moving away from the CEJ and towards the root apex.[27] Studies have reported that a normal CEJ to ABC distance of 1 +/- 0.5 mm exists in the healthy primary dentition,[28,29] and a distance of 2 mm or greater is considered to represent alveolar bone loss.[28] Perio-pathogenic bacteria drive alveolar bone loss through the induction of a chronic pro-inflammatory host immune response, that spreads deep into the gingival connective tissue as an inflammatory cell infiltrate.[30] This pro-inflammatory state dysregulates fibroblast-mediated remodeling of the gingival connective tissue and the PDL, which leads to reduced collagen content and compromised tissue integrity.[31,32] As this process continues, irreversible detachment of PDL collagen fibers occurs at the root surface, which results in the junctional epithelium extending apically.[31,32] As the subgingival biofilms extend apically toward alveolar bone and the periodontal pocket deepens, pro-inflammatory immune response mediators stimulate osteoclast mediated alveolar bone destruction.[33,34]

The formation of the alveolar bone is dependent on the development, eruption, and maintenance of the teeth.[35] The main function of the alveolar bone complex is to protect the roots of the teeth and support masticatory function.[35] The alveolar bone is subjected to continual and rapid remodeling/turnover associated with tooth eruption and the functional demands of mastication.[36] Alveolar bone is a unique osseous tissue due to its integration with the dentition and its close proximity to the resident oral microbiota colonizing the teeth and gingival tissues.[37] The alveolar bone complex is composed of alveolar bone proper, supporting trabecular bone, and supporting cortical bone, which consists of the lingual and buccal cortical plates **(Figure 1).**[35] The mandible is primarily composed of cortical bone, whereas the maxilla is primarily made up of trabecular bone.[38] The cortical bone is the thick outer layer of bone formed from compact bone on the facial and lingual surfaces of the alveolar bone.[36] The trabecular bone consists of spongy cancellous bone that is found between the alveolar bone proper and the plates of cortical bone.[39] The alveolar bone is rich in marrow spaces, which serve as a reservoir for hematopoietic and mesenchymal lineage cells.[39] While the architecture and morphology of the alveolar bone are unique to the functional demands of the periodontium, cellular processes and activities within alveolar bone are similar to non-oral skeletal sites.[36]

<u>General background on commensal oral microbiota / Host immune response in the oral cavity</u>

Early life host-microbe interactions regulate the development of the host immune system and the formation of a diverse microbial community, which is referred to as the commensal microbiota.[40,41] The oral microbiota, the community of microbes colonizing the oral cavity, play a critical role in regulating human health and disease.[42] The oral microbiota is the second most diverse microbial community colonizing the human body

with more than 1000 different bacterial species that colonize the hard surfaces of teeth and the soft tissues of the oral mucosa.[2,42-44] The predominant bacterial phyla communities that make up the human oral microbiota include Proteobacteria, Actinobacteria, Bacteroidetes, Firmicutes, Fusobacteria, and Spirochaetes.[2]

The oral microbiota has symbiotic effects that benefit the host, including the development and refinement of the local and systemic immune system, and protection against invading pathogenic microbes.[42] The immune system consists of the innate and adaptive immune responses. The innate immune response regulates the composition of resident microbes within commensal microbiota communities, supporting a mutualistic interaction where the host benefits directly from the microbiota's metabolic activities.[45] If the immune cells dominating the innate response lose proper recognition of colonizing bacteria, a dysbiosis between the host and microbiota can occur. Dysbiosis refers to the disruption of symbiotic interactions between the host and microbiota and can often lead to health consequences, such as inflammation or disease states.[46] Periodontal disease is a chronic inflammatory disease in the oral cavity that affects the periodontal tissues and bone supporting the teeth.[47] Periodontal disease is caused by a disruption of homeostasis between the host and oral microbiota.[47] Perio- pathogenic bacteria become more prominent within the oral flora, which stimulates the expression of pro-inflammatory cytokines that induce periodontal tissue destruction.[47] According to recent finding, approximately 47% of American adults have periodontal disease.[48]

The balanced relationship between the oral microbiota and host immune response is dependent on the recognition of commensal microbiota derived microbial-associated molecular patterns (MAMPs) at pattern-recognition receptor (PRR)-expressing host cells.[49-51] PPRs play an important role in innate immunity by recognizing MAMPs, which include microbial cell wall macromolecules, nucleic acids, and other

evolutionary conserved molecular motifs uniquely conserved by microorganisms.[49-51] MAMPs signaling enables the host to distinguish between self and the colonizing microbiota.[49-51] MAMPs activate the PRR-expressing epithelial cells within the oral cavity and function as specific molecular ligands with high affinity to PRRs.[52] When bound to PRR-expressing host cells, MAMPs induce signaling cascades, which lead to the expression of pro-inflammatory cytokines (IL-1B, IL-6, TNF) and type 1 interferons (IFN-a, IFN-B).[49-51]

The innate immune response constitutes a homeostatic system in which innate immune cells are able to recognize invading microorganisms as non-self and prompt immune responses to eliminate them.[53] As a part of the innate immune response of the oral cavity, saliva and the gingival crevicular fluid serve as a liquid barrier by flushing microbes and provide antimicrobial activity to maintain a symbiotic environment.[54] Important to the innate immune response, the periodontal epithelial barrier excludes environmental pathogens, exogenous substances, and resists mechanical stress.[54] Loss of integrity of the periodontal epithelium leads to the recruitment of pro-inflammatory immune cells within the underlying gingival connective tissue. As the pro-inflammatory cellular infiltrate spreads, apically towards the alveolar bone, pro-inflammatory cytokines upregulate osteoclast mediated bone resorption.[54]

Neutrophils are the most abundant leukocytes in blood and the first responders in the host immune defense.[55] Neutrophils use adhesion molecules to attach to endothelial cells within the blood vessels of the gingival connective tissue.[55] Neutrophils exit the gingiva blood vessels and travel through the gingival junctional epithelium until they reach the gingival crevice. At the gingival crevice, neutrophils accumulate and create a barrier wall to prevent the bacterial biofilm from growing and invading the underlying tissues.[55] While the lack of neutrophils has been proven to lead to periodontal

breakdown, the excess of neutrophils has also been reported to lead to periodontal tissue destruction.[55] This innate immune cell population has generated a continued interest in periodontitis due to its close proximity to the oral microbiota and its modulation of other immune cells in periodontal health and disease.[55]

The influx of neutrophils in the innate immune response is closely followed by monocytes that can differentiate into macrophages. In the inflamed periodontium, monocytes are released from the bloodstream in gingival capillaries and produce inflammatory cytokines, such as IL-1 and TNF.[54] Monocyte-derived macrophage cells engulf particular antigens, microbes, and apoptotic cells in the oral cavity.[54] Macrophages can differentiate into two subpopulations: M1 and M2 macrophages. M1 and M2 macrophages have antigen presenting processes specific to effector $CD4^+$ T-cells, thus providing a link between the innate and adaptive immune responses.[54] M1 macrophage cells have been shown to be activated by IFNG and LPS,[54] and produce high levels of pro-inflammatory cytokines such as TNF, IL1B, and IL6.[56] M2 macrophages have the ability to respond to IL4 and IL-3,[54] and express high levels of anti-inflammatory cytokine such IL10.[56] M1 macrophages in the periodontium are pro-inflammatory in nature, and mediate the elimination of invading bacteria.[56] M2 macrophages are anti-inflammatory in nature, and play a dominant role in periodontal tissue repair and homeostasis.[56]

Dendritic cells (DCs) are innate immune cells that capture, process, and present antigens to lymphocytes, which initiates and prompts the adaptive immune response.[57] DCs are derived from the bone marrow and can be divided in to two subpopulations: plasmacytoid DCs and conventional DCs.[57] Plasmacytoid DCs are derived from lymphoid progenitors and terminally differentiate in the bone marrow.[57] Plasmacytoid DCs mostly recognize viral antigens and specialize in the production and secretion of

type 1 interferons and pro-inflammatory chemokines.[57] This subpopulation of DCs enters the lymphoid nodes directly through the bloodstream and can act as antigen presenting cells, but less efficiently than conventional DCs.[57] Conventional DCs patrol various tissues in the periodontium to recognize foreign antigens.[57] Upon maturation, conventional DCs migrate to the lymph nodes draining the oral cavity to present microbial peptides to activate T-cells.[57] DCs can potentially enhance periodontal disease and the progression of alveolar bone loss through the upregulation of the T_H1 and T_H17 response.[57]

Table 1: Helper CD4+ T-Cell subsets, transcription factors, and cytokines

$CD4^+$ T-cell subset	Transcription factor	Characteristic cytokine
T_H1	T-BET	IFNG
T_H17	RORγt	IL17A
T_H22	AHR	IL22
T_{REG}	FOXP3	IL10, TGFβ

Adaptive immune cells are the second line of defense and respond slower to MAMPs than innate immune cells. Adaptive immunity differs from innate immunity in that is it highly specific to antigens and has immunological memory, a concept providing rapid and specific responses to reinfection.[58] Adaptive immune cells are derived from pluripotent hematopoietic stem cells in the bone marrow, and can differentiate into T-cells or B-cells.[58,59] T-cell differentiation and maturation occurs within the thymus and is characterized by ordered expression of various CD surface molecules.[60] B-cell maturation occurs in the bone marrow.[58]

In periodontal health and disease, $CD4^+$ helper T-cells protect the host against microbial invasion and regulate alveolar bone homeostasis.[61] Demonstrating the contribution of helper T-cells to periodontal tissue destruction, mice lacking $CD4^+$ T-cells

are resistant to bacteria induced alveolar bone loss.[12] Important to the current study, $CD4^+$ helper T-cell subsets are defined by the expression of transcription factors and secretion of specific cytokines **(Table 1)**. $CD4^+$ helper T-cell subsets examined in this study have been characterized to play the following roles: T_H1 cells generate cell mediated immunity, T_H17 cells maintain mucosal barrier function and have pro-inflammatory activity beneficial to the host during infection, T_H22 cells defend against tissue inflammation, and T_{REG} cells regulate pro-inflammatory cytokine production and overall immune homeostasis.[62]

In periodontitis, T_H1 cells enhance the apoptotic activity of macrophages to engulf oral pathogens and upregulate the generation of cytotoxic $CD8^+$ T-cells that eliminate intracellular pathogens in the oral environment.[32] T_H1 activity has been reported to parallel the increase of mature DCs in the gingival tissue in periodontitis disease states.[63] *Porphyromonas gingivalis* is a gram negative perio-pathogenic bacteria. In chronic periodontitis patients, *P. gingivalis* has been reported to stimulate mature DCs to secrete IL12 and IFNG.[64] Both cytokines can promote T_H1 responses and lead to sustained inflammation in the periodontium.[63] With regard to periodontitis, IFNG is the signature cytokine released by T_H1 cells and is associated with activating phagocytosis and the upregulation of other inflammatory cytokines and chemokines.[63] T_H1 responses in the periodontium have also associated with increased receptor activator of NF-kB ligand (RANKL) expression[65] enhanced osteoclast formation, and alveolar bone loss *in vivo*.[66] In addition, the T_H1 characteristic cytokine IFNG is presented at high levels in periodontal disease afflicted lesions and has been shown to be linked to progressive inflammation or more severe periodontal disease states.[32]

T_H17 cells protect the oral environment against invading bacteria by promoting mucosal immune responses as well as inducing bone damage.[67] The characteristic

cytokine synthesized by T_H17 cells is IL17A. T_H17 cells have been shown to increase neutrophil recruitment to the dental plaque through IL17A signaling for effective bacterial clearance.[68] When orally infected with *P. gingivalis*, the number of conventional DCs increases, which has been positively correlated with the generation of a T_H17 cell response.[63] Bacterial oral infection stimulates the migration of conventional DCs to the lymph nodes and gingiva, which has been associated with upregulation in IL17A levels and other pro-inflammatory signaling factors such as TNF, IL6, and IL1B, which contribute to alveolar bone loss.[69] In human studies, IL17A levels are also associated with increased mature conventional DCs and increased severity of periodontal bone loss.[63] T_H17 cells function as a bone damaging T-cell subset by promoting osteoclastogenesis through the secretion of IL17A and the induction of pro-inflammatory and osteoclastic mediators such as RANKL and TNF.[67,70]

In contrast to T_H1 and T_H17 cells, T_{REG} cells limit excessive inflammation within the periodontium and function to support alveolar bone homeostasis.[32] In inflamed periodontal disease states, T_{REG} cell characteristic cytokine levels (i.e., IL10, TGFβ) have been reported to be suppressed.[71] When T_{REG} cell function is inhibited, higher levels of IFNG, TNF, and RANKL are expressed in the periodontium, which exacerbates osteoclast mediated alveolar bone loss.[72]

T_H22 cells have been extensively studied in dermal conditions, but their role in periodontal health and disease still remains unclear.[73] These cells are characterized by high production of IL22 and low production of IL17A and IFNG.[74] T_H22 cells are found to be localized in the epithelium and associated with the production of antimicrobial peptides like defensins, which aid protection against tissue inflammation.[73] Due to the high expression of β-defensins in the gingival epithelium, T_H22 cells appear to have anti-inflammatory properties that support periodontal tissue homeostasis.[73]

The Novince group has previously shown that the commensal gut microbiota modulates the host immune response at non-oral skeletal sites.[75] T_H17 cells, $CD4^+IL17A^+$T-cells, and TNF were upregulated in the long bone marrow of specific-pathogen-free mice (SPF) vs. germ-free (GF) mice, which reveals that the commensal gut microbiota regulates $CD4^+$ T-cell hematopoiesis at non-oral skeletal sites.[75] Specific to the current study, Irie, Novince, and Darvaeu (2014) have shown that the commensal oral microbiota critically regulates osteoimmune response mechanisms in the healthy periodontium.[76] 12-week-old GF vs. SPF mice were utilized to determine the commensal oral microbiota's osteoimmunoregulatory effects on alveolar bone homeostasis. The burden of the commensal microbiota in SPF mice increased neutrophils, $CD4^+$ T-cells and $IL17^+$ T-cells in the junctional epithelium, upregulated RANKL expression and osteoclast cell numbers lining alveolar bone, which exacerbated linear alveolar bone loss.[76] The authors concluded that the commensal oral microbiota induction of the periodontal immune defense response results in a low-grade basal inflammation which causes alveolar bone loss during health.[76]

General background on osteoimmunology and alveolar bone homeostasis

Osteoimmunology is the study of the close interrelationship between bone and the immune system. Osteoimmunology research has revealed that innate immunity, adaptive immune cells, and the endocrine system play key roles in regulating skeletal modeling (bone growth) and remodeling (bone turnover).[77,78] Bone modeling directs longitudinal skeletal growth and bone mass accrual in the developing skeleton, while remodeling is important for the maintenance of bone mass and homeostasis of the mature adult skeleton.[37] The current research will focus on osteoimmune processes that influence bone remodeling / turnover in the mature alveolar bone complex. Bone

remodeling is regulated by mesenchymal-derived osteoblasts, which secrete and mineralize the bone matrix, and hematopoietic-derived osteoclasts, which demineralize and resorb bone.[79,80] Bone homeostasis depends upon the tightly coupled process of bone forming osteoblasts and bone resorbing osteoclasts.[79] At physiological conditions the actions of osteoclast and osteoblasts are balanced. However, when the balance is disturbed, bone architecture or function is compromised.[79] At the molecular level, the *Tnfsf11*(RANKL):*Tnfrsf11b*(OPG) (RANKL-OPG) axis is an important regulator of osteoclastogenesis and bone remodeling, which has implications for skeletal homeostasis.[81]

Osteoblasts are bone forming cells that are derived from the mesenchymal cell lineage. Osteoblast lineage cells consist of osteoblast precursors, osteoblasts, bone lining cells, and osteocytes.[82,83] Osteoclasts are multinucleated bone resorbing cells that originate from mononuclear cells derived from the hematopoietic lineage. Osteoclasts function to resorb the bone matrix under the influence of several factors.[84] The factors essential and necessary for osteoclastogenesis are macrophage colony-stimulating factor (CSF1) and receptor activator of nuclear factor kappa B ligand (RANKL).[85,86] CSF1 is a secreted factor required for pre-osteoclastic cells to differentiate into osteoclast precursor cells, and importantly induces the expression of the RANKL receptor, RANK.[86] RANKL signaling at the RANKL receptor drives osteoclast differentiation, maturation, function, and survival.[81,86]

RANKL is a member of the tumor necrosis factor (TNF) cytokine family and plays a critical role in periodontal bone resorption.[87] The major cellular sources of RANKL in the periodontium are B-cells and T-cells.[88] RANKL expression was found mainly in lymphocytes and macrophages within the lesions of periodontal disease afflicted lesions.[89] Osteoclast differentiation is regulated by transcription factors that are induced

by RANKL signaling at the RANK receptor.[90] When RANKL binds to RANK on osteoclast precursors, it causes the activation of nuclear factor for activated T-cells, cytoplasmic 1 (NFATC1).[91] NFATC1 is known as the master regulator of osteoclast differentiation as it transcribes a number of osteoclast specific genes responsible for differentiation, maturation, and function.[91] Dendritic cell specific transmembrane protein (DCSTAMP) is an RANKL induced fusion protein critical for osteoclast maturation.[92]

Osteoprotegerin (OPG) functions as the RANK decoy receptor. OPG is expressed in the bone marrow environment by stromal cells, osteoblasts, T-cells, B-cells and DCs.[84,86,93] This soluble decoy receptor binds RANKL to inhibit the interaction between RANKL and the RANK receptor, which in turn prevents osteoclast differentiation and function.[79] Thus, the ratio of RANKL to OPG is critical when evaluating RANKL-mediated osteoclastogenesis.

Pro-inflammatory cytokines, such as IL1B, IL17A, IL6, IFNG and TNF, have been identified as mediators of bone resorption. These pro-resorptive cytokines can enhance RANKL-signaling mediated osteoclastogensis.[94] Early studies identified an osteoclast activating factor produced in response to periodontal plaque bacteria, which was later recognized as interleukin-1 (IL1).[85] Within the IL1 family, IL1B upregulates the production of RANKL, enhancing its activity and stimulating osteoclastogenesis.[95,96] IL1B also has the ability to upregulate the expression of other pro-inflammatory cytokines in order to promote osteoclastogenesis and inhibit osteoblastogenesis.[95,96] IL1B also has synergistic effects on TNF-signaling induced osteoclastogenesis, as many pro-inflammatory effects of TNF on osteoclasts are upregulated by IL1B.[97] IL1B is secreted by a variety of cells consisting of macrophages, B-cells, neutrophils, fibroblasts and epithelial cells, and has received considerable attention as a potential inflammatory marker for active periodontal bone loss.[85]

TNF has been reported to play a critical role in the pro-inflammatory immune response, alveolar bone resorption, and loss in the attachment of connective tissue in the periodontium.[32,98] TNF is highly expressed in both the gingival crevicular fluid and diseased periodontal tissues, in which it is positively associated with matrix metalloproteinases (MMPs) and RANKL expression.[32] In addition, experimental periodontitis in TNF-a p55 receptor deficient mice was characterized by suppressed RANKL and MMPs expression, which was associated with the significant reduction in alveolar bone loss.[32] TNF actions can influence and support osteoclastogenesis by acting in concert with RANKL-signaling to promote the differentiation and function of osteoclasts.[99] TNF has also been shown to be involved in the induction of pre-osteoclast fusion and differentiation by activating cellular autophagy, which leads to bone resorption.[100]

Another important inflammatory mediator found in the periodontium, IL6, has been characteristically associated with inflammatory cell migration and osteoclastogenesis processes.[98] IL6 has been found in the gingival crevicular fluid of the oral cavity during the progression of periodontal destruction.[101] In immunohistochemistry studies, increased IL6 expression was present in inflamed gingival tissue isolates[102], and in tissue retrieved from periodontitis compared to gingivitis afflicted sites.[103,104] Supporting the association of IL6 expression in the inflamed gingiva, the concentration of IL6 in gingival tissue has been reported to be increased in inflamed compared to normal tissue from young adults.[105] IL6 has been shown to inhibit osteoclastogenesis via inducing the expression of RANKL by osteoblasts.[106] One study demonstrated that IL6 directly acts on osteoclast progenitor and inhibits their differentiation by specifically suppressing RANKL-mediated signaling pathways.[106]

The signature cytokine of the T_H17 cell response, IL17A also plays a critical role as a pro-inflammatory, pro-osteoclastic cytokine in the induction of periodontal bone destruction.[32,67] In one study, IL17A enhanced the expression of RANKL and inhibited the expression of OPG in human periodontal ligament cells, leading to an increased RANKL:OPG ratio, which suggests that IL17A plays a pro-catabolic role in the pathogenesis of periodontal bone loss.[107] A separate experimental study demonstrated that IL17A deficient mice have decreased osteolytic bone lesions in response to perio-pathogen challenge,[108] which further supports the notion that IL17A contributes to alveolar bone resorption.

The signature cytokine of the T_H1 cell response, IFNG, plays a more controversial role in osteoclast differentiation and function.[32] IFNG has been shown to have direct anti-osteoclastogenic actions and indirect pro-osteoclastic actions, which are dependent of the local cellular micro-environment.[109] IFNG is characteristically associated with the production of inflammatory cytokines and chemokines, and has been shown to have actions supporting osteoclastogenesis.[110-112]

Composition of the healthy oral microbiota

The oral microbiota refers to the collection of microbes inhabiting the human oral cavity.[113] The oral microbiome refers to the gene complement of that community. While each individual's oral microbiome consists of a distinct set of microorganisms, these microbes play an important role in maintaining the homeostatic environment within the mouth.[113] The human mouth is colonized by viruses, protozoa, fungi, archaea, and bacteria.[44] The mouth supports one of the most diverse microbial communities compared to other sites found within the human body. This is due to its heterogeneity of the oral microbes and the interrelationships between the different anatomical structures

of the oral cavity.[44] Microbial habitats of the oral cavity are represented by the hard tissue (teeth), soft tissues (cheek, tongue, lip, gingival sulcus, attached gingiva, and the hard/soft palate), and the interface of the two (subgingival and supragingival margins, and gingival crevices around the teeth).[114] The contiguous extensions of the oral cavity, such as the tonsils, pharynx, eustachian tube, middle ear, trachea, lungs, and cervical lymph nodes (CLNs), are also inhabited by the oral microbiota. However, the majority of oral microbiota studies are centered on evaluating samples from the oral cavity, such as gingiva, dental plaque, or saliva.[114] Oral cavity structures are continuously humidified by two physiological fluids, saliva and gingival crevicular fluid, which contribute to maintaining homeostasis in the oral environment by providing water, nutrients, antibodies, and antimicrobial and adherence factors.[115]

Studies have shown that different oral structures and tissues in the normal oral microbiota are colonized by distinct microbial communities.[43,116] The majority of studies defining the composition of the oral microbiota are primarily focused on bacteria. Approximately 280 bacterial species from the oral cavity have been isolated in culture and formally identified.[2] In the mouth, approximately half of the bacteria present are able to be cultivated using aerobic microbiological methods, while there are likely 500 to 700 common oral species.[2] Complex bacterial communities in the oral cavity have been identified and characterized by culture-independent methods based on the analysis of the sequences of conserved housekeeping genes, including the 16S rRNA gene.[2]

The bacterial community of the oral cavity is dominated by the phyla Firmicutes, Bacteriodetes, Proteobacteria, Actinobacteria, Spirochaetes, and Fusobacteria, which account for approximately 96% of bacterial species present.[2] The precise composition of the healthy oral microbiome is difficult to determine as the mouth is an open system and frequently exposed to exogenous factors.[2] The oral cavity can be considered as a major

gateway to the human body.[43] Food enters the mouth and is chewed and mixed with saliva on its way to stomach and intestinal tract for digestion. Air continuously passes through the nose and the mouth on the way to the trachea and lungs. Therefore, microorganisms specific to one area of the oral cavity have a high probability of migrating and spreading on contiguous epithelial surfaces to neighboring sites.[43] Within the oral environment, the highest microbiota richness has been found in gingival plaque and saliva sites, while the lowest richness has been described in the keratinized gingiva.[117] The supragingival or subgingival tooth surfaces provide the most stable environment for bacterial species colonizing in the oral cavity.[114] These non-shedding surfaces are covered by persisting biofilms which represent the earliest colonizers of the teeth[114].

The commensal microbiota plays an important role in maintaining oral and systemic health.[44,113] The presence of commensal microbes in the oral cavity inhibits colonization of pathogens and invading bacteria.[44] Because all surfaces of the mouth are colonized by commensals, there are limited binding sites available for pathogens.[44] While the complex equilibrium between resident species in the oral cavity is responsible for the maintenance of a healthy state, microorganisms within the oral cavity can become disturbed to enter a state of dysbiosis, which can lead to pro-inflammatory oral disease states such periodontal disease.[2]

Antibiotic perturbation of the oral microbiota

The establishment and preservation of a symbiotic relationship with the colonizing commensal microbiota critically supports host health.[14] Extrinsic factors can influence the composition of the commensal microbiota at distinct sites in the human body and ultimately effect overall health.[113] Studies of these microbes in the gut and oral

cavity have uncovered important interactions between bacteria and human hosts in a wide variety of normal and pathological states.[14,118] The commensal microbiota composition and function has been shown to be influenced by variations in host diet, lifestyle, hygiene, or use of antibiotics.[14] Unlike the host genome which is resistant to extrinsic mediators, the microbiome is dramatically impacted by exogenous factors.[14]

The Novince lab has previously demonstrated that antibiotic perturbation of the commensal gut microbiota dysregulates normal osteoimmunological processes at non-oral skeletal sites.[17] A broad-spectrum antibiotic cocktail (ABX) consisting of vancomycin (500mg/L) targeting gram-positive bacteria, imipenem/cilastatin (500mg/L) targeting gram-positive/gram-negative bacteria and anaerobes, and neomycin (1000mg/L) targeting gram-positive/gram-negative bacteria, was employed to broadly disrupt the indigenous gut microbiota.[17,119] Antibiotic treatment was initiated via supplementation of drinking water to male and female C57BL/6T mice from the age of 6 to 12 weeks.[17] The experimental design in this study provided the opportunity to evaluate the antibiotic disruption of the gut microbiota and the secondary osteoimmunomodulatory effects during a critical window of skeletal development.[17]

While ABX treatment reduced the overall gut bacterial load in both male and female mice versus sex-matched vehicle treated mice, bacterial phylum level alterations in the gut microbiota were sex-dependent.[17] ABX treated male mice had increased Proteobacteria and decreased Bacteriodetes, whereas ABX treated female mice had increased Proteobacteria and decreased Bacteriodetes and Firmicutes.[17] Antibiotic disruption of gut microbiota lead to impaired trabecular bone mass and microarchitecture properties.[17] ABX induced a pro-inflammatory hyperimmune response in lymphoid tissues draining the gut, which lead to increased levels of circulating factors that enhanced osteoclastogenesis at distant skeletal sites.[17] The seminal report revealed that

antibiotic disruption of the indigenous gut microbiota has the capacity to dysregulate normal osteoimmune processes at non-oral skeletal sites. Currently unknown, antibiotic perturbation of the indigenous oral microbiota may dysregulate osteoimmune mechanisms in the alveolar bone complex which leads to deleterious effects on periodontal health and homeostasis.

While the majority of studies on antibiotics and the microbiota are focused within the gut, there is emerging research on the effect that antibiotics have on the oral microbiota. Treatment with a broad spectrum antibiotic cocktail (500mg/L ampicillin, 500mg/L vancomycin, and 1g/L metronidazole) has been shown to deplete the resident bacteria in the oral microbiota, which diminished host immune response protective effects and exacerbated oral mucosa tissue destruction.[120] The authors found that the combination of the antibiotics in their experimental treatment diminished salivary short chain fatty acid levels and T_H17 and T_{REG} cells in the oral mucosa, which depleted the host immune response responsible for fungal clearance and reducing inflammation.[120] Other studies on the effect of antibiotics on the oral microbiota have reported that antibiotics such as azithromycin, amoxicillin, clindamycin, and ciprofloxacin affect the amount and diversity of oral microbes.[121,122] Abeles et al. (2016) examined the effects of two commonly prescribed antibiotics, amoxicillin and azithromycin, to discern whether short term antibiotic courses may have prolonged effects on the human commensal microbiota.[122] A significant change in the microbiota diversity was found in the gut and mouth in response to antibiotics, but no analogous patterns were observed in the skin.[122] Amoxicillin treatment for 7 days demonstrated greater reductions in oral microbial diversity compared to treatment duration up to 3 days, which was in contrast to the highly diverse oral microbiota seen at the early time point in subjects treated with azithromycin.[122] The authors concluded that as few of 3 days of treatment with

commonly prescribed antibiotics can result in alterations in oral microbiota diversity, which could have implications for the maintenance of human health and resilience to disease.[122] In a similar study, Zaura et al. (2015) reported that treatment with widely used antibiotics, such as clindamycin and ciprofloxacin, have effects on the oral microbiota.[121] At the one week time point of antibiotic treatment, a microbial shift was observed in saliva samples in response to both clindamycin and ciprofloxacin, resulting in phylum level alterations in Proteobacteria and candidate division TM7.[121] Exposure to clindamycin resulted in the most pronounced and long-lasting change on oral microbial profiles of salivary samples, which remained significant up to 1 month following treatment.[121]

General background on minocycline

Minocycline is a potent, broad spectrum antibiotic within the tetracycline class of antibiotics.[123] Tetracyclines are bacteriostatic antibiotics considered to be broad spectrum due to their activity against a broad range of aerobic and anaerobic gram-positive and gram-negative bacteria.[123] The basic chemical structure of these antibiotics consists of a tetracyclic napthacene carboxamide ring with substituents at different positions.[124] For higher efficiency in these tetracyclines, structural changes have been developed, such as the ring D modification through carbons 7-9 within the semi-synthetic compounds minocycline and doxycycline.[124] The mechanism of action behind the antibiotic properties of minocycline is related to the drug's ability to bind to the bacterial 30S ribosomal subunit and interfere with protein synthesis.[123] Tetracyclines enter bacterial cells through porin channels by coordinating with cations like magnesium and becoming positively charged complexes.[125] This complex enables tetracycline to enter the periplasm and disassociate, which allows a lipophilic tetracycline to diffuse into

bacterial cytoplasm.[125] Tetracyclines are able to prevent aminocyl-tRNA from binding to the 30S ribosome and inhibit protein synthesis in susceptible bacterial microbes.[123,125] Minocycline has been shown to present a better pharmacokinetic profile than its parent, tetracycline, when used orally.[123] Oral minocycline administration allows rapid and complete absorption, a longer half-life, and excellent tissue penetration with almost complete bioavailability.[123] Minocycline is the most frequently prescribed oral antibiotic for the treatment of dermatological conditions in the United States,[126] which highlights the clinical significance of the drug. Minocycline is excreted in high concentrations in the gingival crevicular fluid, and thus has the potential to influence the indigenous oral microbiota.[127]

Tetracyclines present a high affinity for calcified tissues as they are able to bind to calcium and form a tetracycline-calcium orthophosphate complex, which can be deposited and persistent in osteogenic regions of bone.[127] As the rate of mineralization increases, the more tetracycline can become deposited in bone.[128] These agents have also been shown to remain in ossification zones for relatively long periods of time after systemic administration.[128] As minocycline is absorbed, minocycline becomes bound to plasma proteins and is distributed to various tissues in the human body through blood supply.[129] Within these tissues, the antibiotic can then become oxidized and transformed to a pigmented byproduct.[129] Minocycline has been reported to cause pigmentation in a variety of tissues, such as skin, thyroid, nails, teeth, tongue, and bone.[130-132] Minocycline pigmentation of bone is termed “black bone disease” and has been evident in a number of cases presenting within the oral cavity.[131]

Minocycline has intriguingly been shown to exhibit anti-apoptotic, immunosuppressive and anti-inflammatory properties in several pathological conditions, including acne vulgaris, periodontitis (Arestin), rheumatoid arthritis, neural ischemic

damage, Parkinson's disease, and Huntington disease.[133-136] A rheumatoid arthritis study reported that $CD4^+$ T-cells derived from the synovium of diseased patients were altered by minocycline treatment. Minocycline disrupted activated T-cell-induced proliferation and inflammatory cytokine production, which suggests that minocycline has immunomodulatory effects on human cloned synovial T-cells.[136]

Minocycline is a potent, broad spectrum antibiotic that has a high affinity for the bone matrix and reported biological actions independent of their antimicrobial activity, which underscores the need to advance our understanding of the relationship between minocycline, the oral microbiota, and osteoimmunology. This study will begin to delineate the impact that oral antibiotic administration has on the periodontal immune response and alveolar bone remodeling processes. The application of novel osteoimmunology research techniques in the alveolar bone complex will provide mechanistic insight into antibiotic effects on osteoimmune mechanisms that critically regulate periodontal health and homeostasis.

CHAPTER 2: MATERIALS AND METHODS

Specific-Pathogen-Free (SPF) Mice

Five-week-old murine-pathogen-free C57BL/6T mice were purchased from Taconic Biosciences (Rensselaer, NY) and housed under SPF conditions at Medical University of South Carolina (MUSC). Antibiotic cocktail (ABX) treatment model: Male mice were administered a broad spectrum antibiotic cocktail [vancomycin (500mg/L), imipenem/cilastatin (500mg/L), neomycin (1 g/L)] or vehicle control in drinking water from age 6 weeks to 12 weeks; animals were euthanized at age 12 weeks. Minocycline (MINO) treatment model: Sex-matched male / female mice were administered minocycline [100mg/L] or vehicle control in drinking water from age 6 weeks to 12 weeks; animals were euthanized at age 12 weeks and at age 18 weeks. Mice were euthanized by terminal cardiac blood draw following profound anesthesia, which was achieved through intraperitoneal injection of ketamine (100mg/mL) and xylazine (20mg/mL). All work with mice was approved by the MUSC Animal Protocols Review Board and was performed in accordance with the National Institute of Health Guide for Care and Use of Laboratory Animals.

Germ-Free (GF) Mice

GF C57BL/6T mice were acquired from Taconic Biosciences (Rensselaer, NY). GF mice were bred and maintained in sterile isolators at MUSC Gnotobiotic Animal Core. Minocycline (MINO) treatment model: Male mice were administered minocycline [100mg/L] or vehicle control in drinking water from age 6 weeks to 12 weeks; animals were euthanized at age 12 weeks. Mice were euthanized by terminal cardiac blood draw following profound anesthesia, which was achieved through intraperitoneal injection of ketamine (100mg/mL) and xylazine (20mg/mL). All work with mice was approved by the

MUSC Animal Protocols Review Board and was performed in accordance with the National Institute of Health Guide for Care and Use of Laboratory Animals.

Micro-CT

Isolated maxillae and mandibles were fixed in 10% phosphate-buffered-formalin for 24 hours at room temperature and thereafter stored in 70% ethanol. Specimens were scanned with Scanco Medical μCT 40 Scanner, using the following acquisition parameters: X-ray tube potential = 70 kVp; X-ray intensity = 114 μA; Integration time = 200 ms; Isotropic voxel size = 10 μm^3. Calibrated three-dimensional images were reconstructed for analyses. A fixed threshold of 1250 Hounsfield units was utilized to determine mineralized bone tissue for morphometric analysis.

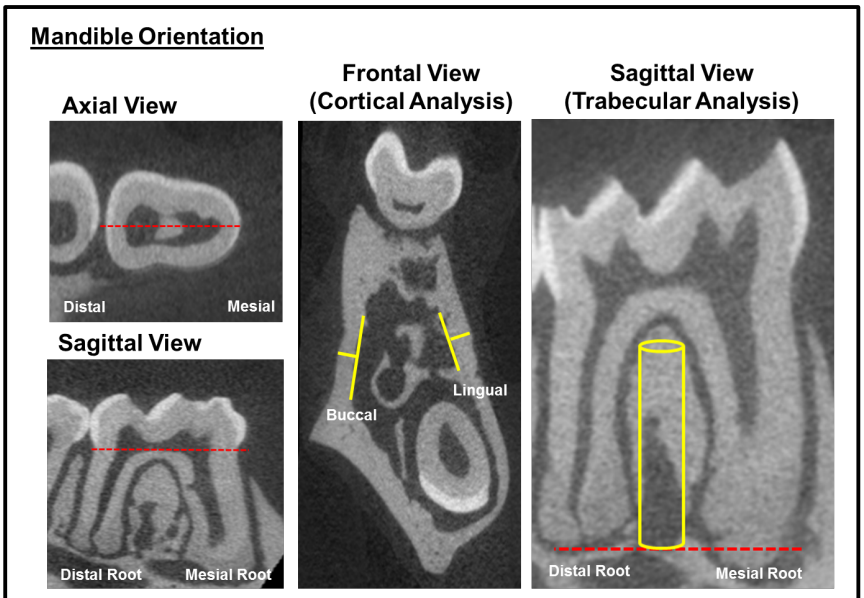

Figure 2: Mandible Orientation for Micro-CT Analysis

Cortical and trabecular alveolar bone morphology was assessed in the bifurcation of the mandibular first molar using AnalyzePro Analysis software (Analyze Direct, Seattle, WA). Each specimen was consistently oriented before determining the

region of interest (ROI) for cortical analysis and the volume of interest (VOI) for trabecular analysis **(Figure 2)**. The mandibular first molar was oriented in the axial plane such that the mid-buccal lingual aspects of the mesial and distal roots were aligned to a horizontal plane at 0 degrees. The first molar was oriented in the sagittal plane such that the CEJ at the mesial and distal aspect of the tooth were aligned to a horizontal plane at 0 degrees **(Figure 2)**.

Alveolar bone cortical thickness was assessed in a 200μm mesial-distal ROI, at both the buccal cortical plate and lingual cortical plate, within the bifurcation of the mandibular first molar. The ROI was centered at the midpoint between the mesial and distal roots in the axial view. Cortical thickness was assessed in a 100 μm (10 slices) region mesial to the midpoint and a 100μm (10 slices) region distal to the midpoint. Buccal cortical plate measurements were performed via drawing a perpendicular line from the endocortical surface to the periosteal surface of the buccal cortical plate. Lingual cortical plate measurements were performed via drawing a perpendicular line from the endocortical surface to the periosteal surface of the lingual cortical plate **(Figure 2)**. Outcomes reported include buccal cortical thickness, lingual cortical thickness, and an average of the two sites of interest. Data are reported in accordance with standardized nomenclature.[137]

Alveolar bone trabecular bone volume fraction was assessed in a defined volume of interest (VOI), within the bifurcation of mandibular first molar. The VOI was created by linearly morphing a cylinder within the bifurcation, excluding the periodontal ligament lining the mesial and distal roots and the endocortical surface of the buccal and lingual cortical plates **(Figure 2)**. The height of the cylinder was set so that the superior aspect of the cylinder was positioned at the fornix of the bifurcation and the inferior aspect of the cylinder was positioned at the distal root apex **(Figure 2)**. Fixed threshold of 1250

Housnfield units was used in order to discriminate mineralized tissue. Outcomes reported include bone volume per tissue volume. Data are reported in accordance with standardized nomenclature.[137]

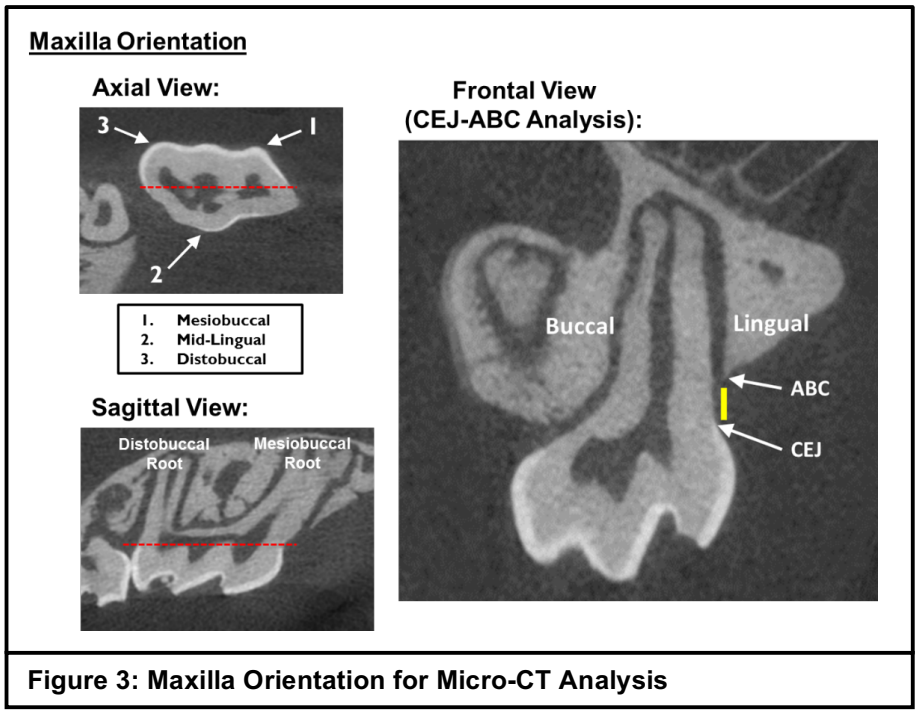

Figure 3: Maxilla Orientation for Micro-CT Analysis

Linear alveolar bone loss was assessed at the maxillary first molar using the AnalyzePro Analysis software (Analyze Direct, Seattle, WA). Linear alveolar bone loss was evaluated by measuring the linear distance from the CEJ to ABC, at the mesiobuccal line angle, distobuccal line angle, and mid-lingual aspect of the maxillary first molar **(Figure 3)**. The CEJ to ABC measurement began at CEJ, the anatomical site where the enamel meets the cementum, and ended at the ABC, the anatomical site where the cortical plates merge with the alveolar bone proper.[138] Reconstructed maxilla images were consistently oriented prior to measuring the CEJ to ABC linear distance at each anatomical line angle **(Figure 3)**. The maxillary first molar was oriented in the axial plane such that the mid-buccal lingual aspect of the mesiobuccal and distobuccal roots

were aligned to a horizontal plane at 0º. The first molar was oriented in the sagittal plane such that the CEJ at the mesial and distal aspect of the tooth were aligned to a horizontal plane at 0 degrees **(Figure 3)**.

Within the axial plane, the coronal height of contour was determined at the mesiobuccal line angle, distobuccal line angle, and mid-lingual aspect of the molar. These landmarks served as the midpoint for carrying out CEJ to ABC linear measurements. 5 total measurements were made at each anatomical site of interest. Measurements were made at the midpoint and +/-10 and +/-20 slices from the midpoint. Outcomes reported for CEJ to ABC analysis consisted of an average of the five measurements performed for each anatomical site of interest. Data are reported in accordance with standardized nomenclature.

Histomorphometry

Maxillae were fixed in 10% phosphate-buffered-formalin for 24 hours at room temperature. Maxillae were then decalcified in 14% ethylenediaminetraacetic acid (EDTA) for 21 days at room temperature and submitted for paraffin embedded histological processing. Sagittal sections were cut through the maxillary first molar. Tartrate-resistant acid phosphatase (TRAP) stain with an aniline blue counterstain was performed for histomorphometric analysis of osteoclast cellular endpoints. Osteoclast were scored lining the alveolar bone within the furcation, which was contained by the mesiobuccal root and distobuccal root. The ROI excluded the periodontal ligament space and the basal bone. TRAP+ multinucleated (three or more nuclei) cells lining the alveolar bone surface within the furcation were considered osteoclasts. Images were acquired at 200x via the Nikon Eclipse TS1000 microscope (Nikon Inc., Melville, NY). Images were stitched using Adobe Photoshop (Adobe, San Jose, CA). Blinded

histomorphometric analysis of TRAP+ osteoclast cellular endpoints was performed using ImageJ software (ImageJ 1.52a, NIH, Bethesda, MD). Stitched maxilla images were analyzed at a set scale of 2.8346 pixels/mm. Osteoclast endpoints include number of osteoclasts per bone perimeter (N.Oc/B.Pm), osteoclast area per osteoclast (Oc.Ar/Oc), and percent osteoclast perimeter per bone perimeter (Oc.Pm/B.Pm). Data are reported in accordance with standardized nomenclature.[139]

Quantitative Real-Time PCR (qRT-PCR) for 16S rDNA Analysis

DNA Extraction: Left maxillary gingiva, right / left mandibular gingiva, and right / left buccal vestibule mucosa were isolated at sacrifice. Mucogingival isolates were flash frozen upon collection and stored at -80°C. Deoxyribonucleic acid (DNA) was extracted from mucogingival isolates using the DNEasy Powersoil Pro Kit (Qiagen, Hilden, Germany). Manufacture's protocol was modified to include additional homogenization steps, in order to increase the quantity of eluted DNA.

PowerBead Pro tubes were briefly spun down. The mucogingival isolates were weighed and delivered to the tubes for homogenization. Optimized homogenization steps were performed as follows: 1) Solution CD1 was added to the PowerBead Pro tube and vortexed for 10 minutes. 2) Using sterile sharp tweezers and 1000ul pipette, the samples were homogenized by clamping and pulverizing the isolates against the bottom of the PowerBead Pro tube within the CD1 solution. 3) An additional vortex for 5 minutes was required to complete the homogenization. Thereafter, DNA extraction continued following the manufacturer's protocol. Genomic DNA was eluted and stored at -20°C for downstream applications.

DNA Quantification: Total DNA was quantified via NanoDrop 1000 (Thermo Scientific, Waltham, MA). DNA was read on a spectrophotometer to determine

concentration of DNA in ng/μL and purity of DNA at absorbance wavelength ratio of 260/280nm. Genomic DNA was then used for 16S rDNA qRT-PCR analysis evaluating alterations in total bacterial load (universal primer) and bacterial phyla (phylum specific primers).

16S rDNA Primers: Forward / Reverse primer sequences are reported in **Table 2**. All primers were ordered from Integrated DNA Technology (Integrated DNA Technologies, Carolville, IA) and were reconstituted at a concentration of 100uM.

Table 2: 16S rDNA Primer Sequences	
Bacterial gene target	Primer sequence
Universal 16S[140]	F: 5'- AAACTCAAAKGAATTGACGG -3' R: 5'- CTCACRRCACGAGCTGAC -3'
α-Proteobacteria[140]	F: 5'- CIAGTGTAGAGGTGAAATT -3' R: 5'- CCCCGTCAATTCCTTTGAGTT -3'
γ-Proteobacteria[140]	F: 5'- TCGTCAGCTCGTGTYGTGA -3' R: 5'- CGTAAGGGCCATGATG -3'
Actinobacteria[140]	F: 5'- TACGGCCGCAAGGCTA -3' R: 5'- TCRTCCCCACCTTCCTCCG -3'
Bacteroidetes[140]	F: 5'- CRAACAGGATTAGATACCCT -3' R: 5'- GGTAAGGTTCCTCGCGTAT -3'
Firmicutes[140]	F: 5'- TGAAACTYAAAGGAATTGACG -3' R: 5;- ACCATGCACCTGTC -3'
Fusobacteria[141]	F: 5'- GGATTTATTGGGCGTAAAGC -3' R: 5'- GGCATTCCTACAAATATCTACGA -3'
Spirochaetes[2]	F: 5'- GAGAGTTTGATYCTGGCTCA -3' R: 5'- GTTACGACTTCACCCTCCT-3'

16S rDNA qRT-PCR: Genomic DNA (gDNA) was amplified via the StepOnePlus System (Applied Biosystems, Foster City, CA), SYBR Green Fast Master Mix (Applied Biosystems), forward / reverse primers **(Table 2)**. A 20 μL PCR reaction was performed using 10 μL of SYBR Master Mix (2x), 6.4 μl of primers (800nM/uL), and 3.6 μL of sample gDNA (5ng/uL). PCR samples were subjected to a 40-cycle thermocycler protocol using the StepOnePlus System (Applied Biosystems). Cycle number 30 was

used as the cutoff for non-specific amplification. Initial denaturing step at 95°C for 5 min, followed by 40 cycles of 95°C for 15 min, 61.5°C for 15 min, 72°C for 20 min, ending with a final elongation step of 72°C for 5 min.[140] Relative quantification of DNA was performed via the comparative CT method ($2^{-\Delta\Delta CT}$).[142] Universal 16S outcomes are reported relative to 12.5ug/uL of a bacterial DNA standard ladder (Microbial Community DNA Standard; 200ng/Catalog Nos. D6306) (ZymoBIOMICS, Irvine, CA) for overall bacterial load analysis. Phylum level outcomes were normalized to the Universal 16S gene, and are reported as relative expression. Specimens were run in triplicate (3 technical replicates). Technical replicates were subjected to a Grubbs outlier analysis test (α=0.05). Biological replicates were subjected to a ROUT outlier analysis test (Q=0.5%). Replicates determined as outliers were excluded from analysis.

qRT-PCR for mRNA Analysis

Mandible Bone Marrow (MBM) Isolation: Mandibles were hemisected at the midline, and bone marrow was isolated from the right / left mandibular ramus. A 27G x 1/2" hypodermic needle (Becton Dickinson, Franklin Lakes, NJ) attached to a 1ml syringe was rotated through the buccal cortical plate inferior to the midpoint between the articular surface and coronoid process and superior to the incisor canal space. The MBM from each animal was flushed with 1.0ml of TRIzol (Invitrogen, Carlsbad, CA, USA), and banked at -80° for subsequent processing.

Gingiva Homogenization: Gingiva isolates from each animal were submerged in 1.0ml of TRIzol reagent, and banked at -80° for subsequent processing. Gingival isolates were thoroughly homogenized in TRIzol reagent prior to performing the RNA extraction. Each isolate was subjected to vortexing, followed by thorough homogenization with a 1000uL pipette.

RNA Extraction (TRIzol Method): RNA extraction of the MBM and gingival isolates were performed using TRIzol (Invitrogen, Carlsbad, CA, USA) extraction method via Phasemaker Separation Tubes, following manufacturer's protocol.

Quantify RNA and cDNA Synthesis: Total RNA was quantified via NanoDrop 1000 (Thermo Scientific). Complementary deoxyribonucleic acid (cDNA) was synthesized from RNA isolates using Taqman Random Hexamers and Reverse Transcription Reagents (Applied Biosystems, Foster City, CA), according to manufacturer's protocol.

Table 3: qRT-PCR Primer-Probes

Gene target	Taqman Primer-Probe
Il1b	Mm00434228_m1
Il6	Mm00446190_m1
Il17a	Mm00439618_m1
Tnf	Mm00443258_m1
Ifng	Mm00439560_m1
S100a8	Mm00496696_g1
S100a9	Mm00656925_m1
Tnfsf11 (Rankl)	Mm00441908_m1
Tnfrsf11b (Opg)	Mm00435451_m1
Dcstamp	Mm04209236_m1
Gapdh	Mm99999915_g1

qRT-PCR gene expression analysis: Synthesized cDNA was amplified via the StepOnePlus System (Applied Biosystems) protocol, using TaqMan Fast Advanced qPCR Master Mix and TaqMan gene expression primer probes **(Table 3)**. A 20 µL PCR reaction was performed using 10 µL of Taqman MM (2x), 1 µL of primer probes (20x), 2 µL of sample cDNA (10x), and 7 µL of RNase free water. PCR samples were then subjected to a 40-cycle thermocycler protocol using the StepOnePlus System (Applied Biosystems); 50°C for 2 minutes, 95°C for 2 minutes, followed by 40 cycles of 95°C for 1

second, 60°C for 20 seconds. Relative quantification of mRNA was performed via the comparative CT method ($2^{-\Delta\Delta CT}$)[142]; *Gapdh* was utilized as an internal control gene.

Flow Cytometric Analysis

Live Cell Analysis: MBM and CLN cells were isolated, washed, and counted. Live cells were resuspended at 100,000 cells/50uL in FACS-buffer. Cells were treated with FcR-block (Miltenyi Biotec, Bergisch Glabach, Germany) and cell specific stains were performed **(Table 4)**. Dead cells were excluded from analysis by labelling with propidium iodide viability dye (Miltenyi Biotec). Data was acquired by the MACSQuant System (Miltenyi Biotec). Analyses were performed via FlowJo VX software (TreeStar).

Table 4. Flow Cytometry Live Cell Analysis				
Immune Cell	Antibody	Fluorescent Tag	Clone	Vendor
Neutrophils	$CD11b^+$ $Ly6C^-$ $Ly6G^+$	APC FITC VB	REA592 REA796 1A8	Milltenyi Biotec
Monocytes	$CD11b^+$ $Ly6G^-$ $F4/80^+$ $Ly6C^+$	APC VB PE FITC	REA592 1A8 REA126 REA796	Milltenyi Biotec
M1 Macrophages	$CD11b^+$ MHC II^+ $CD64^+$	APC FITC APC-Vio770	REA592 REA528 REA286	Milltenyi Biotec
M2 Macrophages	$CD11b^+$ MHC II^+ $CD64^-$ $CD206^+$	APC FITC APC-Vio770 PE	REA592 REA528 REA286 MR6F3	Milltenyi Biotec
Plasmacytoid DCs	$CD11c^+$ $B220^+$ MHC II^{lo}	PE-Vio770 VB FITC	REA754 REA755 REA528	Milltenyi Biotec
Conventional DCs	$CD11c^+$ $CD11b^-$ $B220^-$ MHC II^+	PE-Vio770 APC VB FITC	REA754 REA592 REA755 REA528	Milltenyi Biotec
$CD4^+$ Helper T-Cells	$CD3^+$ $CD8^-$ $CD4^+$	PE-Vio770 PE VB	REA641 REA601 REA604	Milltenyi Biotec
Naïve $CD4^+$ T-cells	$CD3^+$ $CD8^-$ $CD4^+$ $CD62L^+$ $CD69^-$	PE-Vio770 PE VB FITC APC	REA641 REA601 REA604 REA828 H1.2F3	Milltenyi Biotec
Activated $CD4^+$ T-cells	$CD3^+$ $CD8^-$ $CD4^+$ $CD62L^-$ $CD69^+$	PE-Vio770 PE VB FITC APC	REA641 REA601 REA604 REA828 H1.2F3	Milltenyi Biotec
$CD8^+$ Cytotoxic T-Cells	$CD3^+$ $CD4^-$ $CD8^+$	PE-Vio770 VB PE	REA641 REA604 REA601	Milltenyi Biotec
Naïve $CD8^+$ T-cells	$CD3^+$ $CD4^-$ $CD8^+$ $CD62L^+$ $CD69^-$	PE-Vio770 VB PE FITC APC	REA641 REA604 REA601 REA828 H1.2F3	Milltenyi Biotec
Activated $CD8^+$ T-cells	$CD3^+$ $CD4^-$ $CD8^+$ $CD62L^-$ $CD69^+$	PE-Vio770 VB PE FITC APC	REA641 REA604 REA601 REA828 H1.2F3	Milltenyi Biotec

Transcription Factor Analysis: MBM and CLNs cells were isolated, washed, and counted. Cells were re-suspended at 100,000 cells/50uL in FACS-buffer. Cells were treated with FcR-block (Miltenyi Biotec), and labeled with cell surface markers for 30 minutes. Intracellular stains were carried out following the fixation-permeabilization buffer manufacturer's protocol (eBioscience, Santa Clara, CA).

Fixation/Permeabilization: Cells were washed with phosphate-buffered saline (PBS) and centrifuged for 5 minutes at 1,500 RPM at 4°C. The supernatant was aspirated and this process was repeated for 3 washes. eFlour 780 viability dye (eBioscience) was added to the cells and incubated at 4°C for 30 minutes, to exclude dead cells. Following incubation, cells were washed twice via: FACS buffer added, centrifuged for 5 minutes at 1,500 RPM at 4°C, and supernatant was aspirated. Then the fixation permeabilization solution (1 part eBioscience fixation / permeabilization concentrate + 3 parts eBioscience fixation / permeabilization diluent) was added to the cells and plates were incubated overnight, protected from light at 4°C. The next morning, two washes were performed with permeabilization buffer, centrifuged for 5 minutes at 1,500 RPM at 4°C, and supernatant was aspirated. Samples were resuspended in permeabilization buffer. The cells were incubated with intracellular antibodies for 30 minutes at room temperature, protected from light. Two washes were carried out with permeabilization buffer. The samples were resuspended in FACS buffer to run for analysis. Data was acquired by the MACSQuant System. Analyses were performed via FlowJo VX software.

T_{REG} cells: anti-CD3-APC-Vio770 (Miltenyi Biotec, clone REA641), anti-CD4-FITC (Miltenyi Biotec, clone REA604), anti-CD25-PE-Vio770 (Miltenyi Biotec, clone 7D4), anti-FoxP3-PE (Miltenyi Biotec, clone REA788).

- T_{REG} Cells: $CD3^+CD4^+CD25^+FoxP3^+$ (% $CD3^+CD4^+$ cells)

T_H1 cells: anti-CD3-PE-Vio770 (Miltenyi Biotec, clone REA641), anti-CD4-FITC (Miltenyi Biotec, clone REA604), anti-CD183-PE (Miltenyi Biotec, clone CXCR3-173), anti-T-bet-APC (Miltenyi Biotec, clone REA102).

- T_H1 Cells: $CD3^+CD4^+CD183^+T\text{-}BET^+$ (% $CD3^+CD4^+$ cells)

T_H17 / T_H22 cells: anti-CD3-APC-Vio770 (Miltenyi Biotec, clone REA641), anti-CD4-FITC (Miltenyi Biotec, clone REA604), anti-CD196-PE (Miltenyi Biotec, clone REA277), anti-RORγt-APC (Miltenyi Biotec, clone REA278), anti-AHR-PE-Vio770 (eBioscience, clone 4MEJJ).

- T_H17 Cells: $CD3^+CD4^+CD196^+ROR\gamma t^+AHR^-$ (% $CD3^+CD4^+$ cells)
- T_H22 Cells: $CD3^+CD4^+CD196^+ROR\gamma t^-AHR^+$ (% $CD3^+CD4^+$ cells)

In Vitro Osteoclast Assays

Right and left mandible marrow were flushed with 1mL a-MEM media, 10% FBS (Hyclone), 1% PSG utilizing a 27G needle and 1ml syringe and plated in a 48 well plate. Whole marrow cultures were incubated overnight. The following morning, non-adherent hematopoietic cells were isolated for *in vitro* osteoclastogenesis assays. Cells were plated in 96 well plates and primed for 36 hours in a-MEM media, 10% FBS (Hyclone), 1% PSG, supplemented with 10ng/mL CSF1 (R&D Systems, Minneapolis, MN). Cultures were subsequently stimulated with control (25ng/ml CSF1 and 50 ng/mL RANKL; R&D Systems) or minocycline treatment (0.125ug/ml minocycline (Sigma-Aldrich, St. Louis, MO), 25 ng/mL CSF1, and 50ng/mL RANKL). The media was changed every other day for 6 days. Day 6 control and treatment cultures were stained via the TRAP method. Images were acquired at 100x magnification via a Nikon Eclipse TS100 microscope. TRAP stain assay was carried out in triplicate (technical replicate) culture wells; four images per sample were methodically acquired in the same locations within the culture

wells. The image locations were designated at north/south/east/west and accounted for 0.166cm^2 of the 0.32 cm^2 total surface area per well. Osteoclast cellular outcomes (TRAP+ cells with 3 nuclei were scored as osteoclasts) were evaluated within four fields of view per well at 100x magnification. Cytomorphometric analysis of TRAP+ osteoclast cells was performed using ImageJ software, version 1.51a, (NIH, Bethesada, MD, USA). Osteoclast outcomes included number of osteoclasts (N.Oc), average osteoclast area (Oc.Ar/Oc), and nuclei number per osteoclast (N.Nc/Oc).

Faxitron Micro-Radiographs / Gross Clinical Photos

Isolated mandibles were fixed in 10% phosphate-buffered-formalin for 24 hours at room temperature and then stored in 70% ethanol. Two-dimensional X-ray images were acquired using a Faxitron Microradiograph (Faxitron LX-60, Faxtiron X-ray Corporation, Tucson, Arizona) for qualitative radiographic analysis. Mandibles specimens were oriented uniformly with the buccal aspect facing down; X-ray exposure time was 40 seconds with an X-ray beam energy of 36 kV. The micro-radiographs were developed using a Medical Film Processor (Konica SRX-101A, Konica Minolta Medical & Graphic, Inc., NJ, USA). Gross clinical photos were acquired using an Olympus SZ61 Compact Stereo Microscope (Olympus Life Sciences, Waltham, Massachusetts) with an Infinity 2 camera (Version 5.0.3, Lumenera Corporation, Ottawa, Canada) and Infinity Analyze imaging software (Lumenera).

Statistical Analysis

Unpaired t tests were performed using Graphpad Prism 8.0 (GraphPad, La Jolla, CA, USA). Data are presented as mean ± SEM. Significant is indicated as *$p < 0.050$,

**p < 0.010, ***p < 0.001. Power analysis consultation was carried out with the Biostatistical Unit of the Medical University of South Carolina Bioinformatics Core.

CHAPTER 3: RESULTS

3.1 Aim 1 Results

Studies investigating the commensal microbiota's role in immunity have shown that microbial communities at tissue-specific sites play important roles in prompting the immune system, which can have secondary effects on tissue homeostasis. The commensal oral microbiota is an emerging topic in osteoimmmunology research and has recently been shown to play a key role in regulating alveolar bone homeostasis in the healthy periodontium.[5,6,67,76]

Previous studies in the Novince Research Lab have shown an association between the antibiotic perturbation of gut microbiota and dysregulated bone modeling/remodeling at non-oral skeletal sites.[17] To broadly disrupt the indigenous gut microbiota, a broad spectrum antibiotic cocktail was orally administered to C57BL/6T sex-matched mice from 6 weeks of age until euthanization at age 12 weeks.[17] 16S rDNA qRT-PCR analysis revealed that antibiotic perturbation of indigenous gut microbiota had sex dependent effects on the composition of bacterial communities at the phyla level.[17] Male antibiotic treated mice were found to have higher levels of α-Proteobacteria and γ-Proteobacteria communities and lower levels of Bacteriodetes, while female antibiotic treated mice showed increases in α-Proteobacteria and decreases in Bacteriodetes and Firmicutes communities.[17] Furthermore, micro-CT analysis showed that antibiotic disruption of gut microbiota induced sex dependent tissue level alterations in bone mineral density and trabecular bone morphology at non-oral skeletal sites.[17]

Irie, Novince, and Darvaeu (2014) have shown that the commensal oral microbiota has an impact on alveolar bone homeostasis.[76] Utilizing the specific-pathogen-free (SPF) vs. germ-free (GF) mouse model, this investigation began to elucidate osteoimmune mechanisms regulating the oral microbiota's impact on alveolar

bone homeostasis during health.[76] Through histomorphometric analysis of the distance from CEJ to ABC, the commensal bacteria were shown to increase linear alveolar bone loss in the maxillary molars of SPF vs. GF mice.[4] This was the first known histomorphometric study to discern upregulated osteoimmune mechanisms and exacerbated alveolar bone loss SPF vs. GF mice.[76]

Tsukasaki et al. (2018) have recently shown that bone damaging T-cells impact the host defense against oral microbiota by regulating protection against bacterial infection and induction of bone destruction in the oral cavity.[67] In this periodontitis model, silk ligature placement around the maxillary second molar lead to an accumulation of oral bacteria, which caused inflammation and bone destruction.[67] Utilizing 16S sequence analysis, the total amount of bacterial DNA was increased and the composition of oral bacteria was altered in Il17a-/-Il17f-/- double knockout mice.[67] These results suggest that T_H17 cells play a key role in the host defense against invasion of oral bacteria through the induction of alveolar bone loss.[67]

Considering the previous studies from the Novince lab investigating antibiotic perturbation of the gut microbiota[17] and the oral commensal microbiota impact on alveolar bone loss,[4-6,67] the oral microbiota composition and linear alveolar bone loss were evaluated in response to treatment with an oral antibiotic therapy, specifically minocycline.

Aim 1: Evaluate the persistence of minocycline induced changes in the oral microbiome and alveolar bone homeostasis.

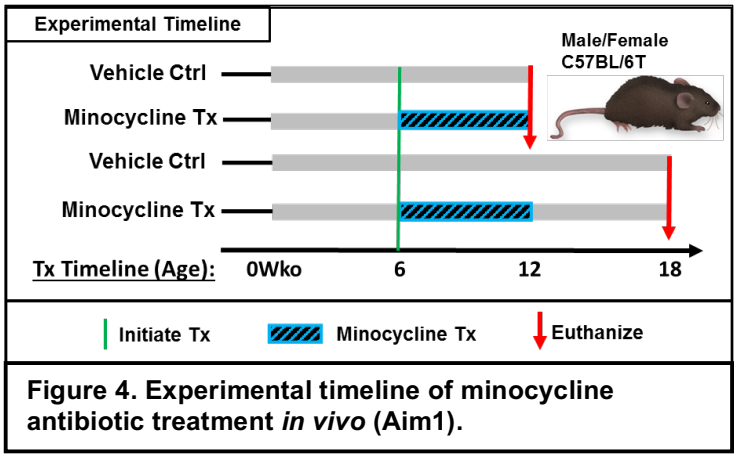

Figure 4. Experimental timeline of minocycline antibiotic treatment *in vivo* (Aim1).

Minocycline or vehicle control treatment was supplemented to the drinking water of sex-matched C57BL/6T SPF mice from age 6 to 12 weeks **(Figure 4)**. Minocycline *in vivo* treatment was orally administered in drinking water at a clinically relevant dose of 100mg/L**.** Based on the human pediatric dosage of minocycline prescribed per day to adolescents for treatment of acne (2.0mg/kg), the mouse equivalent dosage of minocycline treatment is 24.6mg/kg.[143] Based on a 20g mouse, the amount of minocycline the mice would receive per day is 0.492 mg (0.02kg mouse x 24.6mg/kg). On average, a mouse consumes 4.92 mL of water per day, thus the concentration of minocycline in drinking water to receive a human equivalent dosage is 0.1mg/mL (100mg/L).[144] Treatment was initiated at the age of 6 weeks, the developmental age when C57BL/6T mice immune system is considered mature.[145,146] Also at the 6-week time point, the murine teeth have fully erupted and alveolar bone formation is considered complete.[33,147] Mice were euthanized at 12 weeks of age to assess the immediate impact of minocycline treatment effects on the oral microbiome and alveolar bone homeostasis. Other groups of mice were taken off minocycline treatment at 12 weeks of age, and

aged to 18 weeks to allow for a 6-week recovery period of no antibiotic treatment **(Figure 4)**. Mice were euthanized at 18-weeks of age to assess persistent minocycline effects on the oral microbiome and alveolar bone homeostasis. This experimental model provides the opportunity to evaluate sex-dependent alterations and the persistence of minocycline treatment effects on the oral microbiome and alveolar bone homeostasis **(Figure 4)**.

16S rDNA qPCR analysis of gingival isolates was performed to determine minocycline perturbation of overall bacterial load and phylum level alterations in the oral bacteriome, in male **(Figure 5)** and female mice **(Figure 6)**. MINO vs. VEH treatment caused a 20X fold increase in total bacterial load **(Figure 5a)** and caused phylum level alterations **(Figure 5b)** in male mice at age 12-weeks immediately following 6 weeks MINO treatment. 12-week-old male MINO vs. VEH mice demonstrated a significant increase in Proteobacteria, a significant decrease in Firmicutes, and a trending decrease in Actinobacteria bacteria communities **(Figure 5b)**. MINO vs. VEH treatment caused a sustained disruption of the oral microbiota at age 18 weeks, following the 6-week window of recovery after the withdrawal of minocycline treatment **(Figure 5c-d)**. While there was no difference in the overall bacterial load **(Figure 5c)**, 18-week-old male MINO vs. VEH mice demonstrated significant increases in Actinobacteria and Firmicutes bacteria communities **(Figure 5d).**

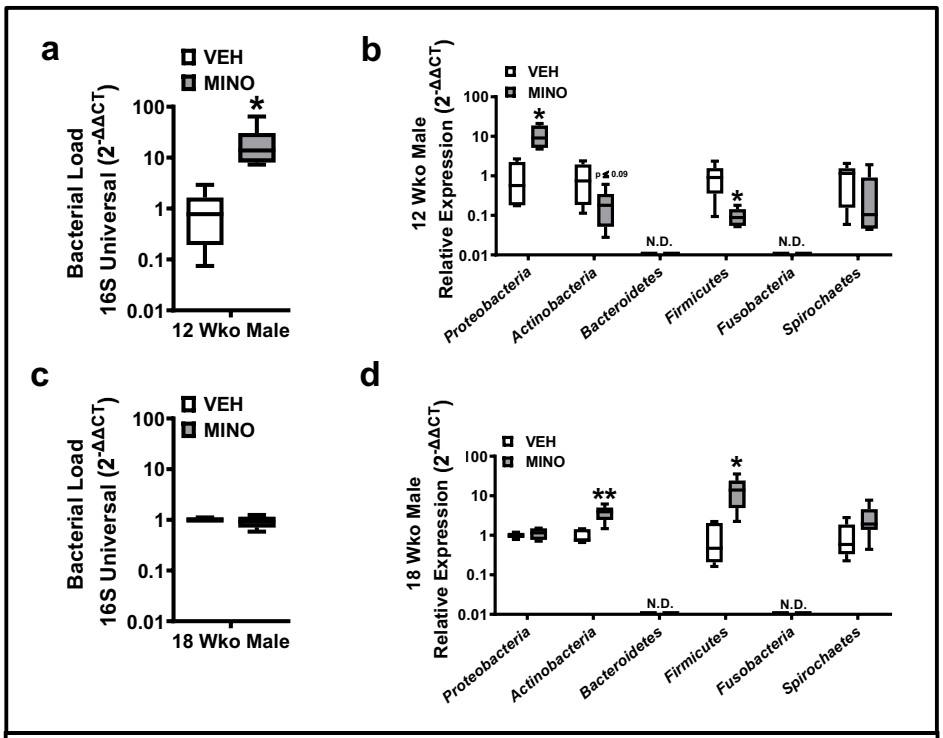

Figure 5: Minocycline (MINO) perturbation of oral microbiota composition in male mice. (a-d) 16S rDNA analysis of gingival isolates. (a,c) Universal 16S gene analysis for total bacterial load in (a) 12-week-old and (c) 18-week-old male mice; reported relative to 12.5ng/ul DNA Standard via the comparative CT method ($2^{-\Delta\Delta CT}$). (c-d) Phylum-level gene analysis in (b) 12-week-old and (d) 18-week-old male mice; reported relative to universal 16S gene expression via the comparative CT method (2-ΔΔCT). Unpaired t-test statistical analysis was used. Data are expressed as mean ± SEM. (n=5-6/pg) *p<0.05 vs. VEH. **p<0.01 vs. VEH. ***p<0.001 vs. VEH.

Overall bacterial load and phylum level alterations in MINO vs. VEH treated mice were sex dependent **(Figure 6)**. Contrary to male mice, 12-week-old female MINO vs. VEH mice showed no differences in overall bacterial load **(Figure 6a)** or phylum level alterations **(Figure 6b)**. Demonstrating that minocycline continued to have no effect on the oral microbiota of female mice after withdrawal of antibiotic treatment, 18-week-old female MINO vs. VEH mice also showed no differences in overall bacterial load **(Figure 6c)** or phylum level alterations **(Figure 6d)**.

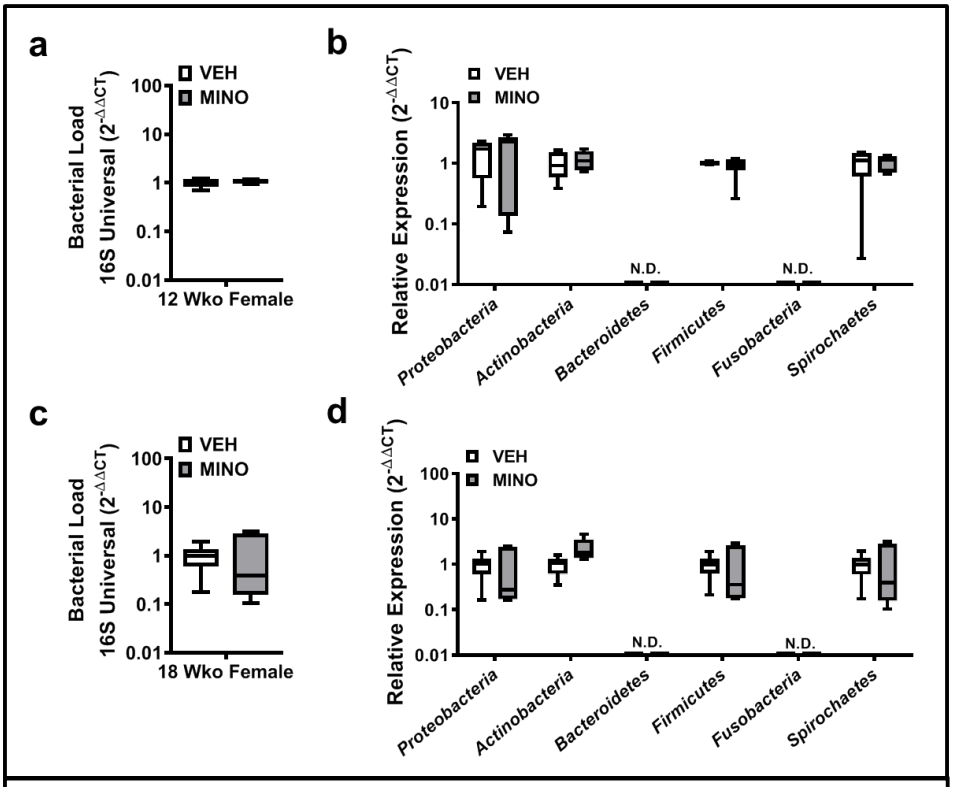

Figure 6: Minocycline (MINO) perturbation of oral microbiota composition in female mice. (a-d) 16S rDNA analysis of gingival isolates. (a,c) Universal 16S gene analysis for total bacterial load in (a) 12-week-old and (c) 18-week-old female mice; reported relative to 12.5ng/ul DNA Standard via the comparative CT method ($2^{-\Delta\Delta CT}$). (b,d) Phylum-level gene analysis in (b) 12-week-old and (d) 18-week-old female mice; reported relative to universal 16S gene expression via the comparative CT method (2-ΔΔCT). Unpaired t-test statistical analysis was used. Data are expressed as mean ± SEM. (n=5-6/pg) *p<0.05 vs. VEH.

Micro-CT analysis of linear alveolar bone loss was executed in the maxillary first molar of male and female mice **(Figure 7-8)**. Linear measurements assessing the distance from CEJ to ABC were made at the mesiobuccal, mid-lingual, and distobuccal line angles. Male MINO vs. VEH treatment demonstrated an increase in linear alveolar bone loss at all three anatomic landmarks at age 12 weeks **(Figure 7a,c)**. At the 18-week time point in male mice, minocycline-induced alveolar bone loss was sustained after the 6-week window of recovery following the withdrawal of antibiotic treatment. The sustained increase in alveolar bone loss was found at the mesiobuccal and mid-lingual line angle of the maxillary first molar, in 18-week-old male MINO vs. VEH treated mice **(Figure 7b,d)**.

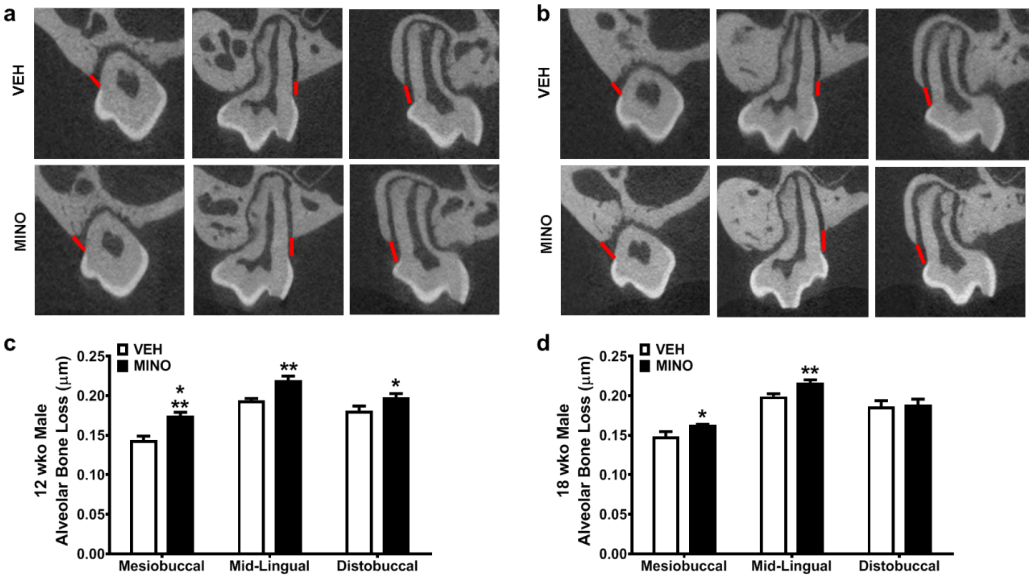

Figure 7: Minocycline (MINO) effects on linear alveolar loss bone in male mice. 12-week-old and 18-week-old, male VEH vs. MINO mice were euthanized and maxillae were harvested for micro-CT analysis. (a-d) Linear alveolar bone loss was assessed in the maxillary first molar via measurements of the distance from the CEJ-ABC at mesiobuccal, mid-lingual, and distobuccal line angles. (a-b) Representative images of CEJ-ABC measurements at mesiobuccal, mid-lingual, and distobuccal line angles in 12-week-old (a) and 18-week-old (b) male mice. (c) Alveolar bone loss outcomes in 12-week-old male mice. (d) Alveolar bone loss outcomes in 18-week-old male mice. Unpaired t-test statistical analysis was used. Data are reported as mean ± SEM. *p<0.05 vs. VEH. **p<0.01 vs. VEH. ***p<0.001 vs. VEH.

MINO vs. VEH treatment demonstrated an increase in linear alveolar bone loss, specifically at the mesiobuccal and mid-lingual line angles, in 12-week-old female mice **(Figure 8a,c)**. At the 18-week time point in female mice, minocycline-induced alveolar bone loss was sustained after the 6-week window of recovery following the withdrawal of antibiotic treatment. MINO vs. VEH treatment demonstrated a sustained increase in alveolar bone loss, specifically at the mesiobuccal line angle, in 18-week-old female mice **(Figure 8b,d)**. While no differences were detected at the distobuccal line angle at the 12-week time point, an increase in alveolar bone loss was seen at this anatomical site in the 18-week-old female mice **(Figure 8b,d)**.

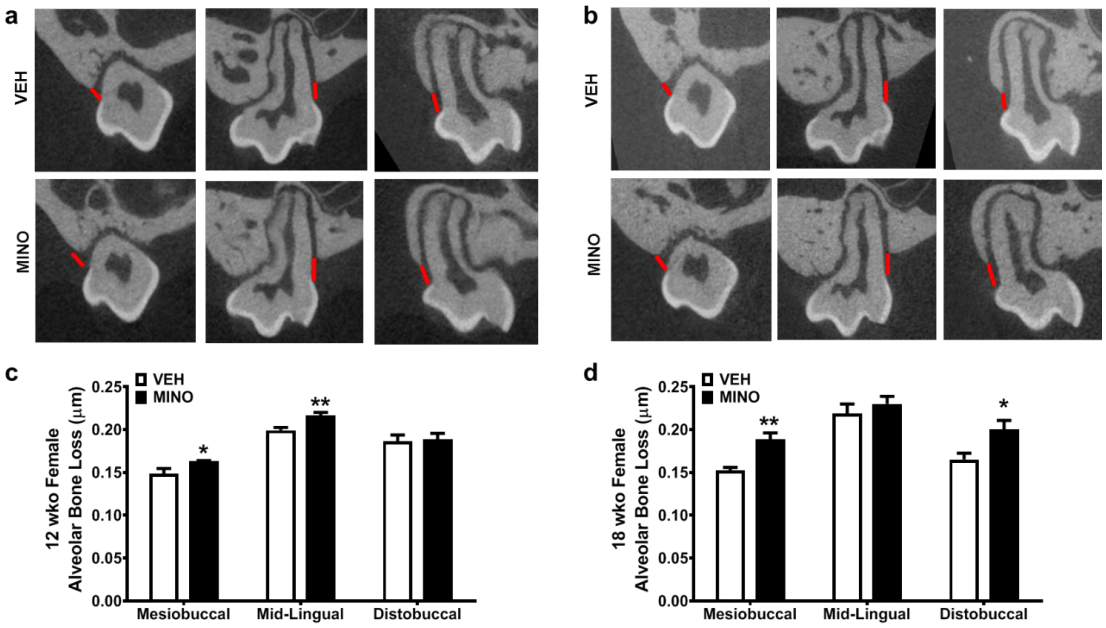

Figure 8. Minocycline (MINO) effects on linear alveolar bone loss in female mice. 12-week-old and 18-week-old, female VEH vs. MINO mice were euthanized and maxillae were harvested for micro-CT analysis. (a-d) Linear alveolar bone loss was assessed in the maxillary first molar via measurements of the distance from the CEJ-ABC at mesiobuccal, mid-lingual, and distobuccal line angles. (a-b) Representative images of CEJ-ABC measurements at mesiobuccal, mid-lingual, and distobuccal line angles in 12-week-old (a) and 18-week-old (b) female mice. (c) Alveolar bone loss outcomes in 12-week-old female mice. (d) Alveolar bone loss outcomes in 18-week-old female mice. Unpaired t-test statistical analysis was used. Data are reported as mean ± SEM. *p<0.05 vs. VEH. **p<0.01 vs. VEH.

To validate that antibiotic perturbation of oral microbiota drives the alveolar bone loss found in SPF mice, germ-free (GF) mice were utilized to investigate the direct effect of minocycline on linear alveolar bone loss under the complete absence of the microbiota. Micro-CT analysis of linear alveolar bone loss was assessed at the maxillary first molar of 12-week-old male GF mice **(Figure 9).** Linear measurements assessing the distance from CEJ to ABC were made at the mesiobuccal, mid-lingual, and distobuccal line angles. MINO vs. VEH treatment demonstrated no differences in the linear distance from CEJ to ABC in 12-week-old GF mice **(Figure 9)**.

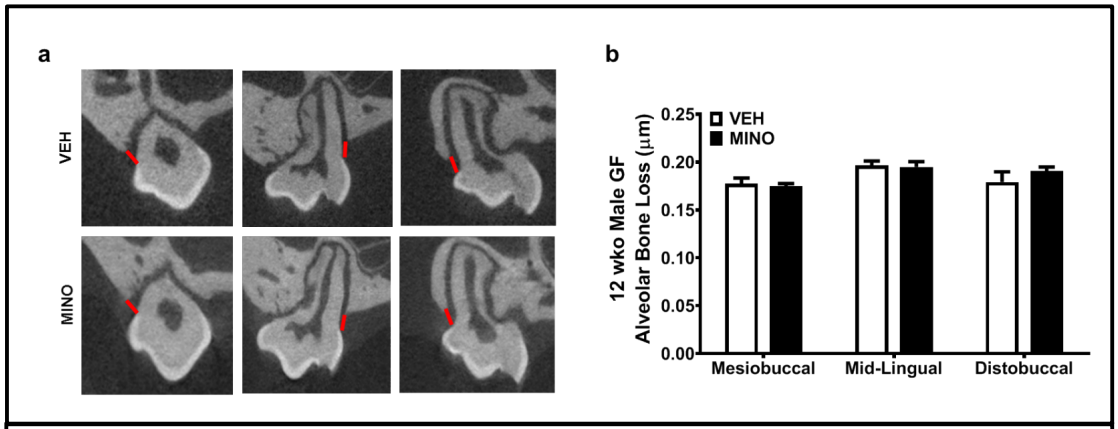

Figure 9. Minocycline (MINO) effects on linear alveolar loss bone in GF mice. 12-week-old male VEH vs. MINO treated GF mice were euthanized and maxillae were harvested for micro-CT analysis. (a-b) Linear alveolar bone loss was assessed in the maxillary first molar via measurements of the distance from the CEJ-ABC at mesiobuccal, mid-lingual, and distobuccal line angles. (a) Representative images of CEJ-ABC measurements at mesiobuccal, mid-lingual, and distobuccal line angles in 12-week-old GF mice. (b) Alveolar bone loss outcomes in 12-week-old GF mice. Unpaired t-test statistical analysis was used. Data are reported as mean ± SEM. *p<0.05 vs. VEH.

3.2 Aim 2 Results

The Novince Lab has shown previously that antibiotic disruption of the gut microbiota dysregulates osteoimmune cross talk at non-oral skeletal sites.[17] These studies utilized a broad-spectrum antibiotic cocktail (ABX) in C57BL/6T mice to investigate exogenous perturbation of commensal gut microbiota osteoimmune effects on osteoblastogenesis and osteoclastogenesis in the late growing skeleton.[17] In ABX treated mice, antibiotic alteration of gut microbiota increased osteoclastogenesis, enhanced local and systemic pro-inflammatory cytokines, and altered innate and adaptive immune cells at non-oral skeletal sites.[17] Through micro-CT analysis, antibiotic disruption of the gut microbiota induced a more profound inferior trabecular bone phenotype in proximal tibia of male mice compared to female mice.[17] Histomorphometric analysis of proximal tibia revealed an increase in osteoclast perimeter per bone perimeter, osteoclast size, and number of osteoclasts in ABX treated mice.[17] Flow cytometry revealed that antibiotic disruption of gut microbiota altered the innate and adaptive immune cell profile in gut draining lymphoid tissues and the bone marrow of non-oral skeletal sites.[17]

Irie, Novince, and Darveau (2014) have shown that homeostasis of healthy periodontal tissues is impacted by innate and adaptive immunosurveillance mechanisms in response to the commensal oral microbiota.[4] The indigenous oral microbiota was reported to cause an exacerbated naturally occurring alveolar bone loss, which was attributed to an increase in osteoclastic cell numbers lining the surface of alveolar bone.[4] To elucidate the mechanisms causing the loss of alveolar bone, the commensal oral flora was shown to drive a host immune response through an increase in $CD3^+$ T-lymphocytes, $CD4^+$ helper T-cells, $IL17A^+$ T-cells, and enhanced RANKL expression in barrier periodontal tissues.[4]

While the effect of antibiotics on commensal gut microbiota has been shown to critically regulate osteoclast/osteoblast mediated bone metabolism at non-oral skeletal sites, antibiotic perturbation of oral commensal microbiota has unclear effects on the osteoimmune mechanisms regulating alveolar bone metabolism.[17]

Aim 2: Evaluate antibiotic treatment effects on skeletal homeostasis and osteoimmune response mechanisms within the alveolar bone complex.

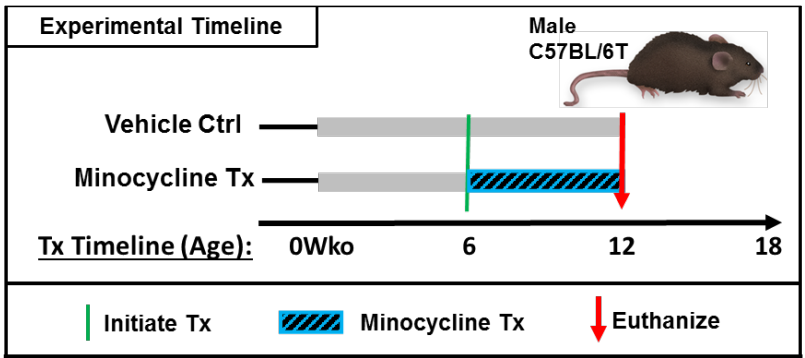

Figure 10. Experimental timeline of minocycline antibiotic treatment *in vivo* (Aim 2).

In order to evaluate antibiotic induced changes in osteoimmune response pathways, minocycline antibiotic (MINO) treatment or vehicle-control (VEH) treatment was orally administered via supplementation of drinking water to male C57BL/6T SPF mice, from age 6 to 12 weeks **(Fig 10)**. Mice were administered minocycline at a human equivalent dose, as previously described. Treatment was initiated at 6 weeks of age, the developmental age when the murine immune system is considered principally complete in the C57BL/6 mouse.[145,146] Also at 6 weeks of age, C57BL/6 mice have reached their stage of development where the teeth have fully erupted and alveolar bone formation is complete.[33,147] Mice were euthanized at 12 weeks of age to evaluate antibiotic-induced

alterations in alveolar bone morphology, osteoclastogenesis, and osteoimmune response effects.

Micro-CT analysis **(Figure 11)** was performed in the mandibular first molar furcation to assess antibiotic induced tissue level alterations in trabecular and cortical bone within the alveolar bone complex. Trabecular bone volume fraction was similar in MINO vs. VEH treated mice **(Figure 11a-b)**. To the contrary, minocycline treatment suppressed cortical bone thickness at the buccal cortical plate **(Figure 11c,e)** and lingual cortical plate **(Figure 11d,f)** of the mandibular first molar. Furthermore, combined analysis at the buccal and lingual cortical plate analyses supported a decreased total cortical bone thickness in MINO vs. VEH treated mice **(Figure 11g)**.

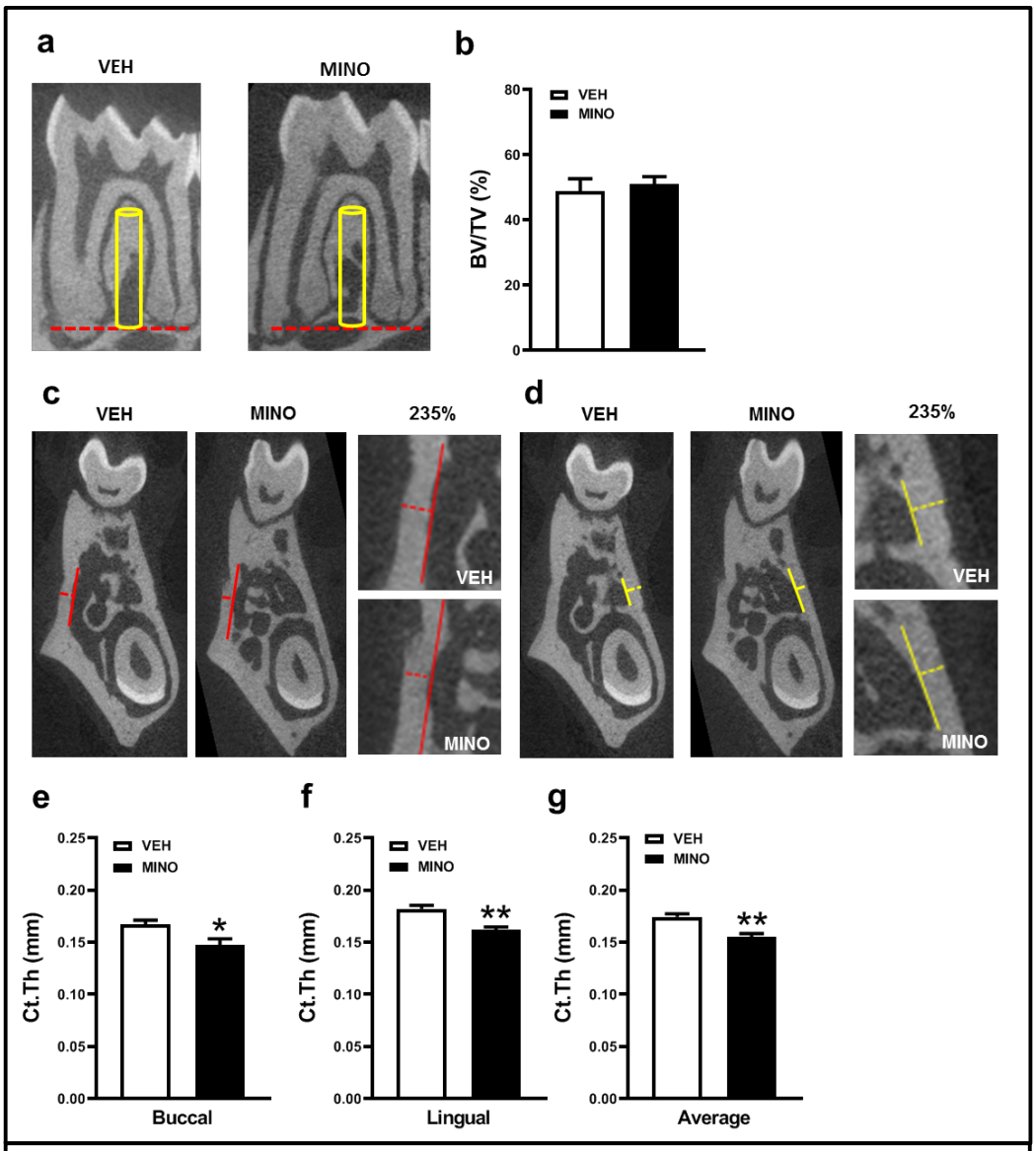

Figure 11. Minocycline (MINO) effects on cortical and trabecular bone microarchitecture. 12-week-old male VEH- and MINO-treated mice were euthanized, and mandibles were harvested for micro-CT analysis. (a-b) Micro-CT analysis of trabecular bone in mandibular first molar furcation. (n=4-6/pg) (a) Representative images of trabecular bone volume fraction using cylindrical method (*region of interest defined by yellow cylinder). (b) BV/TV = trabecular bone volume fraction. (c-g) Micro-CT analysis of cortical bone in mandibular first molar (n=4-6/gp). (c) Representative images of cortical bone thickness at the buccal aspect of inner cortical bone surface (*measurement of interest defined by red perpendicular dashed line). Magnified images were set at 235% Scale Height. (d) Representative images of cortical bone thickness at the lingual aspect of inner cortical bone surface (*measurement of interest defined by yellow perpendicular dashed line). Magnified images were set at 235% Scale Height. Ct.Th = cortical bone thickness outcomes at the (e) buccal cortical plate, (f) lingual cortical plate, and (g) combined average of the buccal / lingual cortical plates. Unpaired t-test statistical analysis was used. Data re reported as mean ± SEM. *p<0.05 vs. VEH. **p<0.01 vs. VEH.

Appreciating that alveolar bone loss is driven by osteoclastic bone resorption actions, studies were performed to investigate the impact of minocycline treatment effects on osteoclastogenesis. Histomorphometric analysis of tartrate-resistant acid phosphatase (TRAP) stained maxilla sections was utilized to investigate the effect of minocycline treatment on osteoclast cell outcomes in the maxillary first molar furcation. MINO vs. VEH treated mice had significantly greater osteoclast perimeter per bone perimeter **(Figure 12e)**, which was attributed to enhanced osteoclast size per osteoclast **(Figure 12d)**. The minocycline-induced increase in osteoclastogenesis *in situ*, parallels

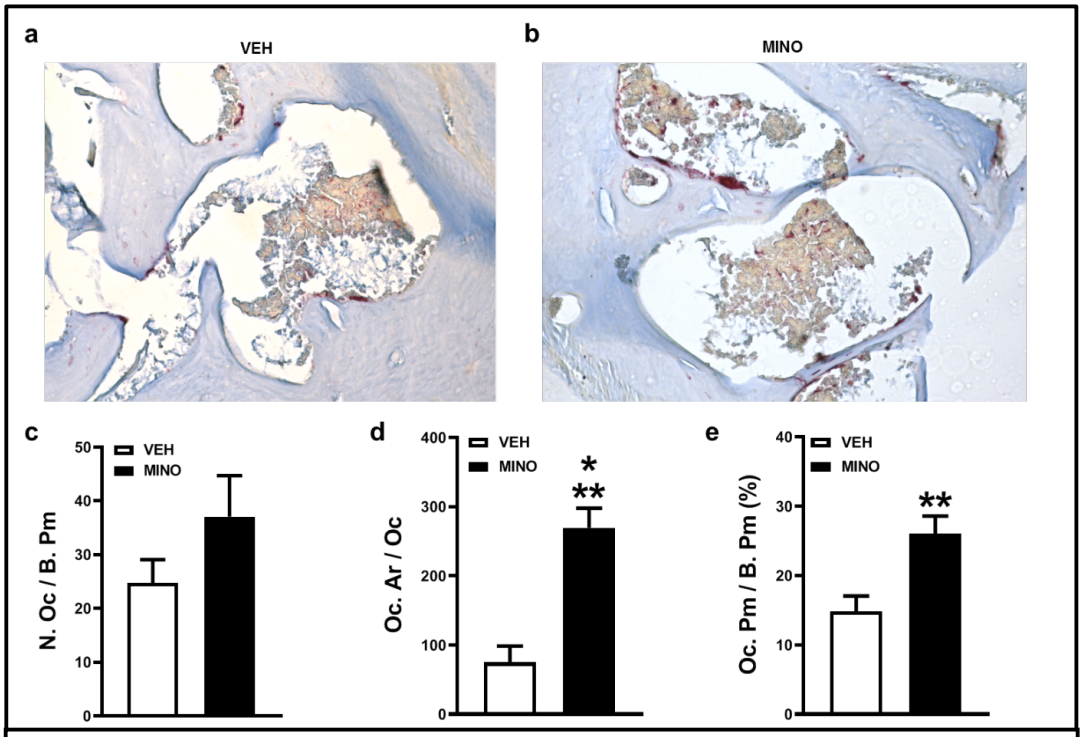

Figure 12. Minocycline (MINO) effects on *in situ* osteoclastogenesis.12-week-old male VEH- and MINO-treated mice were euthanized, and maxilla harvested for histomorphometric analysis. Histomorphometric analysis of osteoclast cellular endpoints were performed in the trabecular bone marrow furcation of tartrate-resistant acid phosphatase (TRAP) stained maxillary first molar sections; TRAP+ cells lining bone with ≥ 3 nuclei were designated an osteoclast. (a-b) Representative images of furcation region of interest in TRAP-stained maxilla sections. (c) N.OC / B.Pm = osteoclast number per bone perimeter. (d) Oc.Ar / Oc = average osteoclast area. (e) Oc.Pm / B.Pm = osteoclast perimeter per bone perimeter. Unpaired t-test statistical analysis was used. Data are reported as mean ± SEM. **p<0.01 vs. VEH. ***p<0.001 vs. VEH.

the minocycline-induced inferior cortical bone phenotype found through micro-CT analysis **(Figure 11c-g)**.

Recognizing that innate and adaptive immune cells are critical regulators of osteoclastogeneis and inflammatory bone loss[77,78,148,149], investigation of immune cell profiles was carried out in primary and secondary lymphoid tissues drining the oral cavity. MBM and CLN cells were isolated for flow cytometric analysis **(Figure 13-15)**. Innate and adaptive immune cell populations investigated were based on prior research demonstrating the role of specific immune cells in osteoclast mediated periodontal bone loss.

Neutrophils, monocytes, macrophages, and DCs are innate immune cell mediators that play important roles in periodontal health and disease.[150-153] Therefore, antibiotic treatment effects on these innate immune cell populations were assessed **(Figure 13)**. Increased %$CD11b^{+}Ly6C^{lo}Ly6G^{+}$ neutrophils were observed in the CLNs of MINO vs. VEH mice **(Figure 13a)**. While neutrophils were similar in the MBM **(Figure 13a)**, %$CD11b^{+}Ly6G^{-}F4/80^{+}Ly6C^{+}$ inflammatory monocytes were decreased in the MBM of MINO vs. VEH mice **(Figure 13b)**. No differences were found in %$CD11b^{+}MHCII^{+}CD4^{-}CD206^{+}$ anti-inflammatory M2 macrophages **(Figure 13d)**, however, %$CD11b^{+}MHCII^{+}CD64^{+}$ pro-inflammatory M1 macrophages were decreased in the MBM of MINO vs. VEH mice **(Figure 13c)**. %$CD11c^{+}B220^{+}MHCII^{lo}$ pro-inflammatory plasmacytoid DCs showed a significant increase in the MBM and CLNs in response to MINO treatment **(Figure 13e)**. Conversely, %$CD11c^{+}CD11b^{-}B220^{-}MHCII^{+}$ conventional DCs were decreased in the CLNs and increased in the MBM of MINO vs. VEH mice **(Figure 13f)**.

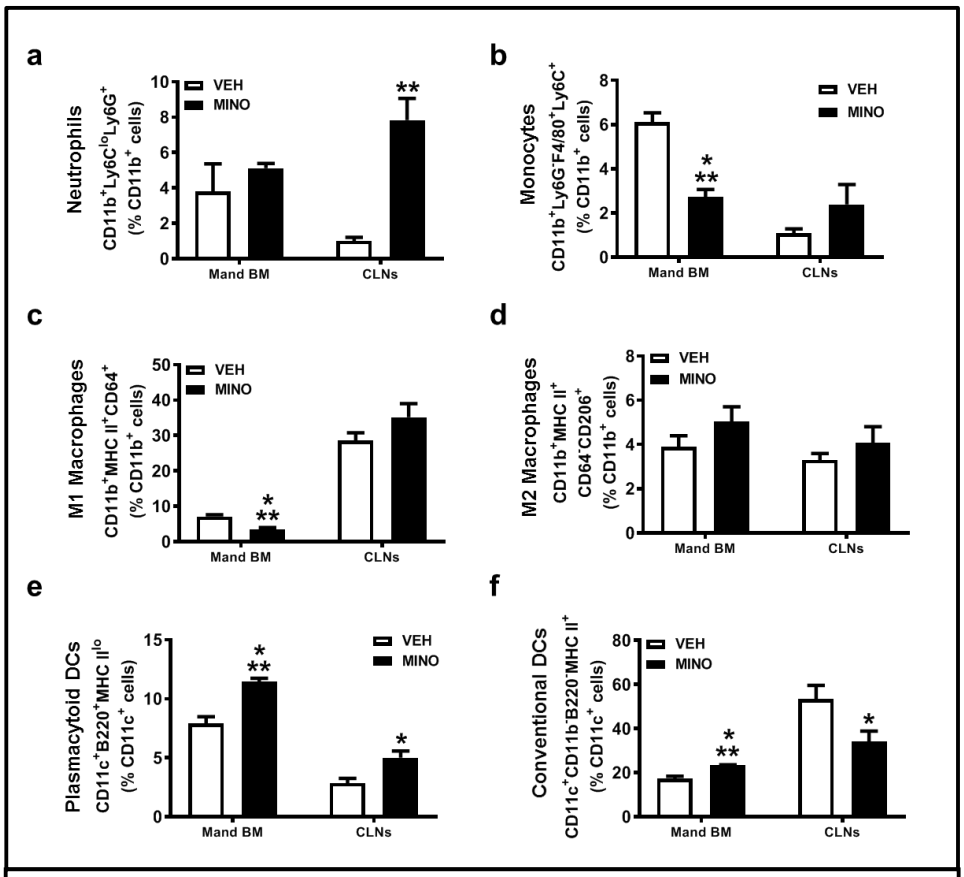

Figure 13. Minocycline (MINO) effects on innate immune cells in mandible bone marrow (MBM) and cervical lymph node (CLN). 12-week-old male VEH- and MINO-treated mice were euthanized; MBM and CLN cells were isolated for flow cytometric analysis (n=4-6/gp). (a-d) Neutrophil, monocyte, and macrophage subsets are expressed relative to the CD11b+ cell population; (a) %$CD11b^{+}Ly6C^{lo}Ly6G^{+}$ neutrophils; (b) %$CD11b^{+}Ly6G^{-}F4/80^{+}Ly6C^{+}$ inflammatory monocytes; (c) %$CD11b^{+}MHCII^{+}CD64^{+}$ M1-macrophages; (d) %$CD11b^{+}MHCII^{+}$ M2-macrophages. (e-f) Dendritic cell (DC) subsets are expressed relative to the CD11c+ cell population; (e) $CD11c^{+}B220^{+}MHCII^{lo}$ plasmacytoid DCs; (f) $CD11c^{+}CD11b^{-}B220^{-}MHCII^{+}$ conventional DCs. Unpaired t-test statistical analysis was used. Data are reported as mean ± SEM, *p<0.05 vs. VEH, **p<0.01 vs. VEH, ***p<0.001 vs. VEH.

Prior research has discerned that $CD4^{+}$ helper T-cells and $CD8^{+}$ cytoxic T-cells regulate alveolar bone homeostasis and periodontal bone loss.[12,154-157] Therefore, flow cytometric analysis was employed to evaluate total and activated vs. naïve $CD4^{+}$ T-cell and $CD8^{+}$ T-cell populations. While no differences were seen in Total $CD4^{+}$ T-cells **(Figure 14a)**, MINO treatment caused an increase in $CD3^{+}CD8^{-}CD4^{+}CD62L^{+}CD69^{-}$

naïve $CD4^+$ T-cells **(Figure 14b)** and a decrease in $CD3^+CD8^-CD4^+CD62L^-CD69^+$ activated $CD4^+$ T-cells in CLNs **(Figure 14c)**. No differences were seen in the MBM of naïve and activated $CD4^+$ T-cell populations in MINO vs. VEH mice **(Figure 14b-c)**. While no differences were seen in Total $CD8^+$ T-cell **(Figure 14d)**, MINO treatment caused a trending increase towards significance in naïve $CD8^+$ T-cells in the MBM and CLNs **(Figure 14e)**. No differences were seen in activated $CD8^+$ T-cell populations in the MBM, however, a trend towards a decrease in the CLNs of MINO vs. VEH mice **(Figure 14f)**.

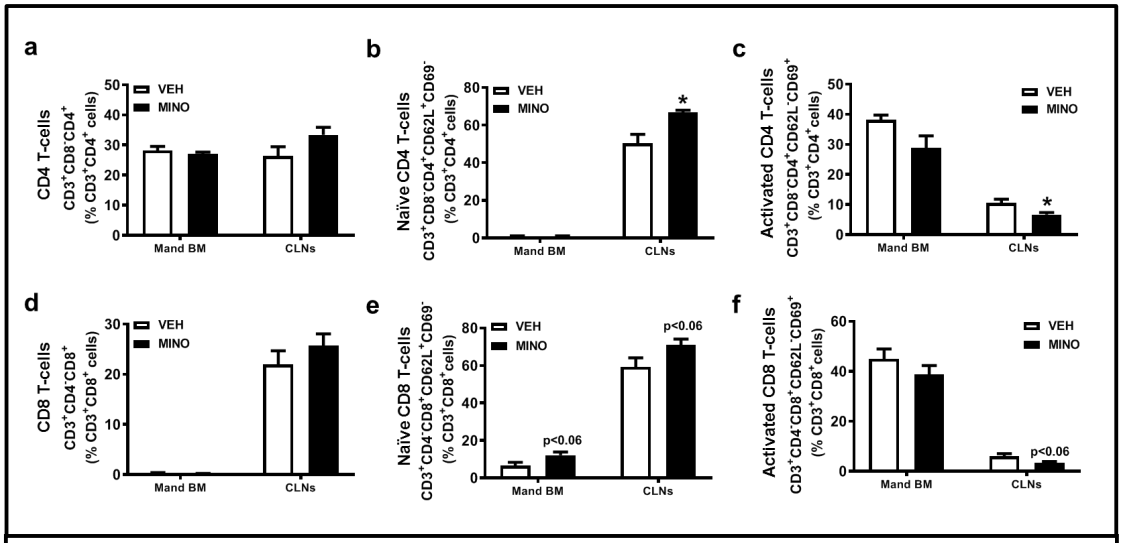

Figure 14. Minocycline (MINO) effects on Total, Naïve, and Activated T-cells in mandible bone marrow (MBM) and cervical lymph nodes (CLNs). 12-week-old male VEH- and MINO-treated mice were euthanized; MBM and CLN cells were isolated for flow cytometric analysis (n=4-6/gp). (a-c) Helper $CD4^+$ T-cell subset composition. (a) $CD3^+CD8^-CD4^+$ Total CD4 Helper T-cells; (b) $CD3^+CD8^-CD4^+CD62L^+CD69^-$ Naïve CD4 T-cells; (c) $CD3^+CD8^-CD4^+CD62L^-CD69^+$ Activated CD4 T-cells. (d-f) Helper $CD8^+$ T-cell subset composition. (d) $CD3^+CD4^-CD8^+$ Helper $CD8^+$ T-cells; (e) $CD3^+CD4^-CD8^+CD62L^+CD69^-$ Naïve CD8 T-cells; (f) $CD3^+CD4^-CD8^+CD62L^-CD69^+$ Activated CD8 T-cells. Data are expressed relative to CD3+CD4+ cells. Unpaired t-test statistical analysis was used. Data are reported as mean ± SEM, *p<0.05 vs. VEH.

Due to the majority of periodontitis studies focused on the association of $CD4^+$ T-cell mediated host immune response and alveolar bone loss[12,154,158], $CD4^+$ helper T-cell subsets were assessed in the local MBM environment and CLNs draining the oral cavity

(Figure 15). There were no differences in anti-inflammatory T_{REG} cell populations in the MBM or CLNs of MINO vs. VEH mice **(Figure 15a)**. However, there was a significant decrease in anti-inflammatory T_H22 cell populations in the MBM and a significant increase in CLNs of MINO vs. VEH mice **(Figure 15b)**. To the contrary, pro-inflammatory $CD3^+CD4^+CD183^+$T-bet$^+$ T_H1 cell and $CD3^+CD4^+$RORyt$^+AHR^-$ T_H17 cell populations were upregulated within the MBM and CLNs of MINO vs. VEH treated mice **(Figure 15c-d)**. Critical to the current study, the increase in pro-inflammatory T_H1 and T_H17 cell populations in the MBM and CLNs appears to contribute to the pro-inflammatory response seen in the oral environment secondary to minocycline treatment.

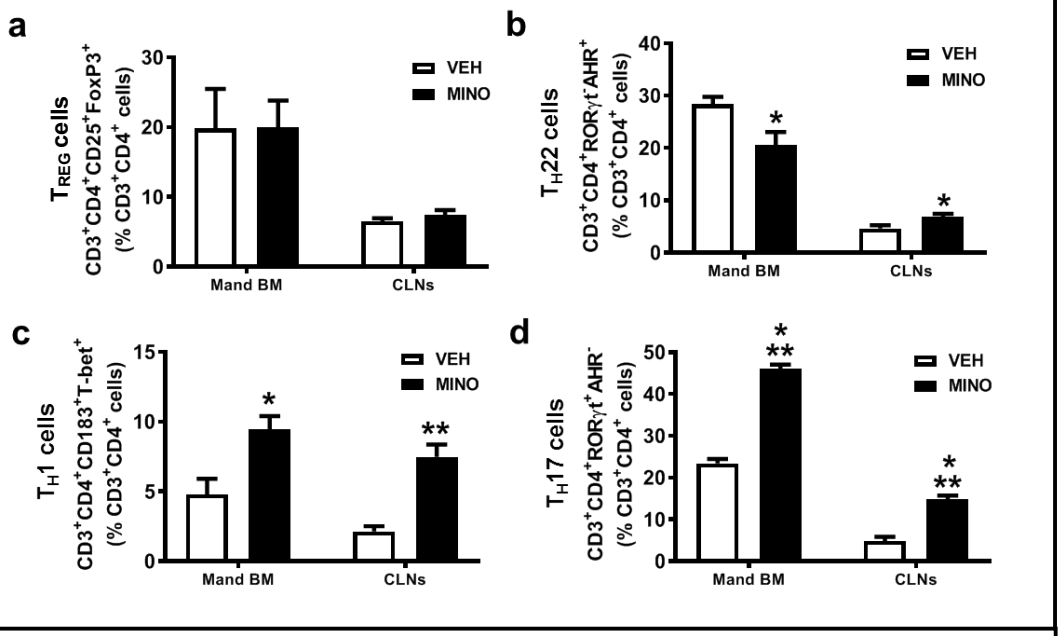

Figure 15. Minocycline (MINO) effects on CD4+ Helper T-cell subsets in mandible bone marrow (MBM) and cervical lymph nodes (CLNs). 12-week-old male VEH and MINO-treated mice were euthanized; MBM and CLN cells were isolated for flow cytometric analysis (n=4-6/gp). (a-d) $CD4^+$ T-cell subsets composition (a) $CD3^+CD4^+CD25^+FoxP3^+$ T_{REG} cells; (b) $CD3^+CD4^+$RORyt$^-$AHR+ T_H22 cells (c) $CD3^+CD4^+CD183^+$T-bet$^+$ T_H1 cells; (d) $CD3^+CD4^+$RORyt$^+AHR^-$ T_H17 cells. Percentages relative to total $CD3^+CD4^+$ T-cells. Unpaired t-test statistical analysis was used. Data

Osteoclast mediated bone resorption is promoted by pro-inflammatory cytokines.[77,81,86,159] Therefore, it was necessary to investigate pro-inflammatory cytokines known to enhance osteoclastogenesis. Gene expression analysis was carried out to evaluate pro-inflammatory/pro-osteoclastic factors known to be upregulated in the barrier gingival tissue of periodontal disease afflicted sites.[160] There were no significant differences in characteristic pro-inflammatory/pro-osteoclastic cytokines in the gingiva of MINO vs. VEH treated mice **(Figure 16)**.

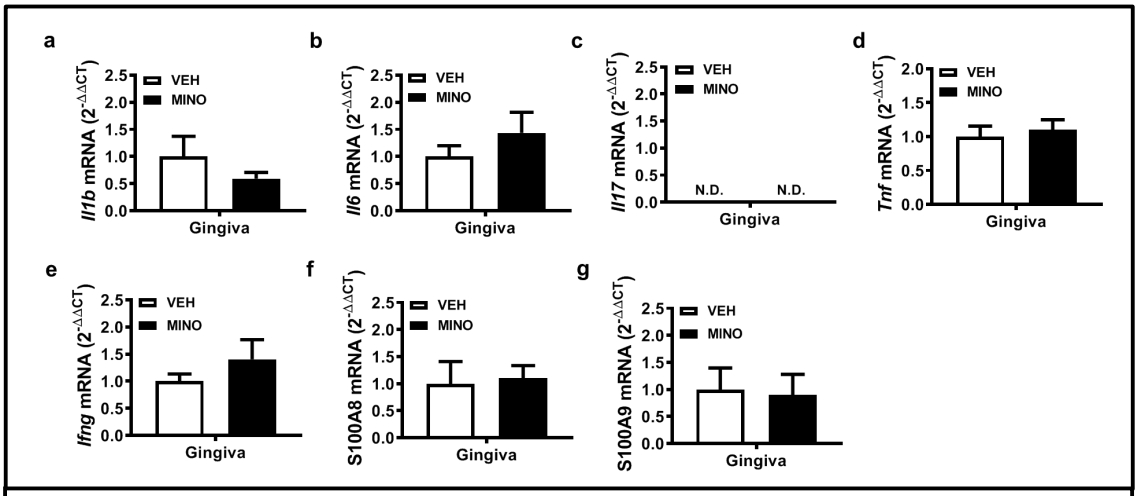

Figure 16. Minocycline (MINO) effects on pro-inflammatory mediators in mandible gingiva. 12-week-old male VEH and MINO treated mice were euthanized and gingiva was isolated for qRT-PCR gene expression analysis (n=4-12/gp). (a) *Il1b* mRNA (pleiotropic inflammatory cytokine); (b) *Il6* mRNA (pleiotropic inflammatory cytokine); (c) *Il17* mRNA (T_H17 cytokine); (d) *Tnf* mRNA (pleiotropic inflammatory cytokine); (e) *Ifng* mRNA (T_H1 cytokine); (f) S100A8 mRNA (neutrophil/monocyte cytokine); (g) S100A9 mRNA (neutrophil/monocyte cytokine). Relative quantification of mRNA was performed via the comparative C_T method ($2^{-\Delta\Delta CT}$); *Rn18s* was utilized as an internal control gene. Data are reported as mean ± SEM. *p<0.05 vs. VEH.

The RANKL:OPG axis, along with pro-osteoclastic signaling factors, was investigated in the MBM to determine whether changes in critical osteoclastic genes regulate the pro-osteoclastic phenotype found in minocycline treated mice **(Figure 12)**. RANKL, which signals to the RANK receptor on pre-osteoclastic and osteoclastic cells, is necessary for the differentiation and function of osteoclasts. Osteoprotegerin (OPG)

functions as the RANK decoy receptor by binding RANKL, preventing signaling at the RANK receptor. Therefore, the RANKL/OPG ratio must be assessed when evaluating potential alterations in RANKL-mediated osteoclastogenesis.[77,81,86,159] DCSTAMP is the surface protein critical for osteoclast fusion and maturation.[92] There were no significant differences in pro-osteoclastic signaling mediators or the RANKL:OPG ratio in the MBM of MINO vs. VEH treated mice **(Figure 17)**.

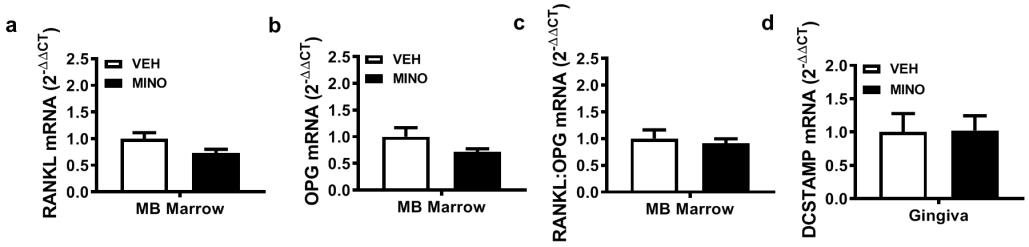

Figure 17. Minocycline (MINO) effects on pro-osteoclastic factors in mandible bone (MB) marrow. 12-week-old, male VEH vs. MINO mice were euthanized and mandible marrow was flushed in TRIzol for gene expression analysis. qRT-gene expression analysis (n=6/gp): (a) *RANKL* mRNA; (b) *OPG* mRNA; (c) *RANKL/OPG* ratio; (d) *Dcstamp* mRNA. Relative quantification of mRNA was performed via the comparative C_T method ($2^{-\Delta\Delta CT}$); *Gapdh* was utilized as an internal control gene. Data are reported as mean ± SEM. *p<0.05 vs. VEH.

To further investigate the pro-osteoclastic effect of minocycline on alveolar bone, additional *in vitro* studies were performed to investigate osteoclast outcomes in MBM cell cultures exogenously treated with minocycline **(Figure 18)**. $TRAP^+$ cytomorphometric analysis revealed a significant increase in osteoclast size **(Figure 18c)** and a trending increase in number of nuclei per osteoclast **(Figure 18d)** in MINO vs. VEH *in vitro* cultures. Both osteoclast size and number of nuclei per osteoclast are surrogate readouts for osteoclast maturation. While the osteoclast maturation phenotype was increased **(Figure 18c,d)**, no differences were seen in number of osteoclast per field **(Figure 18b)** in MINO vs. VEH treated cultures.

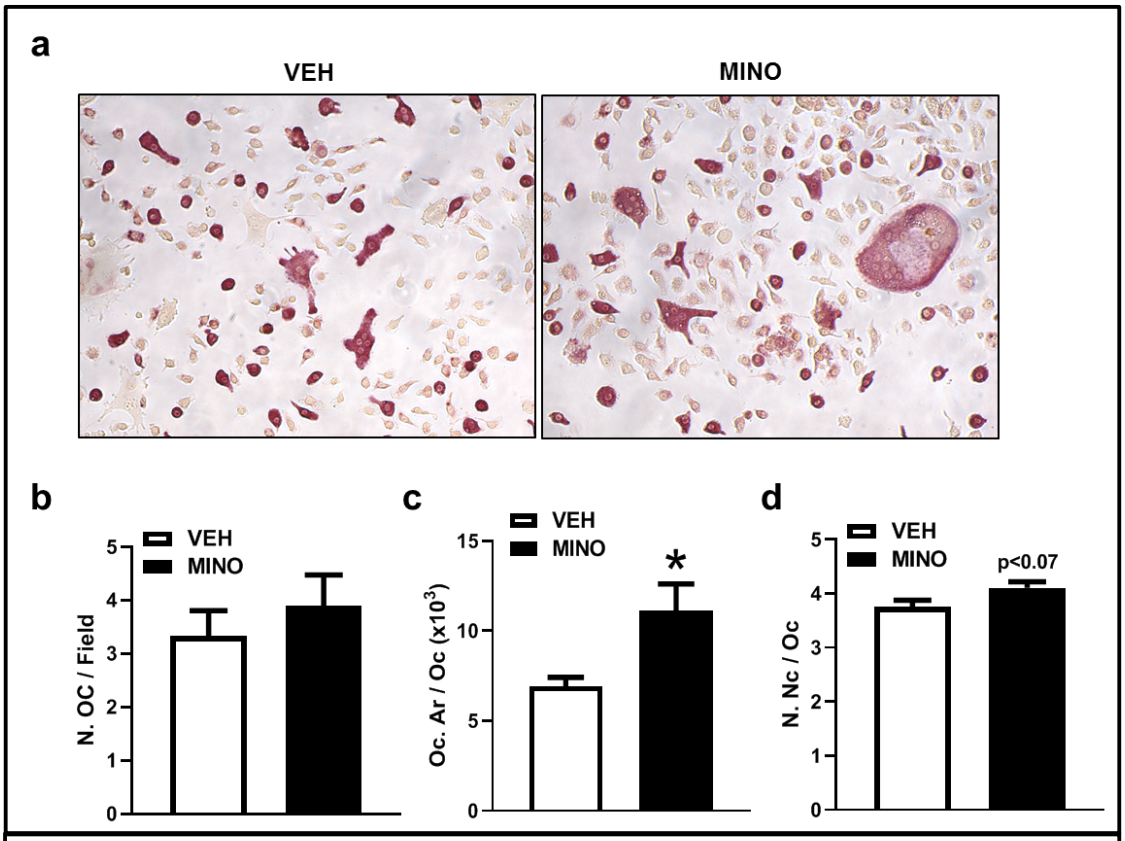

Figure 18. Exogenous *in vitro* minocycline (MINO) treatment in mandible bone marrow derived osteoclastic cell cultures. Non-adherent bone marrow cell cultures were isolated from 12-week-old wild-type C57BL/6T mice and stimulated with 25ng/mL macrophage colony stimulated factor (M-CSF) and 50ng/uL RANKL to induce osteoclastogenesis. Stimulated cultures were treated with vehicle control or minocycline (0.125 µg/ml) until day 6. TRAP+ cytomorphometric analysis of osteoclast cellular outcomes was assessed in exogenously treated minocycline (MINO) vs. vehicle-control (VEH) *in vitro* cultures; TRAP+ cells with ≥ 3 nuclei scored as an osteoclast. (a) Representative images of VEH and MINO treated *in vitro* cultures. (b) N.Oc/Field = number of osteoclast per field. (c) Oc.Ar/Oc ($x10^3$) = average osteoclast area. (d) N.Nc/Oc = number of nuclei per osteoclast. Unpaired t-test statistical analysis was used. Data are reported as mean ± SEM. *p<0.05 vs. VEH.

CHAPTER 4: DISCUSSION AND CONCLUSIONS

The current study utilized VEH vs. MINO treated mice to investigate antibiotic induced alterations in the oral microbiota and its implications on the osteoimmune response and skeletal homeostasis within the alveolar bone complex. The commensal microbiota has been shown to indirectly impact bone growth and modeling in health via interactions of immune cells with osteoclasts and osteoblasts.[75,76,161] While the majority of the literature is focused on gut microbiota immunoregulatory effects impacting non-oral skeletal sites,[17,75,80,161-164] fewer studies have been centered on the oral microbiota and its immunomodulatory effects influencing alveolar bone homeostasis.[76,165,166] Irie Novince, and Darveau (2014) utilized the SPF vs. GF mouse model to discern that the commensal oral microbiota stimulates osteoimmune mechanisms that lead to alveolar bone loss in the healthy periodontium.[76] The current investigation revealed that the antibiotic perturbation of commensal oral microbiota critically regulates osteoimmune response effects, which exacerbate naturally occurring bone loss in the alveolar bone complex.

Hathaway-Schrader et al. (2019) was the first known report to demonstrate that antibiotic perturbation of the gut microbiota impairs bone mass accrual at non-oral skeletal sites.[17] The current report is the first known study to discern that antibiotic disruption of the oral microbiota dysregulates osteoimmune response effects and drives bone loss in the alveolar bone complex. Oral minocycline administration to SPF C57BL/6 mice from age 6 to 12 weeks, induced sex-dependent shifts in the oral bacteriome. Whereas minocycline treatment increased the bacterial load and altered phylum level composition of the oral microbiota in 12-week-old male SPF mice, minocycline treatment did not alter the bacterial load or phylum level composition of the oral microbiota in 12-week-old female SPF mice. However, micro-CT study findings revealed that minocycline

treatment exacerbated linear alveolar bone loss similarly in 12-week-old SPF male and female SPF mice.

Supporting the minocycline treatment effects on the oral microbiota, a previous study administered antibiotics or placebo control for one week duration and then evaluated changes in the oral microbiota composition at the termination of treatment and 1, 2, 4, and 12 months following treatment.[121] Oral administration of either ciprofloxacin or clindamycin initially resulted in a profound microbial shift in saliva specimens immediately after one week of treatment.[121] The study reported that antibiotics induced phyla level changes in the oral bacteriome, including Proteobacteria or candidate division TM7.[121] Proteobacteria was significantly altered by clindamycin immediately following treatment and by ciprofloxacin immediately following treatment and 12 months after treatment.[121] Similar to the aforementioned clinical study on the effect of different antibiotics on the oral microbiota[121], we found that minocycline administration to 6 to 12-week-old C57BL/6T mice resulted in a Proteobacteria-dominated oral microbiota composition in 12-week-old male mice.

Shifts in the gut microbiota favoring the phylum Proteobacteria have been associated with dysbiotic pro-inflammatory states,[167] metabolic conditions,[168] and an imbalanced gut microbiota function.[168] Recognizing that the phylum Proteobacteria has implications for enhanced inflammatory states,[167] and that inflammation of the supporting gingival tissues can lead to alveolar bone loss,[169] the increased presence of phylum Proteobacteria is a possible mediator of the minocycline-induced alveolar bone loss in 12-week-old male mice. Along with the increase in Proteobacteria, a significant decrease in phylum Firmicutes was seen is 12-week-old male MINO vs. VEH mice. Firmicutes are known to contain Gram-positive bacteria and produce mostly butyrate in the human gut.[170] Studies have shown that a decrease in the Firmicutes to Bacteriodetes ratio has

been associated with decreased production of short chain fatty acids, which may decrease the integrity of cellular junctions, increase mucosal permeability, and increase inflammatory cytokines.[171] Therefore, the decreased presence of Firmicutes phylum may partially contribute to the minocycline-induced alveolar bone loss in 12-week-old male mice.

Within the current study, 16S analysis also discerned that minocycline administration resulted in an increased overall bacterial load in the oral microbiota of 12-week-old male mice. While this may seem surprising, previous studies have indicated that the depletion of microbiota required a combination of at least 3 antibiotics for up to 4 weeks,[172,173] and single antibiotics may not be sufficient to reduce the total bacterial load.[174] Supporting the possibility that the increased bacterial load contributed to the increase in linear alveolar bone loss found in MINO vs. VEH treated 12-week old male mice, Abusleme et al. (2013) reported that subgingival plaque from periodontitis vs. healthy patients demonstrated higher bacterial load and richness.[175] Based on the correlation between higher bacterial biomass and disease states, the host immune response eliciting the destruction of periodontal tissue may be secondary to an overall greater bacterial challenge. Considering that periodontal disease has been characterized by an increase in bacterial load[175] and abundance of specific phylum-level taxa,[176] the previous reports provide support that pathogenesis of periodontal alveolar bone loss is secondary to both dysbiotic shifts in the oral microbiota composition and increase in overall bacterial load.

Minocycline treatment exhibited sex-dependent effects on the oral microbiota as no differences were seen in overall bacterial load or phylum level bacterial communities in female mice. While there was significantly increased linear alveolar bone loss in minocycline treated female SPF mice, the role of the oral microbiota is unclear. In a

recently published study, Hathaway-Schrader et al. (2020) showed that specific changes in the bacterial composition of the commensal gut microbiota alters osteoimmune response effects at non-oral skeletal sites.[164] Comparing mice colonized by segmented filamentous bacteria (SFB) to mice not colonized by SFB revealed that the presence of a single commensal gut bacterium has the potential to impair the accrual of bone mass in the late growing skeleton.[164] Notably, the aforementioned seminal manuscript highlights that species level changes in microbiota communities can disrupt osteoimmune processes which ultimately have detrimental effects on the skeleton. This research supports the notion that species level antibiotic-induced alterations in the oral microbiota, could contribute to the alveolar bone loss found in MINO vs. VEH mice. To determine whether minocycline-induced shifts in the oral microbiota of female mice contributed to the increased alveolar bone loss, further investigations evaluating more specific taxonomy levels, such as genus and species, are indicated and necessary.

As means to elucidate whether minocycline-induced linear alveolar bone loss is dependent on the oral microbiota, male GF C57BL/6T mice were administered MINO vs. VEH treatment from age 6 to 12 weeks. Micro-CT analysis revealed that there were no differences in the linear distance from CEJ to ABC in 12-week-old male MINO vs. VEH treated GF mice. Because minocycline treatment did not influence linear alveolar bone loss in GF mice, this supports the notion that the exacerbated linear alveolar bone loss found in minocycline treated SPF mice was attributed antibiotic disruption of the oral microbiota.

In order to determine whether oral minocycline administration had sustained effects on the oral microbiota and linear alveolar bone loss, treatment was withdrawn from sex-matched C57BL/6 SPF mice from age 12 –18 weeks. While antibiotic treatment effects on overall bacterial load were not sustained in 18-week-old male mice following

the withdrawal of minocycline treatment, phylum level alterations in the oral microbiota persisted. At the 18-week time point, MINO treatment reduced the Proteobacteria phylum to baseline and caused a significant increase in Actinobacteria and Firmicutes phyla. Knowing that shifts in the gut microbiota favoring Firmicutes have been associated with decreases in intestinal mucosal protection function,[177] the shift towards a Firmicutes dominated oral microbiota in 18-week-old male MINO treated mice could be contributing to the persistent alveolar bone loss realized. The bacteria of Actinobacteria have been shown to be involved in the modulation of mucosal permeability, the immune system, and metabolism as an unbalanced abundance has been evidenced in several pathological conditions, such as diphtheria, tuberculosis, and leprosy.[178] Actinobacteria have also been reported to dominate the abundance in dental supragingival plaque and have become increasingly evident to play a role in the etiology of dental caries and periodontal disease, which supports the notion that detrimental effects found in 18-week-old male MINO treated mice may be related to an increase in this phylum.[178,179] Supporting the sustained minocycline-induced alterations in the oral microbiota of 18-week-old male MINO treated mice, Zaura et al. (2015) demonstrated that exposure to clindamycin resulted in profound changes in the genus-level oral microbial profile which remained significant one month following cessation of antibiotic treatment.[121]

Minocycline treatment exhibited no significant effects on the oral bacteriome of female mice. Paralleling findings in 12-week-old female mice, there were no differences in overall bacterial load or phylum level composition of MINO vs. VEH treated female mice at age 18 weeks. Because the current study showed sex-dependent minocycline induced changes in oral microbiota composition, future investigations are necessary to determine underlying sex-specific mechanisms, such as the role of sex hormones.

Following the withdrawal of minocycline treatment from 12-18 weeks of age, the linear alveolar bone loss seen in 12-week-old mice was sustained in 18-week-old male and female mice. At the 18-week time point, male mice treated with minocycline from 6 to 12 weeks demonstrated linear alveolar bone loss at the mesiobuccal line angle and mid-lingual aspect of the maxillary first molar. While prior research has been centered on minocycline anti-inflammatory actions that have been linked to bone protective effects during disease states,[123,133] our research shows that minocycline administration to healthy subjects has catabolic effects on alveolar bone. These minocycline-induced adverse effects, which were persistent following cessation of antibiotic administration, appear to be mediated by sustained disruption of the oral microbiota.

Findings in male mice demonstrating that minocycline treatment induced sustained alterations in the oral microbiota and persistent detrimental effects on linear alveolar bone loss, lead to investigating minocycline-induced alterations in osteoimmune mechanisms regulating skeletal homeostasis within the alveolar bone complex. Micro-CT studies revealed decreased cortical bone thickness in the mandibular first molar furcation of MINO vs. VEH treated 12-week-old male SPF mice. Supporting the inferior cortical bone phenotype found in the alveolar bone of minocycline treated 12-week-old male SPF mice, Guss et al. (2017) found that administering broad spectrum oral antibiotics to male C57Bl/6J mice, from 4 to 16 weeks of age, impaired cortical bone morphological properties at non-oral skeletal sites.[180]

Differences in cortical bone parameters and the distance from the CEJ to ABC may be due to alterations in osteoclastogenesis. Therefore, histological sections were stained for tartrate resistance acid phosphatase (TRAP) to investigate osteoclast parameters. Osteoclasts were identified as TRAP+ stained cells with 3 or more nuclei lining the bone. Histomorphometric analysis demonstrated an increase in the size of

osteoclasts and an increase in the perimeter of osteoclasts lining the bone surface in the maxillary first molar furcation of MINO vs. VEH mice. Increased size and perimeter of osteoclasts lining the bone surface, if actively resorbing bone, could result in the decreased bone microarchitecture properties found in MINO vs. VEH treated mice.

MBM cultures were exogenously treated with minocycline to further investigate the pro-osteoclastic effects realized *in situ* in the maxillary alveolar bone of MINO treated mice. While there were no differences in number of osteoclasts, a significant increase in osteoclast size and a trending increase in number of nuclei per osteoclast was found in response to *in vitro* exogenous minocycline treatment. The increase in size and maturation of osteoclasts *in vitro* parallels the increase in osteoclast size and osteoclast perimeter per bone perimeter observed *in situ*, which suggests that minocycline-induced pro-osteoclastic actions are in part independent of the oral microbiota.

To investigate mechanisms mediating the increased size of osteoclasts and perimeter of osteoclasts per bone surface in MINO vs. VEH mice, expression of osteoclast related genes was assessed in MBM. Prior research has discerned that the RANKL/OPG axis critically regulates periodontitis induced alveolar bone loss, and pro-inflammatory signaling mediators can exacerbate periodontal bone loss.[85,89,181] Dental plaque biofilms have been reported to upregulate RANKL, downregulate OPG, and increase the RANKL:OPG ratio.[169,182,183] Although there were no differences in pro-osteoclastic factors (*Rankl*, *Opg*, and *Dcstamp*) or the RANKL:OPG ratio in the MBM of MINO vs. VEH mice, pro-inflammatory cytokines are known to enhance RANKL-mediated osteoclastogenesis.[77,86] Therefore, pro-inflammatory / pro-osteoclastic cytokine gene expression was evaluated in gingival tissue isolates from VEH vs MINO mice.

The gingival epithelium was originally considered to be a physical barrier that protected the host from bacterial invasion, however, we now know that it plays a more

active role in the pathogenesis of inflammatory alveolar bone loss.[20] Pro-inflammatory cytokines known to enhance RANKL-mediated osteoclastogenesis, such as *Il1b*, *Il6*, *Il17a*, *Tnf*, *Ifng, S100a8*, and *S100a9* were investigated. Minocycline treatment induced no differences in pro-inflammatory mediators in the mandible gingiva. Considering that there were no alterations in the expression of cytokines known to modulate RANKL-mediated osteoclastogenesis, further research is indicated to more broadly evaluate biologic mediators in the mandibular gingiva and bone marrow of minocycline treated mice.

The field of osteoimmunology has shown that innate and adaptive immune cells critically regulate osteoclastogenesis in skeletal homeostasis.[77,78,148,149] Therefore, flow cytometric analysis was performed in the MBM and CLNs of MINO vs. VEH treated mice to evaluate changes in immune cells as candidate regulators of minocycline-induced osteoimmune effects. A recent periodontal osteoimmunology study demonstrated that bone damaging T-cells, specifically T_H17 cells converted from FoxP3+ T cells, drive osteolytic alveolar bone destruction secondary to periodontitis-induced changes in the oral microbiota.[67] Tsukasaki et al. (2018) concluded that bacterial invasion lead to the proliferation of specialized T_H17 cells that protect against perio-pathogenic bacteria by promoting mucosal immune responses as well as inducing alveolar bone damage.[67] Irie, Novince, and Darveau (2014) reported that host immune response mechanisms mediating homeostasis with the commensal oral microbiota, including increased neutrophils, $CD3^+$ T-lymphocytes, $CD4^+$ T-helper cells, and $IL17^+$ T-cells in the junctional epithelium, induces basal inflammation supporting osteoclastogenesis and driving bone loss in the healthy periodontium.[76]

Based on the prior reports by Tsukasaki et al. (2018)[67] and Irie, Novince, and Darveau (2014),[76] we investigated alterations in innate immune cell populations and

$CD4^+$ helper T-cell subsets within the MBM environment and oral draining CNLs. Flow cytometry outcomes demonstrating that minocycline treatment increased the frequencies of neutrophils in the CLNs, plasmacytoid DCs in the MBM and CLNs, conventional DCs in the MBM, T_H22 cells in the CLNs, and T_H1 and T_H17 cells in both MBM and CLNs, show that antibiotic perturbation of oral microbiota induced a pro-inflammatory immune response in the MBM and oral draining lymphoid tissues. While we discerned that minocycline altered the oral microbiota at the phylum level, antibiotic-induced pro-inflammatory immune cell response effects may be associated with increased mucosal permeability, translocation of oral microbes, and overgrowth of antibiotic-resistant opportunistic pathogens.[184-191]

The frequency of neutrophil cells was increased in CLNs. Important for bacterial clearance, neutrophils have been suggested to accumulate in periodontal tissues and precipitate in tissue destruction states.[192] There is an abundance of evidence on the phagocytic activity of neutrophils in connection with loose bacterial aggregates in the oral cavity. However, Garant et al. (1976) concluded that “no harmful effects are suffered as a consequence of the transmigration of neutrophils to the junctional epithelium” and the protective wall of leukocytes reflects the host’s intention to wall off and protect itself from bacterial invasion.[193] Studies have reported that minocycline has the ability to decrease the LPS-induced activation of macrophages[194] and suppress the activation of pro-inflammatory monocytes,[195] which in part explains the reduced frequency of inflammatory monocytes and M1-macrophages found in the MBM in response to minocycline treatment. Considering that minocycline treatment suppressed the frequency of inflammatory monocytes and M1-macrophages, this highlights that minocycline administration may have altered DCs in the MBM and CLNs draining the oral cavity.

Two major DC subtypes are critical to periodontal immunity; plasmacytoid DCs terminally differentiate in the bone marrow carrying the ability to produce high amounts of type-1 INFs,[196] whereas conventional DCs migrate to the oral draining lymph nodes to present pathogen-derived peptides to T-cells.[197] Plasmacytoid DCs were increased in the marrow and CLNs, while conventional DCs were increased in the marrow of MINO treated mice. Under inflammatory conditions, peripheral DCs reside in an immature state and serve as sentinels that survey the periodontal tissue for invading microbes.[196] Dendritic cell function has been reported to be modulated by direct interaction with periodontal pathogens.[198-200] One study demonstrated exposure to *P. gingivalis* in the gingiva resulted in production of pro-inflammatory cytokines from non-immune cells in the local tissue.[198] DCs exposed to cytokines produced by gingival tissue cells induced the generation of T_H2 and T_{REG} cells, however, DCs in direct interaction with infiltrating bacteria induced the population of T_H1 cells.[199] As oral DCs are also likely to become exposed to multiple types of bacteria simultaneously, studies have evaluated the impact of polybacterial infection on DCs.[200] While it is known that Gram-negative bacteria are stronger inducers of inflammatory cytokines, DCs exposed to Gram-negative bacteria selectively synergized production of *Il6*, *Tnf,* and *Il12* cytokines.[200] Another study highlighted the contribution of the commensal bacteria to alveolar bone loss, demonstrating that oral exposure of mice to *P. gingivalis* dramatically increases the commensal oral bacteria load, alters the diversity of the oral microbiota, and drives alveolar bone loss.[5] In this regard, periodontal pathogen induced alterations in the oral commensal bacteriome can stimulate maturation of DCs and production of cytokines and chemokines with inflammatory properties.[201] Several studies have demonstrated that among the $CD4^+$ T-cell subsets, upregulation of T_H1/T_H17 cells and downregulation of T_H2 cells are associated with periodontal tissue destruction.[202-204] The minocycline-

induced increase in DCs paralleled the increased frequency of T_H1 and T_H17 cells in the MBM and CLNs, which suggests that the upregulated DCs in the oral environment may drive the development of pro-inflammatory T_H1 / T_H17 cells to exacerbate periodontal tissue destruction.

Also under inflammatory states, oral DCs have been reported to have important roles in antigen presenting processes to prompt the adaptive immune response.[196] Moreover, DCs may migrate to the oral draining CLNs to present MHC Class II and co-stimulatory molecules, which enables potent activation of $CD4^+$ T cells.[196] Because we found a decreased frequency of activated $CD4^+$ T-cells and an increased frequency of naïve $CD4^+$ T-cells in the CLNs of MINO vs. VEH treated mice, this suggest that minocycline dysregulated MHC Class II antigen processing/presentation.

Antigen presentation is an important component of innate and adaptive immune cross talk as antigen presenting cells present self-peptides and non-self-peptides to prompt the adaptive immune system. It has been more recently studied that bone marrow-derived antigen presenting cells are necessary for oral T-cell education, immune tolerance, and T-cell interactions in lymphoid tissues in periodontitis and health.[63,196] Because MHC class II complexes are expressed on antigen presenting plasmacytoid DCs, we propose a mechanism by which plasmacytoid DCs drive a pro-inflammatory immune response secondary to minocycline perturbation of the oral microbiota.

Further demonstrating the role DCs play in activating bone-damaging $CD4^+$ T-cells, one study has reported that in the absence of $CD4^+$ T-cells, mice were resistant to bacteria induced alveolar bone loss.[12] Whereas the oral microbiota is essential for the initiation and progression of periodontitis disease states in the oral cavity, tissue damage is mediated primarily by the host immune response.[61,205] When commensal oral microbiota homeostasis is disrupted, commensals could potentially be presented by oral

DCs to activate T-cells, thus facilitating local inflammation and bone resorption in the alveolar bone complex.

This research demonstrates that antibiotic disruption of the oral microbiota alters host immune response effects, which critically regulates normal osteoimmune processes and skeletal homeostasis in the alveolar bone complex. Minocycline-induced up-regulation of DCs in the marrow and lymphoid tissues draining the oral cavity highlights that DCs are a critical modulator of oral microbiota host immune response effects driving alveolar bone loss **(Figure 19)**.

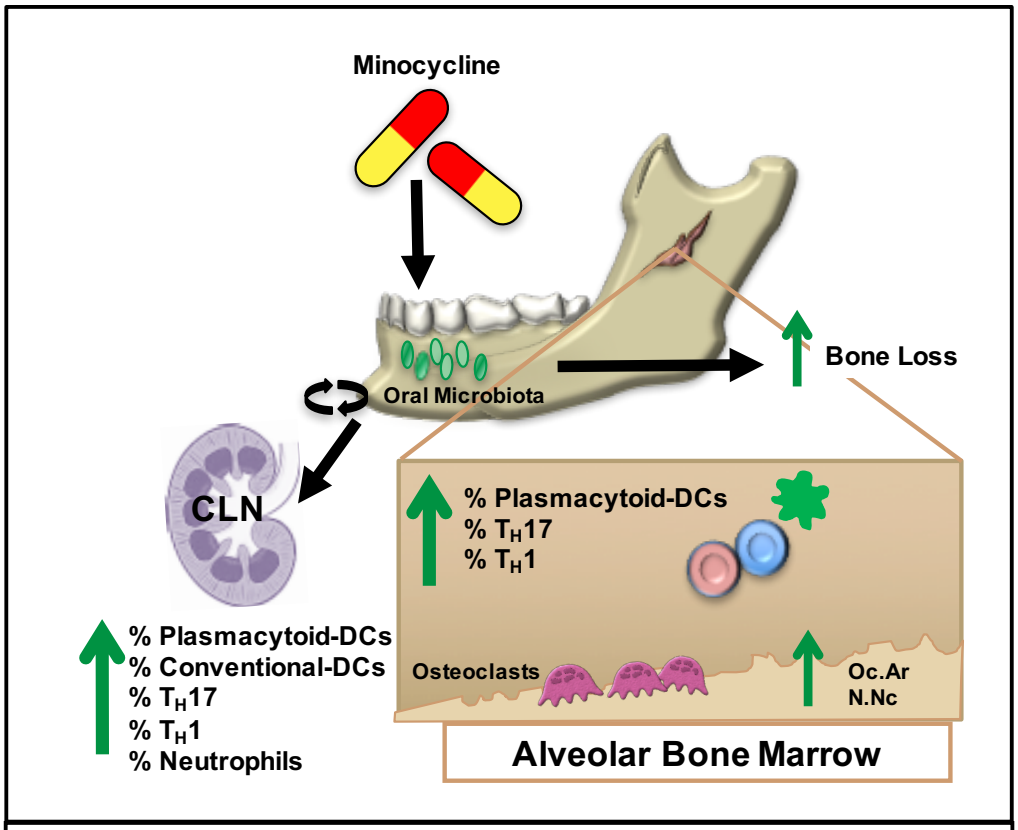

Figure 19: Schematic summarizing findings in minocycline treated mice.

Due to the pharmacological profile of tetracyclines, which combines anti-microbial with anti-inflammatory and anti-apoptotic properties, oral minocycline treatment has previously been experimentally administered in periodontal disease models. When

administered for the treatment of periodontitis, minocycline was detected in gingival crevicular fluid and significantly increased the proliferation of osteoblast cells, whereas long-term exposure of these cells to tetracycline resulted in a proportional increase in mineralized bone matrix. This suggest that minocycline has a therapeutic osteogenic effect when administered for the treatment of periodontitis.[206] These minocycline effects are present without impacting the survival and protein expression of human gingival fibroblasts, epithelial cells, and periodontal ligament fibroblasts.[207] Taken together, these minocycline actions in experimental periodontal disease models may explain the efficacy of minocycline in reducing disease progression and promoting periodontal healing.[208]

Speaking to the clinical implications of this study, minocycline is FDA approved as a local adjunctive therapeutic for the treatment of periodontal disease. Local administration of minocycline microspheres, or Arestin (OraPharma, Inc., Warminster, Pa, USA), has been shown to be advantageous when used as an adjunctive therapy to both nonsurgical and surgical treatment in patients with moderate to severe, chronic periodontitis.[209] Compared to scaling and root planning alone, adjunctive minocycline administration into the periodontal pocket has been shown to significantly reduce probing depths and eliminate red-complex periodontal pathogens.[209] Despite the fact that several clinical studies have shown additional benefits when systemic antibiotics are administered as adjuncts to periodontal treatment, clear guidelines for the use of these agents in clinical practice are unavailable, and their slight additional benefits must be balanced against their adverse side effects. Minocycline is also commonly prescribed to adolescents for the treatment of dermatological conditions.[210] Highlighting the clinical relevance of this study, minocycline was administered at a human equivalent dose for the treatment of acne. The current investigation is the first known study to delineate that oral minocycline therapy induced disruption of the commensal oral microbiota negatively

impacts periodontal health and homeostasis. This suggests that oral minocycline therapy for the treatment of acne may have unintended detrimental clinical effects on the healthy periodontium.

Future studies are needed to further advance knowledge about minocycline effects on the oral microbiota, periodontal immune response, and alveolar bone homeostasis. While there is an increasing prevalence of research focused on the impact of antibiotics on the oral bacteriome, there is a lack of studies discerning effects on the fungal component of the oral microbiota. Antibiotics are known to cause shifts in the fungal flora within the gut, further demonstrating the need for future studies evaluating minocycline induced changes in the oral mycobiome. Minocycline effects on non-oral microbiota communities, such as the gut and skin flora, may contribute to the alveolar bone loss found in response to minocycline treatment. Therefore, future studies should investigate whether minocycline effects on the oral microbiota vs. non-oral microbiota communities are causing alveolar bone loss. While the current osteoimmunology study was focused on osteoclastogensis, ongoing research is needed to evaluate minocycline effects on osteoblastogenesis in the alveolar bone complex. Considering that other tetracycline derivatives, such as doxycycline, are commonly administered by clinicians, future investigations could employ the reported murine antibiotic administration model to evaluate whether other tetracycline class drugs have similar effects on alveolar bone homeostasis and periodontal health.

REFERENCES

1. Hathaway-Schrader JD, Novince CM. Maintaining Homeostatic control of periodontal bone tissue. *Periodontology 2000.* 2020; In Press.

2. Dewhirst FE, Chen T, Izard J, et al. The human oral microbiome. *Journal of bacteriology.* 2010;192(19):5002-5017.

3. Nazir MA. Prevalence of periodontal disease, its association with systemic diseases and prevention. *International journal of health sciences.* 2017;11(2):72-80.

4. Irie K, Tomofuji T, Ekuni D, Morita M, Shimazaki Y, Darveau RP. Impact of Oral Commensal Bacteria on Degradation of Periodontal Connective Tissue in Mice. *Journal of periodontology.* 2015;86(7):899-905.

5. Hajishengallis G, Liang S, Payne MA, et al. Low-abundance biofilm species orchestrates inflammatory periodontal disease through the commensal microbiota and complement. *Cell host & microbe.* 2011;10(5):497-506.

6. Brown LR, Roth GD, Hoover D, Flanagan V, Nielsen AH, Werder AA. Alveolar bone loss in leukemic and nonleukemic mice. *Journal of periodontology.* 1969;40(12):725-730.

7. Dixon DR, Reife RA, Cebra JJ, Darveau RP. Commensal bacteria influence innate status within gingival tissues: a pilot study. *Journal of periodontology.* 2004;75(11):1486-1492.

8. Dutzan N, Kajikawa T, Abusleme L, et al. A dysbiotic microbiome triggers TH17 cells to mediate oral mucosal immunopathology in mice and humans. *Science translational medicine.* 2018;10(463).

9. Assuma R, Oates T, Cochran D, Amar S, Graves DT. IL-1 and TNF antagonists inhibit the inflammatory response and bone loss in experimental periodontitis. *Journal of immunology (Baltimore, Md : 1950).* 1998;160(1):403-409.

10. Delima AJ, Oates T, Assuma R, et al. Soluble antagonists to interleukin-1 (IL-1) and tumor necrosis factor (TNF) inhibits loss of tissue attachment in experimental periodontitis. *Journal of clinical periodontology.* 2001;28(3):233-240.

11. Graves DT, Delima AJ, Assuma R, Amar S, Oates T, Cochran D. Interleukin-1 and tumor necrosis factor antagonists inhibit the progression of inflammatory cell infiltration toward alveolar bone in experimental periodontitis. *Journal of periodontology.* 1998;69(12):1419-1425.

12. Baker PJ, Dixon M, Evans RT, Dufour L, Johnson E, Roopenian DC. CD4(+) T cells and the proinflammatory cytokines gamma interferon and interleukin-6

contribute to alveolar bone loss in mice. *Infection and immunity.* 1999;67(6):2804-2809.

13. Garlet GP, Cardoso CR, Campanelli AP, et al. The dual role of p55 tumour necrosis factor-alpha receptor in Actinobacillus actinomycetemcomitans-induced experimental periodontitis: host protection and tissue destruction. *Clinical and experimental immunology.* 2007;147(1):128-138.

14. Sommer F, Backhed F. The gut microbiota--masters of host development and physiology. *Nature reviews Microbiology.* 2013;11(4):227-238.

15. Cho I, Blaser MJ. The human microbiome: at the interface of health and disease. *Nature reviews Genetics.* 2012;13(4):260-270.

16. Ananthakrishnan AN. Epidemiology and risk factors for IBD. *Nature reviews Gastroenterology & hepatology.* 2015;12(4):205-217.

17. Hathaway-Schrader JD, Steinkamp HM, Chavez MB, et al. Antibiotic Perturbation of Gut Microbiota Dysregulates Osteoimmune Cross Talk in Postpubertal Skeletal Development. *The American journal of pathology.* 2019;189(2):370-390.

18. Ten Cate AR, Mills C. The development of the periodontium: the origin of alveolar bone. *The Anatomical record.* 1972;173(1):69-77.

19. Schroeder HE, Listgarten MA. The gingival tissues: the architecture of periodontal protection. *Periodontology 2000.* 1997;13:91-120.

20. Bosshardt DD, Lang NP. The junctional epithelium: from health to disease. *Journal of dental research.* 2005;84(1):9-20.

21. Nanci A, Bosshardt DD. Structure of periodontal tissues in health and disease. *Periodontology 2000.* 2006;40:11-28.

22. Ji S, Choi YS, Choi Y. Bacterial invasion and persistence: critical events in the pathogenesis of periodontitis? *Journal of periodontal research.* 2015;50(5):570-585.

23. Gottlieb B. The new concept of periodontoclasia. *The Journal of periodontology.* 1946;17:7-23.

24. Liu J, Li Q, Liu S, et al. Periodontal Ligament Stem Cells in the Periodontitis Microenvironment Are Sensitive to Static Mechanical Strain. *Stem cells international.* 2017;2017:1380851.

25. Schroeder HE. *Oral structural biology : embryology, structure, and function of normal hard and soft tissues of the oral cavity and temporomandibular joints.* Stuttgart ;New York: G. Thieme Verlag ; Thieme Medical Publishers; 1991.

26. Zhu W, Liang M. Periodontal ligament stem cells: current status, concerns, and future prospects. *Stem cells international.* 2015;2015:972313.

27. Vandana KL, Haneet RK. Cementoenamel junction: An insight. *Journal of Indian Society of Periodontology.* 2014;18(5):549-554.

28. Sjodin B, Matsson L. Marginal bone level in the normal primary dentition. *Journal of clinical periodontology.* 1992;19(9 Pt 1):672-678.

29. Bimstein E, Soskolne AW. A radiographic study of interproximal alveolar bone crest between the primary molars in children. *ASDC journal of dentistry for children.* 1988;55(5):348-350.

30. Graves DT, Li J, Cochran DL. Inflammation and uncoupling as mechanisms of periodontal bone loss. *Journal of dental research.* 2011;90(2):143-153.

31. Liu YC, Lerner UH, Teng YT. Cytokine responses against periodontal infection: protective and destructive roles. *Periodontology 2000.* 2010;52(1):163-206.

32. Garlet GP. Destructive and protective roles of cytokines in periodontitis: a re-appraisal from host defense and tissue destruction viewpoints. *Journal of dental research.* 2010;89(12):1349-1363.

33. Page RC, Schroeder HE. *Periodontitis in man and other animals: a comparative review.* New York: Karger; 1982.

34. Listgarten MA. Pathogenesis of periodontitis. *Journal of clinical periodontology.* 1986;13(5):418-430.

35. Cho MI, Garant PR. Development and general structure of the periodontium. *Periodontology 2000.* 2000;24:9-27.

36. Sodek J, McKee MD. Molecular and cellular biology of alveolar bone. *Periodontology 2000.* 2000;24:99-126.

37. Huja SS, Fernandez SA, Hill KJ, Li Y. Remodeling dynamics in the alveolar process in skeletally mature dogs. *The anatomical record Part A, Discoveries in molecular, cellular, and evolutionary biology.* 2006;288(12):1243-1249.

38. Novince CM, Kirkwood KL. Alveolar Bone Homeostasis in Health and Disease. *Primer on the Metabolic Bone Diseases and Disorders of Mineral Metabolism*: John Wiley & Sons, Inc. : Hoboken, NJ, USA; 2018:933-940.

39. Morrison SJ, Scadden DT. The bone marrow niche for haematopoietic stem cells. *Nature.* 2014;505(7483):327-334.

40. Ivanov, II, Honda K. Intestinal commensal microbes as immune modulators. *Cell host & microbe.* 2012;12(4):496-508.

41. Brestoff JR, Artis D. Commensal bacteria at the interface of host metabolism and the immune system. *Nature immunology.* 2013;14(7):676-684.

42. Minty M, Canceil T, Serino M, Burcelin R, Terce F, Blasco-Baque V. Oral microbiota-induced periodontitis: a new risk factor of metabolic diseases. *Reviews in endocrine & metabolic disorders.* 2019;20(4):449-459.

43. Aas JA, Paster BJ, Stokes LN, Olsen I, Dewhirst FE. Defining the normal bacterial flora of the oral cavity. *Journal of clinical microbiology.* 2005;43(11):5721-5732.

44. Wade WG. The oral microbiome in health and disease. *Pharmacological research : the official journal of the Italian Pharmacological Society.* 2013;69(1):137-143.

45. Thaiss CA, Zmora N, Levy M, Elinav E. The microbiome and innate immunity. *Nature.* 2016;535(7610):65-74.

46. Slack E, Hapfelmeier S, Stecher B, et al. Innate and adaptive immunity cooperate flexibly to maintain host-microbiota mutualism. *Science (New York, NY).* 2009;325(5940):617-620.

47. Graves DT, Jiang Y, Genco C. Periodontal disease: bacterial virulence factors, host response and impact on systemic health. *Current opinion in infectious diseases.* 2000;13(3):227-232.

48. Eke PI, Dye BA, Wei L, et al. Update on Prevalence of Periodontitis in Adults in the United States: NHANES 2009 to 2012. *Journal of periodontology.* 2015;86(5):611-622.

49. Takeuchi O, Akira S. Pattern recognition receptors and inflammation. *Cell.* 2010;140(6):805-820.

50. Kawai T, Akira S. Toll-like receptors and their crosstalk with other innate receptors in infection and immunity. *Immunity.* 2011;34(5):637-650.

51. Cao X. Self-regulation and cross-regulation of pattern-recognition receptor signalling in health and disease. *Nature reviews Immunology.* 2016;16(1):35-50.

52. Song B, Zhang Y, Chen L, et al. The role of Toll-like receptors in periodontitis. *Oral diseases.* 2016.

53. Silva N, Abusleme L, Bravo D, et al. Host response mechanisms in periodontal diseases. *Journal of applied oral science : revista FOB.* 2015;23(3):329-355.

54. Meyle J, Dommisch H, Groeger S, Giacaman RA, Costalonga M, Herzberg M. The innate host response in caries and periodontitis. *Journal of clinical periodontology.* 2017;44(12):1215-1225.

55. Cortes-Vieyra R, Rosales C, Uribe-Querol E. Neutrophil Functions in Periodontal Homeostasis. *Journal of immunology research.* 2016;2016:1396106.

56. Yu T, Zhao L, Huang X, et al. Enhanced Activity of the Macrophage M1/M2 Phenotypes and Phenotypic Switch to M1 in Periodontal Infection. *Journal of periodontology.* 2016;87(9):1092-1102.

57. Song L, Dong G, Guo L, Graves DT. The function of dendritic cells in modulating the host response. *Molecular oral microbiology.* 2018;33(1):13-21.

58. Chaplin DD. Overview of the immune response. *The Journal of allergy and clinical immunology.* 2010;125(2 Suppl 2):S3-23.

59. Mathur A, Michalowicz BS. Cell-mediated immune system regulation in periodontal diseases. *Critical reviews in oral biology and medicine : an official publication of the American Association of Oral Biologists.* 1997;8(1):76-89.

60. Takahama Y. Journey through the thymus: stromal guides for T-cell development and selection. *Nature reviews Immunology.* 2006;6(2):127-135.

61. Gaffen SL, Hajishengallis G. A new inflammatory cytokine on the block: re-thinking periodontal disease and the Th1/Th2 paradigm in the context of Th17 cells and IL-17. *Journal of dental research.* 2008;87(9):817-828.

62. Sun B, Zhang Y. Overview of orchestration of CD4+ T cell subsets in immune responses. *Advances in experimental medicine and biology.* 2014;841:1-13.

63. Souto GR, Queiroz-Junior CM, de Abreu MH, Costa FO, Mesquita RA. Pro-inflammatory, Th1, Th2, Th17 cytokines and dendritic cells: a cross-sectional study in chronic periodontitis. *PloS one.* 2014;9(3):e91636.

64. Cury PR, Carmo JP, Horewicz VV, Santos JN, Barbuto JA. Altered phenotype and function of dendritic cells in individuals with chronic periodontitis. *Archives of oral biology.* 2013;58(9):1208-1216.

65. Teng YT, Mahamed D, Singh B. Gamma interferon positively modulates Actinobacillus actinomycetemcomitans-specific RANKL+ CD4+ Th-cell-mediated alveolar bone destruction in vivo. *Infection and immunity.* 2005;73(6):3453-3461.

66. Alayan J, Ivanovski S, Farah CS. Alveolar bone loss in T helper 1/T helper 2 cytokine-deficient mice. *Journal of periodontal research.* 2007;42(2):97-103.

67. Tsukasaki M, Komatsu N, Nagashima K, et al. Host defense against oral microbiota by bone-damaging T cells. *Nature communications.* 2018;9(1):701.

68. Yu JJ, Ruddy MJ, Wong GC, et al. An essential role for IL-17 in preventing pathogen-initiated bone destruction: recruitment of neutrophils to inflamed bone requires IL-17 receptor-dependent signals. *Blood.* 2007;109(9):3794-3802.

69. Beklen A, Ainola M, Hukkanen M, Gurgan C, Sorsa T, Konttinen YT. MMPs, IL-1, and TNF are regulated by IL-17 in periodontitis. *Journal of dental research.* 2007;86(4):347-351.

70. Cardoso CR, Garlet GP, Crippa GE, et al. Evidence of the presence of T helper type 17 cells in chronic lesions of human periodontal disease. *Oral microbiology and immunology.* 2009;24(1):1-6.

71. Dutzan N, Gamonal J, Silva A, Sanz M, Vernal R. Over-expression of forkhead box P3 and its association with receptor activator of nuclear factor-kappa B ligand, interleukin (IL) -17, IL-10 and transforming growth factor-beta during the progression of chronic periodontitis. *Journal of clinical periodontology.* 2009;36(5):396-403.

72. Garlet GP, Cardoso CR, Mariano FS, et al. Regulatory T cells attenuate experimental periodontitis progression in mice. *Journal of clinical periodontology.* 2010;37(7):591-600.

73. Arun KV, Talwar A, Kumar TS. T-helper cells in the etiopathogenesis of periodontal disease: A mini review. *Journal of Indian Society of Periodontology.* 2011;15(1):4-10.

74. Wolk K, Witte E, Witte K, Warszawska K, Sabat R. Biology of interleukin-22. *Seminars in immunopathology.* 2010;32(1):17-31.

75. Novince CM, Whittow CR, Aartun JD, et al. Commensal Gut Microbiota Immunomodulatory Actions in Bone Marrow and Liver have Catabolic Effects on Skeletal Homeostasis in Health. *Scientific reports.* 2017;7(1):5747.

76. Irie K, Novince CM, Darveau RP. Impact of the Oral Commensal Flora on Alveolar Bone Homeostasis. *Journal of dental research.* 2014;93(8):801-806.

77. Lorenzo J, Horowitz M, Choi Y. Osteoimmunology: interactions of the bone and immune system. *Endocrine reviews.* 2008;29(4):403-440.

78. Takayanagi H. Osteoimmunology and the effects of the immune system on bone. *Nature reviews Rheumatology.* 2009;5(12):667-676.

79. Walsh MC, Kim N, Kadono Y, et al. Osteoimmunology: interplay between the immune system and bone metabolism. *Annual review of immunology.* 2006;24:33-63.

80. Walsh MC, Takegahara N, Kim H, Choi Y. Updating osteoimmunology: regulation of bone cells by innate and adaptive immunity. *Nature reviews Rheumatology.* 2018;14(3):146-156.

81. Walsh MC, Choi Y. Biology of the RANKL-RANK-OPG System in Immunity, Bone, and Beyond. *Frontiers in immunology.* 2014;5:511.

82. Long F. Building strong bones: molecular regulation of the osteoblast lineage. *Nature reviews Molecular cell biology.* 2011;13(1):27-38.

83. Karner CMH, J. H. Endochondral Ossification. *Primer on the Metabolic Bone Diseases and Disorders of Mineral Metabolism*: John Wiley & Sons, Inc. : Hoboken, NJ, USA; 2018:12-19.

84. Yasuda H, Shima N, Nakagawa N, et al. Osteoclast differentiation factor is a ligand for osteoprotegerin/osteoclastogenesis-inhibitory factor and is identical to TRANCE/RANKL. *Proceedings of the National Academy of Sciences of the United States of America.* 1998;95(7):3597-3602.

85. McCauley LK, Nohutcu RM. Mediators of periodontal osseous destruction and remodeling: principles and implications for diagnosis and therapy. *Journal of periodontology.* 2002;73(11):1377-1391.

86. Boyce BF, Xing L. Functions of RANKL/RANK/OPG in bone modeling and remodeling. *Archives of biochemistry and biophysics.* 2008;473(2):139-146.

87. Takayanagi H, Ogasawara K, Hida S, et al. T-cell-mediated regulation of osteoclastogenesis by signalling cross-talk between RANKL and IFN-gamma. *Nature.* 2000;408(6812):600-605.

88. Chen B, Wu W, Sun W, Zhang Q, Yan F, Xiao Y. RANKL expression in periodontal disease: where does RANKL come from? *BioMed research international.* 2014;2014:731039.

89. Liu D, Xu JK, Figliomeni L, et al. Expression of RANKL and OPG mRNA in periodontal disease: possible involvement in bone destruction. *International journal of molecular medicine.* 2003;11(1):17-21.

90. Park JH, Lee NK, Lee SY. Current Understanding of RANK Signaling in Osteoclast Differentiation and Maturation. *Molecules and cells.* 2017;40(10):706-713.

91. Kim JH, Kim N. Regulation of NFATc1 in Osteoclast Differentiation. *Journal of bone metabolism.* 2014;21(4):233-241.

92. Wisitrasameewong W, Kajiya M, Movila A, et al. DC-STAMP Is an Osteoclast Fusogen Engaged in Periodontal Bone Resorption. *Journal of dental research.* 2017;96(6):685-693.

93. Simonet WS, Lacey DL, Dunstan CR, et al. Osteoprotegerin: a novel secreted protein involved in the regulation of bone density. *Cell.* 1997;89(2):309-319.

94. Weitzmann MN. The Role of Inflammatory Cytokines, the RANKL/OPG Axis, and the Immunoskeletal Interface in Physiological Bone Turnover and Osteoporosis. *Scientifica.* 2013;2013:125705.

95. Nakamura I, Jimi E. Regulation of osteoclast differentiation and function by interleukin-1. *Vitam Horm.* 2006;74:357-370.

96. Weitzmann MN, Pacifici R. The role of T lymphocytes in bone metabolism. *Immunological reviews.* 2005;208:154-168.

97. Ruscitti P, Cipriani P, Carubbi F, et al. The role of IL-1beta in the bone loss during rheumatic diseases. *Mediators of inflammation.* 2015;2015:782382.

98. Graves DT, Fine D, Teng YT, Van Dyke TE, Hajishengallis G. The use of rodent models to investigate host-bacteria interactions related to periodontal diseases. *Journal of clinical periodontology.* 2008;35(2):89-105.

99. Zhang YH, Heulsmann A, Tondravi MM, Mukherjee A, Abu-Amer Y. Tumor necrosis factor-alpha (TNF) stimulates RANKL-induced osteoclastogenesis via coupling of TNF type 1 receptor and RANK signaling pathways. *The Journal of biological chemistry.* 2001;276(1):563-568.

100. Lin NY, Stefanica A, Distler JH. Autophagy: a key pathway of TNF-induced inflammatory bone loss. *Autophagy.* 2013;9(8):1253-1255.

101. Masada MP, Persson R, Kenney JS, Lee SW, Page RC, Allison AC. Measurement of interleukin-1 alpha and -1 beta in gingival crevicular fluid: implications for the pathogenesis of periodontal disease. *Journal of periodontal research.* 1990;25(3):156-163.

102. Takahashi K, Takashiba S, Nagai A, et al. Assessment of interleukin-6 in the pathogenesis of periodontal disease. *Journal of periodontology.* 1994;65(2):147-153.

103. Yamazaki K, Nakajima T, Gemmell E, Polak B, Seymour GJ, Hara K. IL-4- and IL-6-producing cells in human periodontal disease tissue. *Journal of oral pathology & medicine : official publication of the International Association of Oral Pathologists and the American Academy of Oral Pathology.* 1994;23(8):347-353.

104. Gamonal J, Acevedo A, Bascones A, Jorge O, Silva A. Levels of interleukin-1 beta, -8, and -10 and RANTES in gingival crevicular fluid and cell populations in adult periodontitis patients and the effect of periodontal treatment. *Journal of periodontology.* 2000;71(10):1535-1545.

105. Yakovlev E, Kalichman I, Pisanti S, Shoshan S, Barak V. Levels of cytokines and collagen type I and type III as a function of age in human gingivitis. *Journal of periodontology.* 1996;67(8):788-793.

106. Yoshitake F, Itoh S, Narita H, Ishihara K, Ebisu S. Interleukin-6 directly inhibits osteoclast differentiation by suppressing receptor activator of NF-kappaB signaling pathways. *The Journal of biological chemistry.* 2008;283(17):11535-11540.

107. Lin D, Li L, Sun Y, et al. IL-17 regulates the expressions of RANKL and OPG in human periodontal ligament cells via TRAF6/TBK1-JNK/NF-kappaB pathways. *Immunology.* 2014.

108. Oseko F, Yamamoto T, Akamatsu Y, et al. IL-17 is involved in bone resorption in mouse periapical lesions. *Microbiology and immunology.* 2009;53(5):287-294.

109. Gao Y, Grassi F, Ryan MR, et al. IFN-gamma stimulates osteoclast formation and bone loss in vivo via antigen-driven T cell activation. *J Clin Invest.* 2007;117(1):122-132.

110. Fox SW, Chambers TJ. Interferon-gamma directly inhibits TRANCE-induced osteoclastogenesis. *Biochem Biophys Res Commun.* 2000;276(3):868-872.

111. Kotake S, Nanke Y, Mogi M, et al. IFN-gamma-producing human T cells directly induce osteoclastogenesis from human monocytes via the expression of RANKL. *Eur J Immunol.* 2005;35(11):3353-3363.

112. Madyastha PR, Yang S, Ries WL, Key LL, Jr. IFN-gamma enhances osteoclast generation in cultures of peripheral blood from osteopetrotic patients and normalizes superoxide production. *Journal of interferon & cytokine research : the official journal of the International Society for Interferon and Cytokine Research.* 2000;20(7):645-652.

113. Kilian M, Chapple IL, Hannig M, et al. The oral microbiome - an update for oral healthcare professionals. *British dental journal.* 2016;221(10):657-666.

114. Klimesova K, Jiraskova Zakostelska Z, Tlaskalova-Hogenova H. Oral Bacterial and Fungal Microbiome Impacts Colorectal Carcinogenesis. *Frontiers in microbiology.* 2018;9:774.

115. Marcotte H, Lavoie MC. Oral microbial ecology and the role of salivary immunoglobulin A. *Microbiology and molecular biology reviews : MMBR.* 1998;62(1):71-109.

116. Mager DL, Ximenez-Fyvie LA, Haffajee AD, Socransky SS. Distribution of selected bacterial species on intraoral surfaces. *Journal of clinical periodontology.* 2003;30(7):644-654.

117. Huse SM, Ye Y, Zhou Y, Fodor AA. A core human microbiome as viewed through 16S rRNA sequence clusters. *PloS one.* 2012;7(6):e34242.

118. Lamont RJ, Koo H, Hajishengallis G. The oral microbiota: dynamic communities and host interactions. *Nature reviews Microbiology.* 2018;16(12):745-759.

119. Iida N, Dzutsev A, Stewart CA, et al. Commensal bacteria control cancer response to therapy by modulating the tumor microenvironment. *Science (New York, NY).* 2013;342(6161):967-970.

120. Bhaskaran N, Quigley C, Paw C, Butala S, Schneider E, Pandiyan P. Role of Short Chain Fatty Acids in Controlling Tregs and Immunopathology During Mucosal Infection. *Frontiers in microbiology.* 2018;9:1995.

121. Zaura E, Brandt BW, Teixeira de Mattos MJ, et al. Same Exposure but Two Radically Different Responses to Antibiotics: Resilience of the Salivary Microbiome versus Long-Term Microbial Shifts in Feces. *mBio.* 2015;6(6):e01693-01615.

122. Abeles SR, Jones MB, Santiago-Rodriguez TM, et al. Microbial diversity in individuals and their household contacts following typical antibiotic courses. *Microbiome.* 2016;4(1):39.

123. Garrido-Mesa N, Zarzuelo A, Galvez J. Minocycline: far beyond an antibiotic. *British journal of pharmacology.* 2013;169(2):337-352.

124. Nelson ML. Chemical and biological dynamics of tetracyclines. *Advances in dental research.* 1998;12(2):5-11.

125. Chopra I, Roberts M. Tetracycline antibiotics: mode of action, applications, molecular biology, and epidemiology of bacterial resistance. *Microbiology and molecular biology reviews : MMBR.* 2001;65(2):232-260 ; second page, table of contents.

126. Gollnick H, Cunliffe W, Berson D, et al. Management of acne: a report from a Global Alliance to Improve Outcomes in Acne. *Journal of the American Academy of Dermatology.* 2003;49(1 Suppl):S1-37.

127. Dhem A, Piret N, Fortunati D. Tetracyclines, doxycycline and calcified tissues. *Scandinavian journal of infectious diseases Supplementum.* 1976(9):42-46.

128. Milch RA, Rall DP, Tobie JE. Bone localization of the tetracyclines. *Journal of the National Cancer Institute.* 1957;19(1):87-93.

129. Bowles WH, Bokmeyer TJ. Staining of adult teeth by minocycline: binding of minocycline by specific proteins. *Journal of esthetic dentistry.* 1997;9(1):30-34.

130. Kerbleski GJ, Hampton TT, Cornejo A. Black bone disease of the foot: a case study and review of literature demonstrating a correlation of long-term minocycline therapy and bone hyperpigmentation. *The Journal of foot and ankle surgery : official publication of the American College of Foot and Ankle Surgeons.* 2013;52(2):239-241.

131. Odell EW, Hodgson RP, Haskell R. Oral presentation of minocycline-induced black bone disease. *Oral surgery, oral medicine, oral pathology, oral radiology, and endodontics.* 1995;79(4):459-461.

132. Wolfe ID, Reichmister J. Minocycline hyperpigmentation: skin, tooth, nail, and bone involvement. *Cutis.* 1984;33(5):457-458.

133. Sapadin AN, Fleischmajer R. Tetracyclines: nonantibiotic properties and their clinical implications. *Journal of the American Academy of Dermatology.* 2006;54(2):258-265.

134. Thomas M, Le WD. Minocycline: neuroprotective mechanisms in Parkinson's disease. *Current pharmaceutical design.* 2004;10(6):679-686.

135. Chen M, Ona VO, Li M, et al. Minocycline inhibits caspase-1 and caspase-3 expression and delays mortality in a transgenic mouse model of Huntington disease. *Nature medicine.* 2000;6(7):797-801.

136. Kloppenburg M, Verweij CL, Miltenburg AM, et al. The influence of tetracyclines on T cell activation. *Clinical and experimental immunology.* 1995;102(3):635-641.

137. Bouxsein ML, Boyd SK, Christiansen BA, Guldberg RE, Jepsen KJ, Muller R. Guidelines for assessment of bone microstructure in rodents using micro-computed tomography. *Journal of bone and mineral research : the official journal of the American Society for Bone and Mineral Research.* 2010;25(7):1468-1486.

138. Saffar JL, Lasfargues JJ, Cherruau M. Alveolar bone and the alveolar process: the socket that is never stable. *Periodontology 2000.* 1997;13:76-90.

139. Dempster DW, Compston JE, Drezner MK, et al. Standardized nomenclature, symbols, and units for bone histomorphometry: a 2012 update of the report of the ASBMR Histomorphometry Nomenclature Committee. *Journal of bone and mineral research : the official journal of the American Society for Bone and Mineral Research.* 2013;28(1):2-17.

140. Bacchetti De Gregoris T, Aldred N, Clare AS, Burgess JG. Improvement of phylum- and class-specific primers for real-time PCR quantification of bacterial taxa. *J Microbiol Methods.* 2011;86(3):351-356.

141. Boutaga K, van Winkelhoff AJ, Vandenbroucke-Grauls CM, Savelkoul PH. Periodontal pathogens: a quantitative comparison of anaerobic culture and real-time PCR. *FEMS immunology and medical microbiology.* 2005;45(2):191-199.

142. Schmittgen TD, Livak KJ. Analyzing real-time PCR data by the comparative C(T) method. *Nature protocols.* 2008;3(6):1101-1108.

143. Nair AB, Jacob S. A simple practice guide for dose conversion between animals and human. *Journal of basic and clinical pharmacy.* 2016;7(2):27-31.

144. Bachmanov AA, Reed DR, Beauchamp GK, Tordoff MG. Food intake, water intake, and drinking spout side preference of 28 mouse strains. *Behavior genetics.* 2002;32(6):435-443.

145. Landreth KS. Critical windows in development of the rodent immune system. *Human & experimental toxicology.* 2002;21(9-10):493-498.

146. Dietert RR, Etzel RA, Chen D, et al. Workshop to identify critical windows of exposure for children's health: immune and respiratory systems work group summary. *Environmental health perspectives.* 2000;108 Suppl 3:483-490.

147. Malocclusion in the Laboratory Mouse. Spring 2003;JAX® NOTES(489). https://www.jax.org/news-and-insights/2003/april/malocclusion-in-the-laboratory-mouse.

148. Li Y, Toraldo G, Li A, et al. B cells and T cells are critical for the preservation of bone homeostasis and attainment of peak bone mass in vivo. *Blood.* 2007;109(9):3839-3848.

149. Pacifici R. T cells: critical bone regulators in health and disease. *Bone.* 2010;47(3):461-471.

150. Uriarte SM, Edmisson JS, Jimenez-Flores E. Human neutrophils and oral microbiota: a constant tug-of-war between a harmonious and a discordant coexistence. *Immunological reviews.* 2016;273(1):282-298.

151. Zadeh HH, Nichols FC, Miyasaki KT. The role of the cell-mediated immune response to Actinobacillus actinomycetemcomitans and Porphyromonas gingivalis in periodontitis. *Periodontology 2000.* 1999;20:239-288.

152. Gemmell E, Grieco DA, Seymour GJ. Chemokine expression in Porphyromonas gingivalis-specific T-cell lines. *Oral microbiology and immunology.* 2000;15(3):166-171.

153. Cutler CW, Jotwani R. Antigen-presentation and the role of dendritic cells in periodontitis. *Periodontology 2000.* 2004;35:135-157.

154. Teng YT, Nguyen H, Gao X, et al. Functional human T-cell immunity and osteoprotegerin ligand control alveolar bone destruction in periodontal infection. *The Journal of clinical investigation.* 2000;106(6):R59-67.

155. Cole KL, Seymour GJ, Powell RN. Phenotypic and functional analysis of T cells extracted from chronically inflamed human periodontal tissues. *Journal of periodontology.* 1987;58(8):569-573.

156. Cardoso EM, Arosa FA. CD8(+) T Cells in Chronic Periodontitis: Roles and Rules. *Frontiers in immunology.* 2017;8:145.

157. Dutzan N, Konkel JE, Greenwell-Wild T, Moutsopoulos NM. Characterization of the human immune cell network at the gingival barrier. *Mucosal immunology.* 2016;9(5):1163-1172.

158. Hajishengallis G. Periodontitis: from microbial immune subversion to systemic inflammation. *Nature Reviews Immunology.* 2014;15:30.

159. Redlich K, Smolen JS. Inflammatory bone loss: pathogenesis and therapeutic intervention. *Nature reviews Drug discovery.* 2012;11(3):234-250.

160. Pan W, Wang Q, Chen Q. The cytokine network involved in the host immune response to periodontitis. *International journal of oral science.* 2019;11(3):30.

161. Sjogren K, Engdahl C, Henning P, et al. The gut microbiota regulates bone mass in mice. *Journal of bone and mineral research : the official journal of the American Society for Bone and Mineral Research.* 2012;27(6):1357-1367.

162. Schwarzer M, Makki K, Storelli G, et al. Lactobacillus plantarum strain maintains growth of infant mice during chronic undernutrition. *Science (New York, NY).* 2016;351(6275):854-857.

163. Yan J, Herzog JW, Tsang K, et al. Gut microbiota induce IGF-1 and promote bone formation and growth. *Proceedings of the National Academy of Sciences of the United States of America.* 2016;113(47):E7554-e7563.

164. Hathaway-Schrader JD, Poulides NA, Carson MD, et al. Specific Commensal Bacterium Critically Regulates Gut Microbiota Osteoimmunomodulatory Actions During Normal Postpubertal Skeletal Growth and Maturation. *JBMR Plus.* 2020;4(3):e10338.

165. Uchida Y, Irie K, Fukuhara D, et al. Commensal Microbiota Enhance Both Osteoclast and Osteoblast Activities. *Molecules (Basel, Switzerland).* 2018;23(7).

166. Irie K, Tomofuji T, Ekuni D, et al. Age-related changes of CD4(+) T cell migration and cytokine expression in germ-free and SPF mice periodontium. *Archives of oral biology.* 2018;87:72-78.

167. Rizzatti G, Lopetuso LR, Gibiino G, Binda C, Gasbarrini A. Proteobacteria: A Common Factor in Human Diseases. *BioMed research international.* 2017;2017:9351507.

168. Shin NR, Whon TW, Bae JW. Proteobacteria: microbial signature of dysbiosis in gut microbiota. *Trends Biotechnol.* 2015;33(9):496-503.

169. Cochran DL. Inflammation and bone loss in periodontal disease. *Journal of periodontology.* 2008;79(8 Suppl):1569-1576.

170. Riva A, Borgo F, Lassandro C, et al. Pediatric obesity is associated with an altered gut microbiota and discordant shifts in Firmicutes populations. *Environmental microbiology.* 2017;19(1):95-105.

171. Rinninella E, Raoul P, Cintoni M, et al. What is the Healthy Gut Microbiota Composition? A Changing Ecosystem across Age, Environment, Diet, and Diseases. *Microorganisms.* 2019;7(1).

172. Rakoff-Nahoum S, Paglino J, Eslami-Varzaneh F, Edberg S, Medzhitov R. Recognition of commensal microflora by toll-like receptors is required for intestinal homeostasis. *Cell.* 2004;118(2):229-241.

173. Reikvam DH, Erofeev A, Sandvik A, et al. Depletion of murine intestinal microbiota: effects on gut mucosa and epithelial gene expression. *PloS one.* 2011;6(3):e17996.

174. Million M, Lagier JC, Yahav D, Paul M. Gut bacterial microbiota and obesity. *Clinical microbiology and infection : the official publication of the European Society of Clinical Microbiology and Infectious Diseases.* 2013;19(4):305-313.

175. Abusleme L, Dupuy AK, Dutzan N, et al. The subgingival microbiome in health and periodontitis and its relationship with community biomass and inflammation. *The ISME journal.* 2013;7(5):1016-1025.

176. Li Y, He J, He Z, et al. Phylogenetic and functional gene structure shifts of the oral microbiomes in periodontitis patients. *The ISME journal.* 2014;8(9):1879-1891.

177. Sokol H, Seksik P, Furet JP, et al. Low counts of Faecalibacterium prausnitzii in colitis microbiota. *Inflammatory bowel diseases.* 2009;15(8):1183-1189.

178. Keijser BJ, Zaura E, Huse SM, et al. Pyrosequencing analysis of the oral microflora of healthy adults. *Journal of dental research.* 2008;87(11):1016-1020.

179. Baker JJ, Chan SP, Socransky SS, Oppenheim JJ, Mergenhagen SE. Importance of Actinomyces and certain gram-negative anaerobic organisms in the transformation of lymphocytes from patients with periodontal disease. *Infection and immunity.* 1976;13(5):1363-1368.

180. Guss JD, Horsfield MW, Fontenele FF, et al. Alterations to the Gut Microbiome Impair Bone Strength and Tissue Material Properties. *Journal of bone and mineral research : the official journal of the American Society for Bone and Mineral Research.* 2017.

181. Nagasawa T, Kiji M, Yashiro R, et al. Roles of receptor activator of nuclear factor-kappaB ligand (RANKL) and osteoprotegerin in periodontal health and disease. *Periodontology 2000.* 2007;43:65-84.

182. Belibasakis GN, Bostanci N. The RANKL-OPG system in clinical periodontology. *Journal of clinical periodontology.* 2012;39(3):239-248.

183. Belibasakis GN, Meier A, Guggenheim B, Bostanci N. The RANKL-OPG system is differentially regulated by supragingival and subgingival biofilm supernatants. *Cytokine.* 2011;55(1):98-103.

184. Blander JM, Longman RS, Iliev ID, Sonnenberg GF, Artis D. Regulation of inflammation by microbiota interactions with the host. *Nature immunology.* 2017;18(8):851-860.

185. Lichtman JS, Ferreyra JA, Ng KM, Smits SA, Sonnenburg JL, Elias JE. Host-Microbiota Interactions in the Pathogenesis of Antibiotic-Associated Diseases. *Cell reports.* 2016;14(5):1049-1061.

186. Belkaid Y, Harrison OJ. Homeostatic Immunity and the Microbiota. *Immunity.* 2017;46(4):562-576.

187. Knoop KA, McDonald KG, Kulkarni DH, Newberry RD. Antibiotics promote inflammation through the translocation of native commensal colonic bacteria. *Gut.* 2016;65(7):1100-1109.

188. Quirynen M, De Soete M, Dierickx K, van Steenberghe D. The intra-oral translocation of periodontopathogens jeopardises the outcome of periodontal therapy. A review of the literature. *Journal of clinical periodontology.* 2001;28(6):499-507.

189. Danser MM, Timmerman MF, van Winkelhoff AJ, van der Velden U. The effect of periodontal treatment on periodontal bacteria on the oral mucous membranes. *Journal of periodontology.* 1996;67(5):478-485.

190. Preus HR, Lassen J, Aass AM, Christersson LA. Prevention of transmission of resistant bacteria between periodontal sites during subgingival application of antibiotics. *Journal of clinical periodontology.* 1993;20(4):299-303.

191. Mombelli A, Lehmann B, Tonetti M, Lang NP. Clinical response to local delivery of tetracycline in relation to overall and local periodontal conditions. *Journal of clinical periodontology.* 1997;24(7):470-477.

192. Nussbaum G, Shapira L. How has neutrophil research improved our understanding of periodontal pathogenesis? *Journal of clinical periodontology.* 2011;38 Suppl 11:49-59.

193. Garant PR. Plaque-neutrophil interaction in monoinfected rats as visualized by transmission electron microscopy. *Journal of periodontology.* 1976;47(3):132-138.

194. Nikodemova M, Watters JJ, Jackson SJ, Yang SK, Duncan ID. Minocycline down-regulates MHC II expression in microglia and macrophages through inhibition of IRF-1 and protein kinase C (PKC)alpha/betaII. *The Journal of biological chemistry.* 2007;282(20):15208-15216.

195. Campbell JH, Burdo TH, Autissier P, et al. Minocycline inhibition of monocyte activation correlates with neuronal protection in SIV neuroAIDS. *PloS one.* 2011;6(4):e18688.

196. Wilensky A, Segev H, Mizraji G, et al. Dendritic cells and their role in periodontal disease. *Oral diseases.* 2014;20(2):119-126.

197. Heath WR, Carbone FR. Dendritic cell subsets in primary and secondary T cell responses at body surfaces. *Nature immunology.* 2009;10(12):1237-1244.

198. Kinane DF, Shiba H, Stathopoulou PG, et al. Gingival epithelial cells heterozygous for Toll-like receptor 4 polymorphisms Asp299Gly and Thr399ile are hypo-responsive to Porphyromonas gingivalis. *Genes and immunity.* 2006;7(3):190-200.

199. Rimoldi M, Chieppa M, Larghi P, Vulcano M, Allavena P, Rescigno M. Monocyte-derived dendritic cells activated by bacteria or by bacteria-stimulated epithelial cells are functionally different. *Blood.* 2005;106(8):2818-2826.

200. Huang CB, Altimova Y, Strange S, Ebersole JL. Polybacterial challenge effects on cytokine/chemokine production by macrophages and dendritic cells. *Inflammation research : official journal of the European Histamine Research Society [et al].* 2011;60(2):119-125.

201. Chino T, Santer DM, Giordano D, et al. Effects of oral commensal and pathogenic bacteria on human dendritic cells. *Oral microbiology and immunology.* 2009;24(2):96-103.

202. Sato K, Suematsu A, Okamoto K, et al. Th17 functions as an osteoclastogenic helper T cell subset that links T cell activation and bone destruction. *The Journal of experimental medicine.* 2006;203(12):2673-2682.

203. Ebersole JL, Taubman MA. The protective nature of host responses in periodontal diseases. *Periodontology 2000.* 1994;5:112-141.

204. Takeichi O, Haber J, Kawai T, Smith DJ, Moro I, Taubman MA. Cytokine profiles of T-lymphocytes from gingival tissues with pathological pocketing. *Journal of dental research.* 2000;79(8):1548-1555.

205. Gemmell E, Yamazaki K, Seymour GJ. Destructive periodontitis lesions are determined by the nature of the lymphocytic response. *Critical reviews in oral biology and medicine : an official publication of the American Association of Oral Biologists.* 2002;13(1):17-34.

206. Gomes PS, Fernandes MH. Effect of therapeutic levels of doxycycline and minocycline in the proliferation and differentiation of human bone marrow osteoblastic cells. *Archives of oral biology.* 2007;52(3):251-259.

207. Suzuki A, Yagisawa J, Kumakura S, Tsutsui T. Effects of minocycline and doxycycline on cell survival and gene expression in human gingival and periodontal ligament cells. *Journal of periodontal research.* 2006;41(2):124-131.

208. Kirkwood KL, Cirelli JA, Rogers JE, Giannobile WV. Novel host response therapeutic approaches to treat periodontal diseases. *Periodontology 2000.* 2007;43:294-315.

209. Paquette DW, Ryan ME, Wilder RS. Locally delivered antimicrobials: clinical evidence and relevance. *Journal of dental hygiene : JDH.* 2008;82 Suppl 3:10-15.

210. Garner SE, Eady A, Bennett C, Newton JN, Thomas K, Popescu CM. Minocycline for acne vulgaris: efficacy and safety. *The Cochrane database of systematic reviews.* 2012(8):Cd002086.

APPENDIX

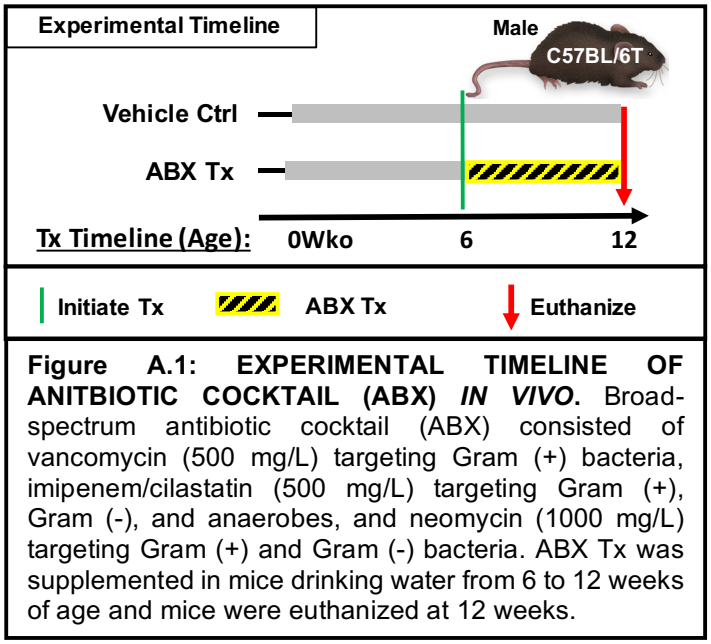

Figure A.1: EXPERIMENTAL TIMELINE OF ANITBIOTIC COCKTAIL (ABX) *IN VIVO*. Broad-spectrum antibiotic cocktail (ABX) consisted of vancomycin (500 mg/L) targeting Gram (+) bacteria, imipenem/cilastatin (500 mg/L) targeting Gram (+), Gram (-), and anaerobes, and neomycin (1000 mg/L) targeting Gram (+) and Gram (-) bacteria. ABX Tx was supplemented in mice drinking water from 6 to 12 weeks of age and mice were euthanized at 12 weeks.

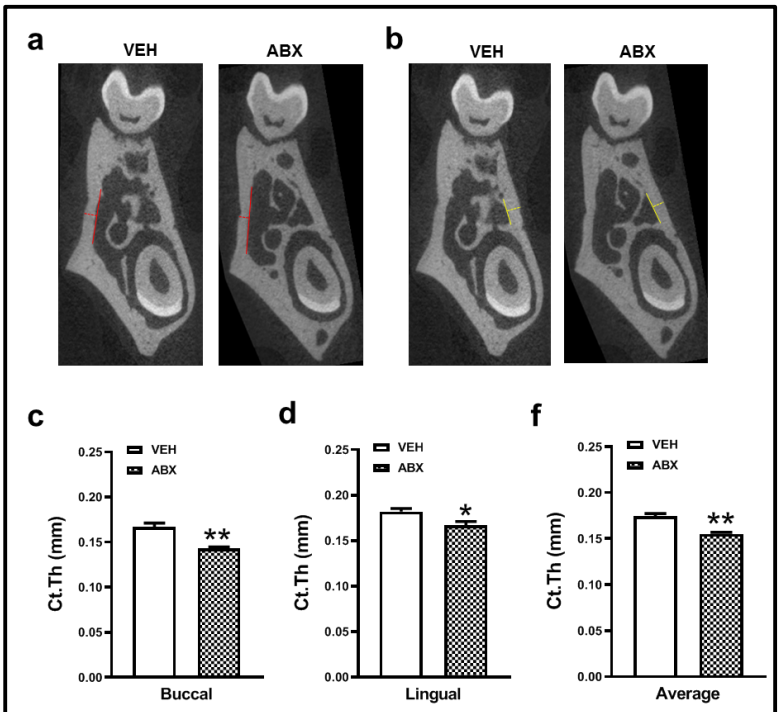

Figure A.2: ANTIBIOTIC COCKTAIL (ABX) EFFECTS ON CORTICAL BONE MICROARCHITECTURE. 12-week-old male VEH- and ABX-treated mice were euthanized, and mandibles were harvested for micro-CT analysis. (a-f) Micro-CT analysis of cortical bone thickness in mandibular first molar furcation. (n=4-6/pg) (a-b) Representative images of cortical bone thickness at the buccal aspect of inner cortical bone surface (*measurement of interest defined by red perpendicular dashed line). (a) Representative images of cortical bone thickness at the lingual aspect of inner cortical bone surface (*measurement of interest defined by yellow perpendicular dashed line). (c-f) Ct.Th = cortical bone thickness outcomes at the (c) buccal cortical plate, (d) lingual cortical plate, and (f) combined average of the buccal / lingual cortical plates. Unpaired t-test statistical analysis was used. Data are reported as mean ± SEM. *$p<0.05$ vs. VEH. **$p<0.01$ vs. VEH.

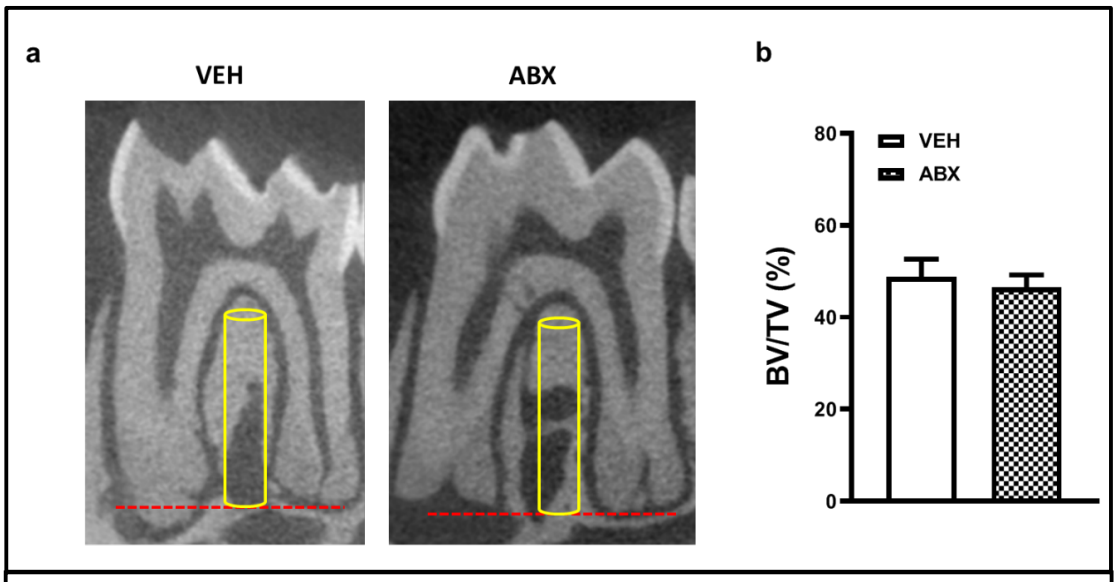

Figure A.3: ANTIBIOTIC COCKTAIL (ABX) EFFECTS ON TRABECULAR BONE MICROARCHITECTURE. 12-week-old male VEH- and ABX-treated mice were euthanized, and mandibles were harvested for micro-CT analysis. (a-b) Micro-CT analysis of trabecular bone in mandibular first molar furcation. (n=4-6/pg) (a) Representative images of trabecular bone volume fraction using cylindrical method (*region of interest defined by yellow cylinder). (b) BV/TV = trabecular bone volume fraction. Unpaired t-test statistical analysis was used. Data are reported as mean ± SEM. *p<0.05 vs. VEH.

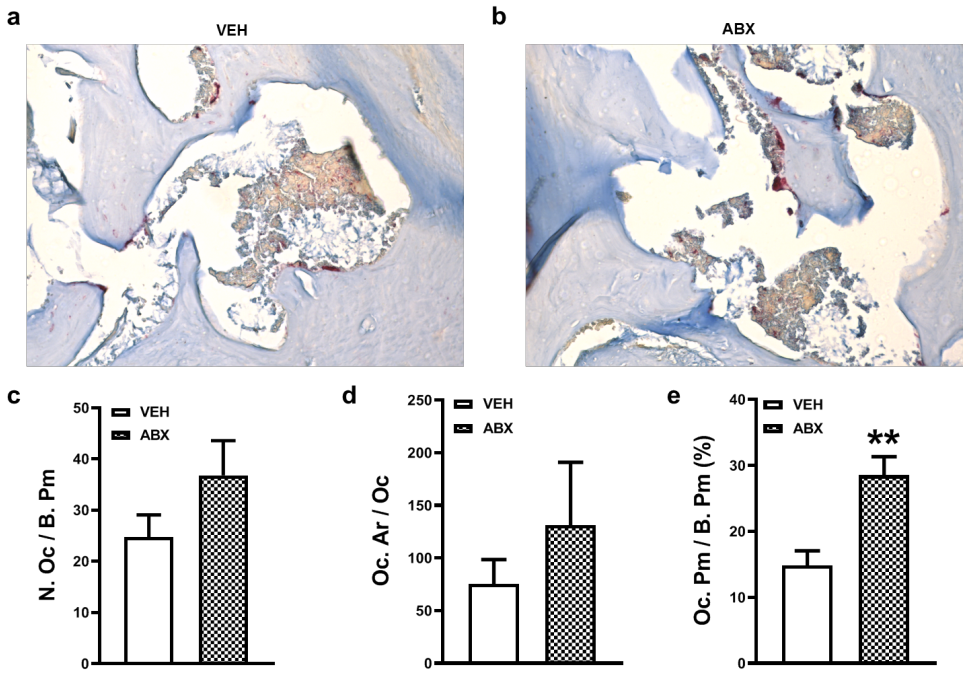

Figure A.4: ANTIBIOTIC COCKTAIL (ABX) EFFECTS ON *IN SITU* OSTEOCLASTOGENESIS. 12-week-old male VEH- and ABX-treated mice were euthanized, and maxilla harvested for histomorphometric analysis. Histomorphometric analysis of osteoclast cellular endpoints were performed in the trabecular bone marrow furcation of tartrate-resistant acid phosphatase (TRAP) stained maxillary first molar sections; TRAP+ cells lining bone with ≥ 3 nuclei were designated an osteoclast. (a-b) Representative images of furcation region of interest in TRAP-stained maxilla sections. (c) N.OC / B.Pm = osteoclast number per bone perimeter. (d) Oc.Ar / Oc = average osteoclast area. (e) Oc.Pm / B.Pm = osteoclast perimeter per bone perimeter. Unpaired t-test statistical analysis was used. Data are reported as mean ± SEM. *p<0.05 vs. VEH. **p<0.01 vs. VEH.

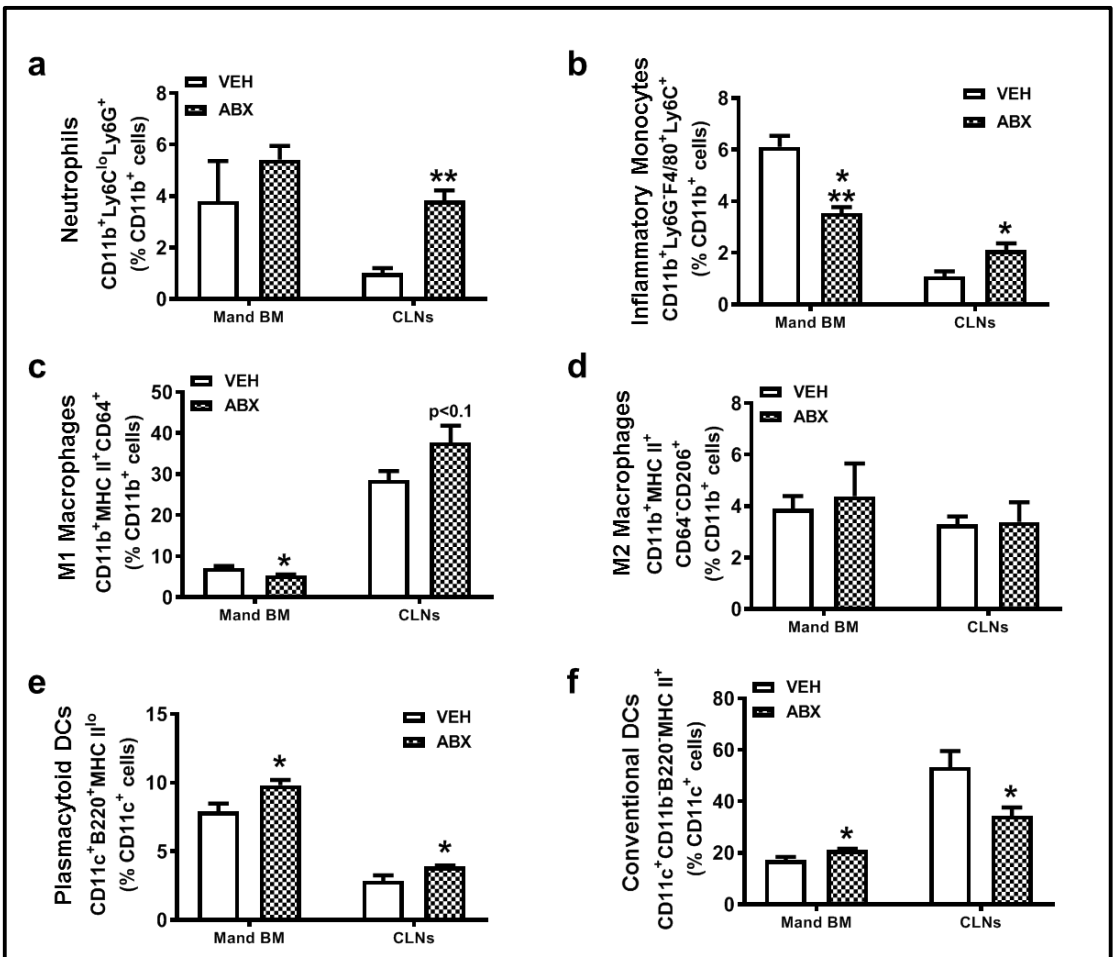

Figure A.5: ANTIBIOTIC COCKTAIL (ABX) EFFECTS ON INNATE IMMUNE CELLS IN MANDIBLE BONE MARROW (MBM) AND CERVICAL LYMPH NODE (CLN). Mandible bone marrow (MBM) and oral draining cervical lymph nodes (CLN) innate immune cell analysis. 12-week-old male VEH- and ABX-treated mice were euthanized; MBM and CLN cells were isolated for flow cytometric analysis (n=4-6/gp). (a-d) Neutrophil, monocyte, and macrophage subsets are expressed relative to the CD11b+ cell population; (a) %$CD11b^{+}Ly6C^{lo}Ly6G^{+}$ neutrophils; (b) %$CD11b^{+}Ly6G^{-}F4/80^{+}Ly6C^{+}$ inflammatory monocytes; (c) %$CD11b^{+}MHCII^{+}CD64^{+}$ M1-macrophages; (d) %$CD11b^{+}MHCII^{+}$ M2-macrophages. (e-f) Dendritic cell (DC) subsets are expressed relative to the CD11c+ cell population; (e) $CD11c^{+}B220^{+}MHCII^{lo}$ plasmacytoid DCs; (f) $CD11c^{+}CD11b^{-}B220^{-}MHCII^{+}$ conventional DCs. Unpaired t-test statistical analysis was used. Data are reported as mean ± SEM, *p<0.05 vs. VEH, **p<0.01 vs. VEH, ***p<0.001 vs. VEH.

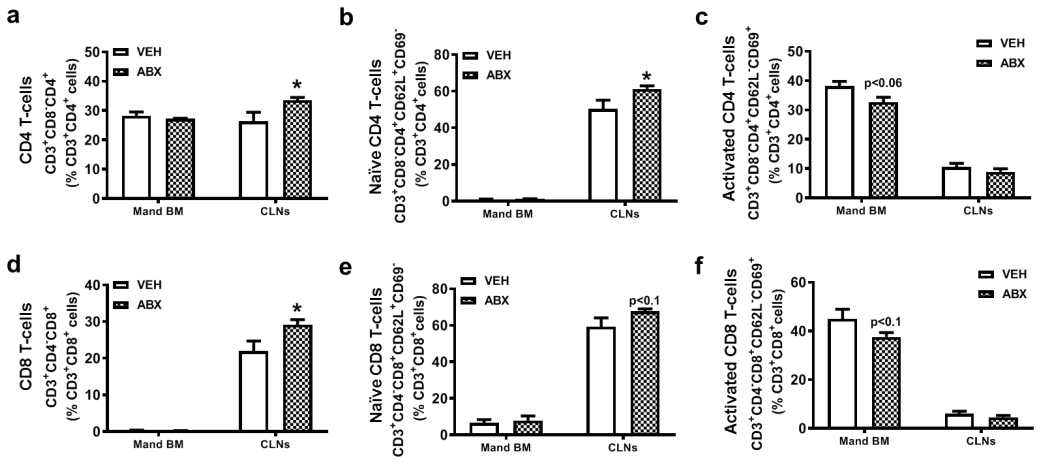

Figure A.6: ANTIBIOTIC COCKTAIL (ABX) EFFECTS ON TOTAL, NAÏVE, AND ACTIVATED T-CELLS IN MANDIBLE BONE MARROW (MBM) AND CERVICAL LYMPH NODES (CLNS). Mandible bone marrow (MBM) and oral draining cervical lymph nodes (CLN) $CD4^+$ T-cell and $CD8^+$ T-cell flow cytometric analysis. 12-week-old male VEH- and ABX-treated mice were euthanized; MBM and CLN cells were isolated for flow cytometric analysis (n=4-6/gp). (a-c) Helper $CD4^+$ T-cell subset composition. (a) $CD3^+CD8^-CD4^+$ Total CD4 Helper T-cells; (b) $CD3^+CD8^-CD4^+CD62L^+CD69^-$ Naïve CD4 T-cells; (c) $CD3^+CD8^-CD4^+CD62L^-CD69^+$ Activated CD4 T-cells. (d-f) Helper $CD8^+$ T-cell subset composition. (d) $CD3^+CD4^-CD8^+$ Helper $CD8^+$ T-cells; (e) $CD3^+CD4^-CD8^+CD62L^+CD69^-$ Naïve CD8 T-cells; (f) $CD3^+CD4^-CD8^+CD62L^-CD69^+$ Activated CD8 T-cells. Data are expressed relative to CD3+CD4+ cells. Unpaired t-test statistical analysis was used. Data are reported as mean ± SEM, *p<0.05 vs. VEH.

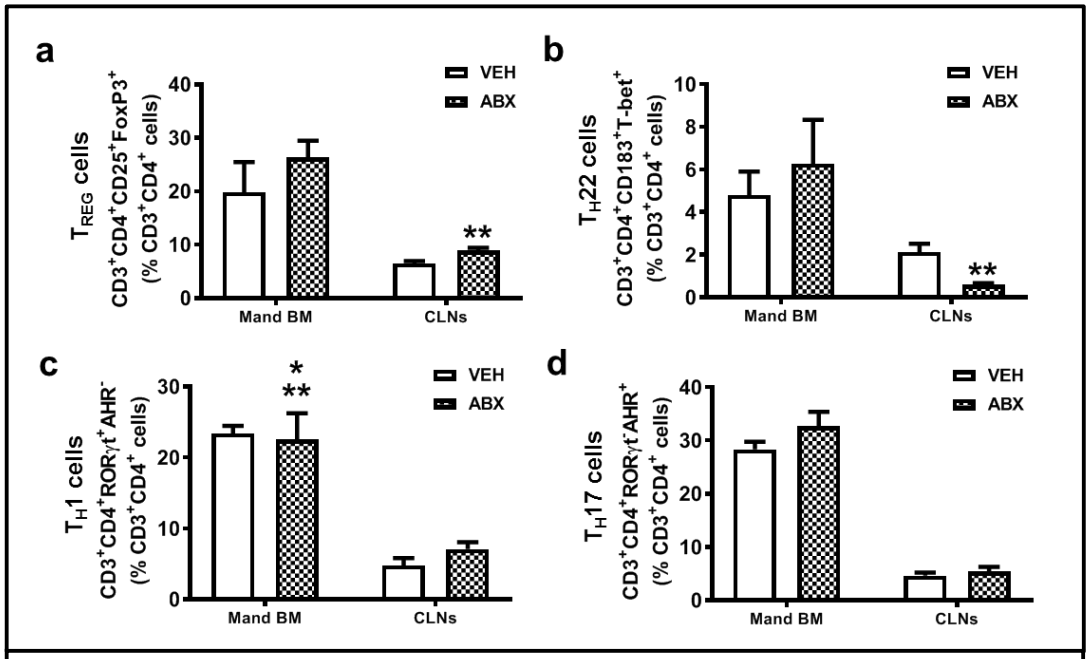

Figure A.7: ANTIBIOTIC COCKTAIL (ABX) EFFECTS ON CD4+ HELPER T-CELL SUBSETS IN MANDIBLE BONE MARROW (MBM) AND CERVICAL LYMPH NODES (CLNS). Mandible bone marrow (MBM) and oral draining cervical lymph nodes (CLN) adaptive immune cell analysis. 12-week-old male VEH- and ABX-treated mice were euthanized; MBM and CLN cells were isolated for flow cytometric analysis (n=4-6/gp). (a-d) $CD4^+$ T-cell subsets composition (a) $CD3^+CD4^+CD25^+FoxP3^+$ T_{REG} cells; (b) $CD3^+CD4^+RORyt^-AHR+$ T_H22 cells (c) $CD3^+CD4^+CD183^+T\text{-}bet^+$ T_H1 cells; (d) $CD3^+CD4^+RORyt^+AHR^-$ T_H17 cells. Percentages relative to total $CD3^+CD4^+$ T-cells. Unpaired t-test statistical analysis was used. Data are reported as mean ± SEM. *p<0.05 vs. VEH. **p<0.01 vs. VEH. ***p<0.001 vs. VEH.

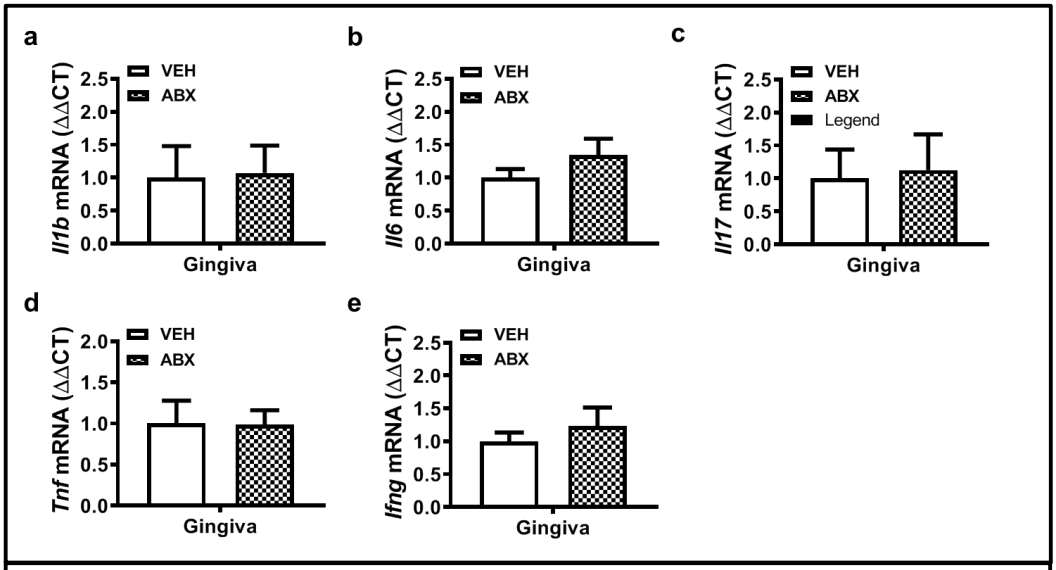

Figure A.8: ANTIBIOTIC COCKTAIL (ABX) EFFECTS ON PRO-INFLAMMATORY MEDIATORS IN MANDIBLE GINGIVA. 12-week-old male VEH and ABX treated mice were euthanized and gingiva was isolated for qRT-PCR gene expression analysis (n=4-6/gp). (a) *Il1b* mRNA (pleiotropic inflammatory cytokine); (b) *Il6* mRNA (pleiotropic inflammatory cytokine); (c) *Il17* mRNA (T_H17 cytokine); (d) *Tnf* mRNA (pleiotropic inflammatory cytokine); (e) *Ifng* mRNA (T_H1 cytokine). Relative quantification of mRNA was performed via the comparative C_T method ($2^{-\Delta\Delta CT}$); *Rn18s* was utilized as an internal control gene. Data are reported as mean ± SEM. *p<0.05 vs. VEH.